# Robust Subspace Tracking With Missing Data and Outliers: Novel Algorithm With Convergence Guarantee

Le Trung Thanh, Nguyen Viet Dung, *Member, IEEE*, Nguyen Linh Trung, *Senior Member, IEEE*, and Karim Abed-Meraim, *Fellow, IEEE*

***Abstract*—In this article, we propose a novel algorithm, namely PETRELS-ADMM, to deal with subspace tracking in the presence of outliers and missing data. The proposed approach consists of two main stages: outlier rejection and subspace estimation. In the first stage, alternating direction method of multipliers (ADMM) is effectively exploited to detect outliers affecting the observed data. In the second stage, we propose an improved version of the parallel estimation and tracking by recursive least squares (PETRELS) algorithm to update the underlying subspace in the missing data context. We then present a theoretical convergence analysis of PETRELS-ADMM which shows that it generates a sequence of subspace solutions converging to the optimum of its batch counterpart. The effectiveness of the proposed algorithm, as compared to state-of-the-art algorithms, is illustrated on both simulated and real data.**

***Index Terms*—Alternating direction method of multipliers (ADMM), missing data, online robust PCA, outliers, robust matrix completion, robust subspace tracking.**

## I. Introduction

SUBSPACE estimation plays an important role in signal processing with numerous applications in wireless communications, radar, navigation, image/video processing, biomedical imaging, etc. [1], especially processing modern datasets in today's big and messy data [2]. It corresponds to estimating an appropriate $r$-dimensional subspace $\mathbf{U}$ of $\mathbb{R}^n$ where $r \ll n$, from a set of $m$ observed data vectors $\{\mathbf{x}_i\}_{i=1}^m$, or equivalently, a measurement data matrix $\mathbf{X}$ of size $n \times m$. To this end, the standard approach is to solve an eigen-problem in a batch manner where the underlying subspace can be obtained from either singular value decomposition of the data matrix or eigenvalue decomposition of its covariance matrix. In certain online or large-scale applications, batch algorithms become inefficient due to their high computational complexity, $\mathcal{O}(nm\min(m,n))$, and memory cost, $\mathcal{O}(nm)$ [3]. Subspace tracking or adaptive (dynamic) principal component analysis (PCA) has been an excellent alternative with a much lower computational complexity as well as memory cost (i.e., linear to the data vector size $n$ and the subspace dimension $r$).

In the signal processing literature, several good surveys of the standard algorithms for subspace tracking can be found, e.g. [1], [4]. The algorithms can be categorized into three classes in terms of their computational complexity: high complexity $\mathcal{O}(n^2r)$, moderate complexity $\mathcal{O}(nr^2)$ and low complexity $\mathcal{O}(nr)$. Note that, there usually exists a trade-off among estimation accuracy, convergence rate and computational complexity. However, the performance of standard algorithms may be degraded significantly if the measurement data are corrupted by even a small number of outliers or missing observations [5]. Recent surveys [6]–[8] show that missing data and outliers are ubiquitous and more and more common in the big data regime. This has led to attempts to define robust variants of subspace learning, namely robust subspace tracking (RST), or online robust PCA. In this work, we aim to investigate the RST problem in the presence of both outliers and missing data.

Our study is also motivated by several emerging applications in diverse fields. In big data analysis, subspace tracking is used to monitor dynamic cardiac magnetic resonance imaging (MRI), track network-traffic anomalies [9] or mitigate radio frequency interference (RFI) in radio astronomy [10]. Moreover, in 5 G wireless communication, subspace tracking have recently been exploited for channel estimation in massive MIMO [11] and millimeter wave multiuser MIMO [12].

### A. Related Works

In the literature, there have been several studies on subspace tracking in the missing data context. Among them, Grassmannian rank-one update subspace estimation (GROUSE) [13] is

Manuscript received February 29, 2020; revised August 15, 2020, November 23, 2020, and February 10, 2021; accepted March 3, 2021. Date of publication March 18, 2021; date of current version April 15, 2021. The associate editor coordinating the review of this manuscript and approving it for publication was Dr. Ali Tajer. This work was supported by the National Foundation for Science and Technology Development (NAFOSTED) of Vietnam under Grant 102.04-2019.14. *(Corresponding author: Nguyen Linh Trung.)*

Le Trung Thanh is with the AVITECH Institute, University of Engineering and Technology, Vietnam National University, Hanoi, Vietnam, and also with the PRISME Laboratory, University of Orléans, 45100 Orleans, France (e-mail: trung-thanh.le@univ-orleans.fr).

Nguyen Viet Dung is with the AVITECH Institute, University of Engineering and Technology, Vietnam National University, Hanoi, Vietnam, and also with the National Institute of Advanced Technologies of Brittany (ENSTA Bretagne), 29200 Brest, France (e-mail: viet.nguyen@ensta-bretagne.fr).

Nguyen Linh Trung is with the AVITECH Institute, University of Engineering and Technology, Vietnam National University, Hanoi, Vietnam (e-mail: linhtrung@vnu.edu.vn).

Karim Abed-Meraim is with the PRISME Laboratory, University of Orleans, 45100 Orleans, France (e-mail: karim.abed-meraim@univ-orleans.fr).

This article has supplementary downloadable material available at https://doi.org/10.1109/TSP.2021.3066795, provided by the authors.

Digital Object Identifier 10.1109/TSP.2021.3066795

an incremental gradient subspace algorithm that performs the stochastic gradient descent on the Grassmannian manifold of the $r$-dimensional subspace. It belongs to the class of low complexity and its convergence has recently been proved in [14]. A robust version of GROUSE for handling outliers is Grassmannian robust adaptive subspace tracking (GRASTA) [15]. GRASTA first uses an $\ell_1$-norm cost function to reduce the effect of sparse outliers and then performs the incremental gradient on the Grassmannian manifold of subspace $\mathbf{U}$ in a similar way as in GROUSE. Although GRASTA is one of the fastest RST algorithms for handling missing data corrupted by outliers, convergence analysis of this algorithm is not available.

Parallel estimation and tracking by recursive least squares (PETRELS) [16] can be considered as an extension of the well-known projection approximation subspace tracking (PAST) algorithm [17] in order to handle missing data. Specifically, PETRELS is a recursive least squares-type algorithm applying the second order stochastic gradient descent to the cost function. Inspired by PETRELS, several variants have been proposed to deal with missing data in the same line such as [9], [18], [19]. The subspace tracking algorithm in [9] is derived from minimizing the sum of squared residuals, but adding a regularization of the nuclear norm of subspace $\mathbf{U}$. Robust online subspace estimation and tracking (ROSETA) in [18] applies an adaptive step size at the stage of subspace estimation to enhance the convergence rate. Meanwhile the main idea of PETRELS-CFAR algorithm [19] is to handle "outliers-removed" data (i.e., outliers are first removed before performing subspace tracking) using a constant false alarm rate (CFAR) detector. However, the convergence of these PETRELS-based algorithms has not been mathematically proved yet.

Recursive projected compressive sensing (ReProCS)-based algorithms [20], [21] are also able to adaptively reconstruct a subspace from missing observations. They provide not only a memory-efficient solution, but also a precise subspace estimation as compared to the state-of-the-arts. However, they require strong assumptions on subspace changes, outlier magnitudes and accurate initialization.

Other subspace tracking algorithms, able to deal with missing data, include pROST [22], APSM [23], POPCA [24] and OVBSL [25]. They either require memorizing previous observations and good initialization or do not provide a convergence guarantee.

Among the subspace tracking algorithms reviewed above, only a few of them are robust in the presence of both outliers and missing observations, including GRASTA [15], pROST [22], ROSETA [18], ReProCS-based algorithms [20], [21] and PETRELS-CFAR [19].

### *B. Contributions*

Adopting the approach of PETRELS-CFAR [19] but aiming to improve RST performance, we are interested in looking for a method that can remove outliers more effectively. Following our preliminary study presented in [26], the main contributions of the paper are as follows.

First, we propose a novel algorithm, namely PETRELS-ADMM, for the RST problem to deal with both missing data and outliers. It includes two main stages: outlier rejection and subspace estimation and tracking. Outliers residing in the measurement data are detected and removed by our ADMM solver in an effective way. Particularly, we design an efficient augmented Lagrangian alternating direction method for the $\ell_1$-regularized loss minimization. Furthermore, we propose an improved version of PETRELS, namely iPETRELS. It is observed that PETRELS is ineffective when the fraction of missing data is too large. We thus add a regularization of the $\ell_{2,\infty}$-norm, which aims to control the maximum $\ell_2$-norm of rows in $\mathbf{U}$, in the objective function to avoid such performance loss. In addition, we introduce an adaptive step size to speed up the convergence rate as well as enhance the subspace estimation accuracy.

Second, we provide a convergence analysis of the proposed algorithm where we show that the solutions $\{\mathbf{U}_t\}_{t=1}^{\infty}$ generated by PETRELS-ADMM converge to a stationary point of the expected loss function $f(\mathbf{U})$ asymptotically. To the best of our knowledge, this is a pioneer analysis for RST algorithm's convergence in the presence of both outliers and missing data, *under mild conditions*.

Finally, we provide extensive experiments on both simulated and real data to illustrate the effectiveness of PETRELS-ADMM in three application contexts: robust subspace tracking, robust matrix completion and video background-foreground separation.

There are several differences between PETRELS-ADMM and the state-of-the-art RST algorithms. In particular, our mechanism for outlier rejection can facilitate the subspace estimation ability of RST algorithms where "clean" data involve the process only, thus improving overall performance. Excepting PETRELS-CFAR, the common principle of the state-of-the-art algorithms is "outlier-resistant" (i.e., to have a "right" direction toward the true subspace). The algorithms thus require robust cost functions as well as additional adaptive parameter selection. For examples, GRASTA and ROSETA use the $\ell_1$-norm robust estimator to reduce the effect of outliers while pROST applies the $\ell_0$-norm one instead. However, there is no guarantee that the $\ell_p$-norm robust estimator (i.e., $p \in [0, 1]$) can provide an optimal solution because of non-convexity. Accordingly, the effect of outliers can not be completely removed in tracking. This is why the algorithms can fail in the appearance of a large fractions of outliers or significant subspace changes in practice. By contrast, 'detect and skip' approach like PETRELS-CFAR can utilize advantage (i.e., competitive performance) of the original PETRELS in missing observations and then treat outliers as missing data to facilitate the subspace tracking.

Compared to PETRELS-CFAR, our ADMM solver may be efficient than CFAR in terms of memory cost and flexibility. The constant false alarm rate method (CFAR) [27] uses a moving window to detect outliers (i.e., using both old and new observations at each time instant). By contrast, our ADMM solver exploits only a new incoming data vector, hence requiring a lower storage complexity. Moreover, the performance of CFAR depends on predefined parameters such as the probability of false alarm and the size of the reference window [19]. Our

ADMM solver does not involve such parameters and hence it is more efficient. Third, PETRELS-CFAR may provide an unstable solution in the presence of a high corruption fraction due to lack of regularization (i.e., in the similar way as PETRELS).

Moreover, PETRELS-ADMM can be classified to a class of provable ST algorithms [20], [21] where a performance guarantee is provided. Our proposed algorithm takes both advantages of streaming solution (need only single-pass of data) and preserved convergence.

The structure of the paper is organized as follows. Section II formulate the RST problem. Section III establishes our PETRELS-ADMM algorithm for RST and Section IV gives its theoretical convergence analysis. Section V presents extensive experiments to illustrate the effectiveness of PETRELS-ADMM as compared to the state-of-the-art algorithms. Section VI concludes the paper.

### C. Notations

We use lowercase (e.g. $a$), boldface lowercase (e.g. $\mathbf{a}$), capital boldface (e.g. $\mathbf{A}$) and calligraphic letters (e.g. $\mathcal{A}$) letters to denote scalars, vectors, matrices and sets respectively. The $i$-th entry of a vector $\mathbf{a}$ is denoted by $\mathbf{a}(i)$. For a matrix $\mathbf{A}$, $(i,j)$-th entry is denoted by $\mathbf{A}(i,j)$; $\mathbf{A}_{:,k}$ and $\mathbf{A}_{l,:}$ are $k$-th column and $l$-th row of $\mathbf{A}$ respectively. Operators $(.)^\top, (.)^\#, \mathbb{E}[.], \mathrm{tr}(.)$ denote the transportation, pseudo-inverse, expectation and trace operator respectively. For $1 \leq p < \infty$, $\ell_p$-norm of a vector $\mathbf{a} \in \mathbb{R}^{n\times 1}$ is $\|\mathbf{a}\|_p \triangleq (\sum_{i=1}^n |\mathbf{a}(i)|^p)^{1/p}$; $\ell_0$-norm is $\|\mathbf{a}\|_0 \triangleq \lim_{p\to 0}(\sum_{i=1}^n |\mathbf{a}(i)|^p)$; $\ell_\infty$-norm is $\|\mathbf{a}\|_\infty \triangleq \max_i |a(i)|$. The $\ell_{2,\infty}$-norm of $\mathbf{A}$ is defined as the maximum $\ell_2$-norm of all rows in $\mathbf{A}$, i.e., $\|\mathbf{A}\|_{2,\infty} = \max_l \|\mathbf{A}_{l,:}\|_2$. The Frobenius norm of a matrix $\mathbf{A} \in \mathbb{R}^{n\times m}$ is $\|\mathbf{A}\|_F \triangleq (\sum_{i=1}^n \sum_{j=1}^m \mathbf{A}(i,j)^2)^{1/2} = \sqrt{\mathrm{tr}(\mathbf{A}^\top\mathbf{A})}$. The condition number of matrix $\mathbf{A}$ is $\kappa(\mathbf{A}) = \frac{\sigma_{\max}(\mathbf{A})}{\sigma_{\min}(\mathbf{A})}$, where $\sigma_{\max}(\mathbf{A})$ and $\sigma_{\min}(\mathbf{A})$ are maximal and minimal singular values of $\mathbf{A}$ respectively.

## II. Problem Formulation

### A. Robust Subspace Tracking

Assume that at each time instant $t$, we observe a signal $\mathbf{x}_t \in \mathbb{R}^n$ satisfying the following model:

$$\mathbf{x}_t = \mathbf{P}_t(\boldsymbol{\ell}_t + \mathbf{n}_t + \mathbf{s}_t), \tag{1}$$

where $\boldsymbol{\ell}_t \in \mathbb{R}^n$ is the true signal that lies in a low dimensional subspace[1] of $\mathbf{U} \in \mathbb{R}^{n\times r}$ (i.e., $\boldsymbol{\ell}_t = \mathbf{U}\mathbf{w}_t$, where $\mathbf{w}_t$ is a weight vector and $r \ll n$), $\mathbf{n}_t \in \mathbb{R}^n$ is the noise vector, $\mathbf{s}_t \in \mathbb{R}^n$ is the sparse outlier vector, while the diagonal matrix $\mathbf{P}_t \in \mathbb{R}^{n\times n}$ is the observation mask indicating whether the $k$-th entry of $\mathbf{x}_t$ is observed (i.e., $\mathbf{P}_t(k,k) = 1$) or not (i.e., $\mathbf{P}_t(k,k) = 0$). For the sake of convenience, let $\Omega_t$ be the set of observed entries at time $t$.

Before introducing the RST formulation, we first define a loss function $\ell(.)$ that remains convex while still promoting sparsity: For a fixed subspace $\mathbf{U} \in \mathbb{R}^{n\times r}$ and a signal $\mathbf{x} \in \mathbb{R}^n$ under an observation mask $\mathbf{P}$, the loss function $\ell(\mathbf{U},\mathbf{P},\mathbf{x})$ with respect to $\mathbf{U}$ and $\{\mathbf{P},\mathbf{x}\}$ is derived from minimizing the projection residual on the observed entries and accounting for outliers as

$$\ell(\mathbf{U},\mathbf{P},\mathbf{x}) \triangleq \min_{\mathbf{s},\mathbf{w}} \tilde{\ell}(\mathbf{U},\mathbf{P},\mathbf{x},\mathbf{w},\mathbf{s}) \tag{2}$$

$$\text{with } \tilde{\ell}(\mathbf{U},\mathbf{P},\mathbf{x},\mathbf{w},\mathbf{s}) = \left\|\mathbf{P}(\mathbf{U}\mathbf{w}+\mathbf{s}-\mathbf{x})\right\|_2^2 + \rho\|\mathbf{s}\|_1, \tag{3}$$

where we here use the $\ell_1$ regularization to promote entry-wise sparsity on $\mathbf{s}$ and $\rho > 0$ is a regularization parameter to control the degree of the sparsity.[2]

Now, given a streaming set of observed signals, $\mathcal{X} = \{\mathbf{x}_i\}_{i=1}^t$ in (1), we wish to estimate a rank-$r$ matrix $\mathbf{U}_t \in \mathbb{R}^{n\times r}$ such that it can cover the span of the complete-data noiseless signal $\boldsymbol{\ell}_t$.

RST can be achieved via the following minimization problem:

$$\mathbf{U}_t = \underset{\mathbf{U}\in\mathbb{R}^{n\times r}}{\mathrm{argmin}} \left[ f_t(\mathbf{U}) \triangleq \frac{1}{t}\sum_{i=1}^t \lambda_i^{t-i}\ell(\mathbf{U},\mathbf{P}_i,\mathbf{x}_i)\right], \tag{4}$$

where the forgetting factor $\lambda_i \in (0,1]$ is to discount the effect of past observations. For the convergence analysis, we will consider the expected cost $f(\mathbf{U})$ on signals distributed by the true data-generating distribution $\mathbb{P}_{\text{data}}$, instead of the empirical cost $f_t(\mathbf{U})$. Thanks to the law of large numbers, expectation of the observations without discounting (i.e., $\lambda = 1$) converges to the true value when $t$ tends to infinity,

$$\hat{\mathbf{U}} = \underset{\mathbf{U}\in\mathbb{R}^{n\times r}}{\mathrm{argmin}} f(\mathbf{U}) \tag{5}$$

$$\text{with } f(\mathbf{U}) \triangleq \mathbb{E}_{\mathbf{x}\overset{\text{i.i.d}}{\sim}\mathbb{P}_{\text{data}}}[\ell(\mathbf{U},\mathbf{P},\mathbf{x})] = \lim_{t\to\infty} f_t(\mathbf{U}). \tag{6}$$

From the past estimations $\{\mathbf{s}_i,\mathbf{w}_i\}_{i=1}^t$, instead of minimizing the empirical cost function $f_t(\mathbf{U})$ in (4), we propose to optimize the surrogate $g_t(\mathbf{U})$ of $f_t(\mathbf{U})$, which is defined as

$$g_t(\mathbf{U}) = \frac{1}{t}\sum_{i=1}^t \lambda_i^{t-i}\left(\left\|\mathbf{P}_i(\mathbf{U}\mathbf{w}_i+\mathbf{s}_i-\mathbf{x}_i)\right\|_2^2 + \rho\|\mathbf{s}_i\|_1\right), \tag{7}$$

where $\{\mathbf{s}_i,\mathbf{w}_i\}_{i=1}^t$ are considered as constants. Note that, the surrogate function provides an upper bound on $f_t(\mathbf{U})$. In our convergence analysis, we will prove that $f_t(\mathbf{U}_t)$ and $g_t(\mathbf{U}_t)$ converge almost surely to the same limit. As a result, the solution $\mathbf{U}_t$ obtained by minimizing $g_t(\mathbf{U})$ is exactly the solution of $f_t(\mathbf{U})$ when $t$ tends to infinity.

### B. Assumptions

We make the following assumptions for convenience of convergence analysis as well as helping deploy our optimization algorithm:

(A-1): The data-generation distribution $\mathbb{P}_{\text{data}}$ has a compact support, $\mathbf{x} \overset{\text{i.i.d}}{\sim} \mathbb{P}_{\text{data}}$. Indeed, real data are often bounded such as

[1] In an adaptive scheme, this subspace might be slowly time-varying, i.e., $\mathbf{U} = \mathbf{U}_t$, and hence the adaptive RST algorithm introduced next would not only estimate $\mathbf{U}$ but also track its variations along the iterations.

[2] The most direct way of enforcing sparsity constraints is to control the $\ell_0$-norm of the solution which counts the number of non-zero entries. Following this way, the problem of (2) is well specified but computationally intractable. Interestingly, the $\ell_1$ relaxation can recover the original sparse solution of the $\ell_0$ problem while still preserving convexity [28].

audio, image and video, hence this assumption naturally holds in many situations.

(A-2): $\mathbf{U}$ is constrained to the set $\mathcal{U} \triangleq \{\mathbf{U} \in \mathbb{R}^{n\times r}, \|\mathbf{U}_{:,k}\|_2 \leq 1, 1 \leq \kappa(\mathbf{U}) \leq \alpha\}$ with a constant $\alpha$. The first constraint $\|\mathbf{U}_{:,k}\|_2 \leq 1$ is not restrictive as it is considered to bound the scale of basis vectors in $\mathbf{U}$ and hence prevents the arbitrarily very large values of $\mathbf{U}$. While the low condition number of the subspace $\kappa(\mathbf{U})$ is to prevent the ill-conditioned computation.

(A-3): Coefficients $\mathbf{w}$ are constrained to the set $\mathcal{W} = \{\mathbf{w} \in \mathbb{R}^r, \omega_1 \leq |w(i)| \leq \omega_2, i = 1, 2, \ldots, r\}$ with two constants $\omega_1$ and $\omega_2$, $0 \leq \omega_1 < \omega_2$. Since the data $\mathbf{x}$ and subspace $\mathbf{U}$ are assumed to be bounded, it is natural that the subspace weight vector $\mathbf{w}$ is bounded too.

(A-4): The subspace changes at two successive time instances is small, i.e., the largest principal angle between $\mathbf{U}_t$ and $\mathbf{U}_{t-1}$ is $0 \leq \theta_{\max} \ll \pi/2$, or the distance between the two subspaces, $\mathrm{d}(\mathbf{U}_t, \mathbf{U}_{t-1}) = \sin(\theta_{\max})$, satisfies $0 \leq \mathrm{d}(\mathbf{U}_t, \mathbf{U}_{t-1}) \ll 1$.

## III. Proposed PETRELS-ADMM Algorithm

In this section, we present a novel algorithm, namely PETRELS-ADMM, for RST to handle missing data in the presence of outliers. The main idea is to minimize the empirical cost function $g_t$ in (7) by updating outliers $\mathbf{s}_t$, weight vector $\mathbf{w}_t$ and subspace $\mathbf{U}_t$ alternatively.

Under the assumption (A-2) that the underlying subspace $\mathbf{U}$ changes slowly, we can detect outliers in $\mathbf{s}_t$ by projecting the new observation $\mathbf{x}_t$ into the space spanned by the formerly estimated subspace $\mathbf{U}_{t-1}$ in the previous phase. Specifically, we solve the following minimization problem:

$$\{\mathbf{s}_t, \mathbf{w}_t\} \triangleq \underset{\mathbf{s},\mathbf{w}}{\operatorname{argmin}}\ \tilde{\ell}(\mathbf{U}_{t-1}, \mathbf{P}_t, \mathbf{x}_t, \mathbf{w}, \mathbf{s}) \text{ with}$$
$$\tilde{\ell}(\mathbf{U}_{t-1}, \mathbf{P}_t, \mathbf{x}_t, \mathbf{w}, \mathbf{s}) = \left\|\mathbf{P}_t(\mathbf{U}_{t-1}\mathbf{w} + \mathbf{s} - \mathbf{x}_t)\right\|_2^2 + \rho\|\mathbf{s}\|_1. \tag{8}$$

In the second phase, the subspace $\mathbf{U}_t$ can be estimated by minimizing the sum of squared residuals:

$$\underset{\mathbf{U}}{\operatorname{argmin}} \frac{1}{t}\sum_{i=1}^{t} \lambda^{t-i} \frac{\mathrm{tr}(\widetilde{\mathbf{P}}_i)}{n} \left\|\widetilde{\mathbf{P}}_i(\mathbf{U}\mathbf{w}_i - \mathbf{x}_i)\right\|_2^2 + \frac{\alpha}{2t}\|\mathbf{U}\|_{2,\infty}^2, \tag{9}$$

where the regularization $\frac{\alpha}{2t}\|\mathbf{U}\|_{2,\infty}^2$ is to bound the scale of vectors in $\mathbf{U}$ while the outliers $\mathbf{s}_t$ has been disregarded and the new observation $\widetilde{\mathbf{P}}_i$ are determined by the following rule:

$$\begin{cases} \widetilde{\mathbf{P}}_i(k,k) = \mathbf{P}_i(k,k), & \text{if } \mathbf{s}_i(k) = 0, \\ \widetilde{\mathbf{P}}_i(k,k) = 0, & \text{otherwise,} \end{cases} \tag{10}$$

which we aim to skip the corrupted entries of $\mathbf{x}_i$.

Our algorithm first applies the ADMM framework in [29], which has been widely used in previous works for solving (8), and then propose a modification of PETRELS [16] to handle (9). In the outlier rejection stage, we emphasize here that we propose to focus on augmenting $\mathbf{s}$ (as shown in (12)) to further annihilate outlier effect, unlike GRASTA and ROSETA which focus on augmenting the residual error only[3]. Meanwhile, we modify the subspace update step in PETRELS by adding an adaptive step size $\eta_t \in (0, 1]$ at each time instant $t$, instead of a constant one as in the original version. The modification can be interpreted as an approximation of Newton method. The proposed method is summarized in Algorithm 1.

**Algorithm 1:** Proposed PETRELS-ADMM.

**Input:** A set of observed signals $\{\mathbf{x}_i\}_{i=1}^t, \mathbf{x}_i \in \mathbb{R}^{n\times 1}$, observation masks $\{\mathbf{P}_i\}_{i=1}^t, \mathbf{P}_i \in \mathbb{R}^{n\times n}$, true rank $r$.
**Output:** $\mathbf{U}_t$
**Procedure:**

**for** $i = 1$ to $t$ **do**
*// Estimate outliers $\mathbf{s}_i$ and coefficient $\mathbf{w}_i$ using Algorithm 2:*
$$\{\mathbf{s}_i, \mathbf{w}_i\} = \underset{\mathbf{s},\mathbf{w}}{\operatorname{argmin}} \left\|\mathbf{P}_i(\mathbf{U}_{i-1}\mathbf{w} + \mathbf{s} - \mathbf{x}_i)\right\|_2^2 + \rho\|\mathbf{s}\|_1.$$
*// New observation $\widetilde{\mathbf{P}}_i$:*
$$\begin{cases} \widetilde{\mathbf{P}}_i(k,k) = \mathbf{P}_i(k,k), & \text{if } \mathbf{s}_i(k) = 0, \\ \widetilde{\mathbf{P}}_i(k,k) = 0, & \text{otherwise.} \end{cases}$$
*// Estimate subspace $\mathbf{U}_i$ using Algorithm 3:*
$$\mathbf{U}_i = \underset{\mathbf{U}}{\operatorname{argmin}} \frac{1}{i}\sum_{j=1}^{i} \lambda^{i-j} \frac{\mathrm{tr}(\widetilde{\mathbf{P}}_j)}{n} \left\|\widetilde{\mathbf{P}}_j(\mathbf{x}_j - \mathbf{U}\mathbf{w})\right\|_2^2 + \frac{\alpha}{2i}\|\mathbf{U}\|_{2,\infty}^2.$$
**end for**

**Algorithm 2:** Outlier Detection.

**Input**: Observed signal $\mathbf{x}_t \in \mathbb{R}^{n\times 1}$, observation mask $\mathbf{P}_t \in \mathbb{R}^{n\times n}$, the previous estimate $\mathbf{U}_{t-1} \in \mathbb{R}^{n\times r}$, maximum iteration $K$, penalty parameters $\rho_1, \rho_2$, absolute and relative tolerances $\epsilon_{\text{abs}}$ and $\epsilon_{\text{rel}}$.
**Output:** $\mathbf{s}, \mathbf{w}$
**Initialization:**
- Choose $\{\mathbf{u}^0, \mathbf{s}^0, \mathbf{w}^0, \mathbf{z}^0, \mathbf{e}^0\}$ randomly.
- $\{\mathbf{r}^0, \mathbf{e}^0\} \leftarrow \mathbf{0}^n$

**Procedure:**

| **for** $k = 0$ to $K$ **do** | **Cost** |
|---|---|
| *// Update* $\mathbf{w}$ | |
| $\mathbf{w}^{k+1} = (\mathbf{P}_t\mathbf{U}_{i-1})^{\#}\mathbf{P}_t(\mathbf{x}_t - \mathbf{s}^k + \mathbf{e}^k)$ | $2\Omega_t r^2 + \Omega_t r$ |
| $\mathbf{z}^{k+1} = \mathbf{P}_t(\mathbf{U}_{t-1}\mathbf{w}^{k+1} + \mathbf{s}^k - \mathbf{x}_t)$ | $\Omega_t r$ |
| $\mathbf{e}^{k+1} = \frac{\rho_2}{1+\rho_2}\mathbf{z}^{k+1} + \frac{1}{1+\rho_2} S_{1+\frac{1}{\rho_2}}(\mathbf{z}^{k+1})$ | $\Omega_t$ |
| *// Update* $\mathbf{s}$ | |
| $\mathbf{u}^{k+1} = \frac{1}{1+\rho_1}\left(\mathbf{P}_t(\mathbf{x}_t - \mathbf{U}_{t-1}\mathbf{w}^{k+1}) - \rho_1(\mathbf{s}^k - \mathbf{r}^k)\right)$ | $\Omega_t r$ |
| $\mathbf{s}^{k+1} = S_{\rho/\rho_1}(\mathbf{u}^{k+1} + \mathbf{r}^k)$ | $\Omega_t$ |
| $\mathbf{r}^{k+1} = \mathbf{r}^k + \mathbf{u}^{k+1} - \mathbf{s}^{k+1}$ | $\Omega_t$ |
| *// Stopping criteria* | |
| **if** $\left\|\mathbf{s}^{k+1} - \mathbf{s}^k\right\|_2 < \sqrt{n}\epsilon_{\text{abs}} + \epsilon_{\text{rel}}\left\|\rho_1\mathbf{r}^{k+1}\right\|_2$ break; | $\Omega_t$ |
| **end if** | |
| **end for** | |

### A. Online ADMM for Outlier Detection

We show in the following how to solve (8) step-by-step:

[3]In GRASTA [15] and ROSETA [18], both the authors aimed to detect outliers $\mathbf{s}$ by solving the augmented Lagrangian of (8) as follows

$$\mathcal{L}(\mathbf{s}, \mathbf{y}, \mathbf{w}) = \|\mathbf{s}\|_1 + \mathbf{y}^\top(\mathbf{P}_t(\mathbf{U}_{t-1}\mathbf{w} + \mathbf{s} - \mathbf{x}_t)) + \frac{\rho}{2}\|\mathbf{P}_t(\mathbf{U}_{t-1}\mathbf{w} + \mathbf{s} - \mathbf{x}_t)\|_2^2.$$

***Update*** $\mathbf{s}_t$*:* To estimate outlier $\mathbf{s}_t$ given $\mathbf{w}$, we exploit the fact that (8) can be cast into the ADMM form as follows:

$$\min_{\mathbf{u},\mathbf{s}} h(\mathbf{u}) + q(\mathbf{s}), \quad \text{subject to } \mathbf{u} - \mathbf{s} = \mathbf{0}, \tag{11}$$

where $\mathbf{u}$ is the additional decision variable, $h(\mathbf{u}) = \frac{1}{2}||\mathbf{P}_t(\mathbf{U}_{t-1}\mathbf{w} + \mathbf{u} - \mathbf{x}_t)||_2^2$ and $q(\mathbf{s}) = \rho\|\mathbf{s}\|_1$. The corresponding augmented Lagrangian with the dual variable vector $\boldsymbol{\beta}$ is thus given by

$$\mathcal{L}(\mathbf{s}, \mathbf{u}, \boldsymbol{\beta}) = q(\mathbf{s}) + h(\mathbf{u}) + \boldsymbol{\beta}^\top(\mathbf{u} - \mathbf{s}) + \frac{\rho_1}{2}\|\mathbf{u} - \mathbf{s}\|_2^2, \tag{12}$$

where $\rho_1 > 0$ is the regularization parameter.[4] Let $\mathbf{r} = \boldsymbol{\beta}/\rho_1$ be the scaled dual variable, we can rewrite the Lagrangian (12) as follows:

$$\mathcal{L}(\mathbf{s}, \mathbf{u}, \mathbf{r}) = q(\mathbf{s}) + h(\mathbf{u}) + \rho_1\mathbf{r}^\top(\mathbf{u} - \mathbf{s}) + \frac{\rho_1}{2}\|\mathbf{u} - \mathbf{s}\|_2^2. \tag{13}$$

The optimization of (13) is achieved iteratively where we have the following update rule using the scaled dual variable at the $k$-th iteration,

$$\mathbf{u}^{k+1} = \underset{\mathbf{u}}{\operatorname{argmin}} \left( h(\mathbf{u}) + \rho_1(\mathbf{r}^k)^\top(\mathbf{u} - \mathbf{s}^k) + \frac{\rho_1}{2}\left\|\mathbf{u} - \mathbf{s}^k\right\|_2^2 \right), \tag{14}$$

$$\mathbf{s}^{k+1} = \underset{\mathbf{s}}{\operatorname{argmin}} \left( q(\mathbf{s}) - \rho_1(\mathbf{r}^k)^\top\mathbf{s} + \frac{\rho_1}{2}\left\|\mathbf{u}^{k+1} - \mathbf{s}\right\|_2^2 \right), \tag{15}$$

$$\mathbf{r}^{k+1} = \mathbf{r}^k + \mathbf{u}^{k+1} - \mathbf{s}^{k+1}. \tag{16}$$

In particular, we first exploit that the minimization (14) can be formulated as a convex quadratic form:

$$\begin{aligned}\mathbf{u}^{k+1} &= \underset{\mathbf{u}}{\operatorname{argmin}} \left( \frac{1+\rho_1}{2}\|\mathbf{u}\|_2^2 \right. \\ &\quad \left. - \left[\mathbf{P}_t(\mathbf{x}_t - \mathbf{U}_{t-1}\mathbf{w}) - \rho_1(\mathbf{s}^k - \mathbf{r}^k)\right]^\top \mathbf{u} \right) \\ &= \frac{1}{1+\rho_1}\left(\mathbf{P}_t(\mathbf{x}_t - \mathbf{U}_{t-1}\mathbf{w}) - \rho_1(\mathbf{s}^k - \mathbf{r}^k)\right). \end{aligned} \tag{17}$$

Meanwhile, the problem (15) is a standard proximal minimization with the $\ell_1$-norm [33] as

$$\begin{aligned}\mathbf{s}^{k+1} &= \underset{\mathbf{s}}{\operatorname{argmin}} \left( \rho\|\mathbf{s}\|_1 + \frac{\rho_1}{2}\left\|\mathbf{s} - (\mathbf{u}^{k+1} + \mathbf{r}^k)\right\|_2^2 \right) \\ &= S_{\rho/\rho_1}(\mathbf{u}^{k+1} + \mathbf{r}^k), \end{aligned} \tag{18}$$

where $S_a(x)$ is a thresholding operator applied element-wise and defined as

$$S_a(x) = \begin{cases} 0, & \text{if } |x| \le a, \\ x - a, & \text{if } x > a, \\ x + a, & \text{if } x < -a, \end{cases}$$

which is a proximity operator of the $\ell_1$-norm.

Finally, a simple update rule for the scaled dual variable $\mathbf{r}$ can be given by the dual ascent, as

$$\mathbf{r}^{k+1} = \mathbf{r}^k + \beta^k\nabla_{\mathcal{L}}(\mathbf{r}^k),$$

where the gradient $\nabla_{\mathcal{L}}(\mathbf{r}^k)$ is computed by $\nabla_{\mathcal{L}}(\mathbf{r}^k) = \rho_1(\mathbf{u}^{k+1} - \mathbf{s}^{k+1})$ and $\beta^k > 0$ is the step size controlling the convergence rate. For ADMM methods, the regularization parameter is often used as the the step size for updating dual variables [29]. Due to the scaled version $\mathbf{r}$ of the dual variable $\boldsymbol{\beta}$, the step size $\beta^k$ is here set to be $\beta^k = 1/\rho_1$ at the $k$-th iteration.

***Update*** $\mathbf{w}_t$*:* To estimate $\mathbf{w}_t$ given $\mathbf{s}$, (8) can be recast into the following ADMM form:

$$\begin{aligned}&\min_{\mathbf{w}\in\mathcal{W},\mathbf{e}\in\mathbb{R}^{n\times 1}} \frac{1}{2}\left\|\mathbf{P}_t(\mathbf{U}_{t-1}\mathbf{w} + \mathbf{s} - \mathbf{x}_t)\right\|_2^2 + y(\mathbf{e}) \\ &\text{subject to } \mathbf{P}_t(\mathbf{U}_{t-1}\mathbf{w} + \mathbf{s} - \mathbf{x}_t) = \mathbf{e}\end{aligned} \tag{19}$$

where $y(\mathbf{e})$ is a convex regularizer function for the noise $\mathbf{e}$, (e.g. $y(\mathbf{e}) = \frac{\sigma}{2}\|\mathbf{e}\|_2^2$, with $\sigma^{-1}$ can be chosen as the signal to noise ratio, SNR). The minimization (19) is equal to the following optimization:

$$\begin{aligned}&\min_{\mathbf{w}\in\mathcal{W},\mathbf{e}\in\mathbb{R}^{n\times 1}} \|\mathbf{e}\|_2^2 \\ &\text{subject to } \mathbf{P}_t(\mathbf{U}_{t-1}\mathbf{w} + \mathbf{s} - \mathbf{x}_t) = \mathbf{e}.\end{aligned} \tag{20}$$

However, the noise $\mathbf{e}$ is still affected by outliers because $\mathbf{s}$ may not be completely rejected in each iteration. Therefore, (20) can be cast further into the ADMM form such that it can lie between least squares (LS) and least absolute deviations to reduce the impact of outliers. The Huber fitting can bring transition between the quadratic and absolute terms of $\mathcal{L}_{\mathbf{w},\mathbf{e}}(\mathbf{w}, \mathbf{e})$[5], as

$$\mathcal{L}_{\mathbf{w},\mathbf{e}}(\mathbf{w}, \mathbf{e}) = f^{\text{Hub}}(\mathbf{e}) + \frac{\rho_2}{2}\left\|\mathbf{P}_t(\mathbf{U}_{t-1}\mathbf{w} + \mathbf{s} - \mathbf{x}_t) - \mathbf{e}\right\|_2^2, \tag{21}$$

where $\rho_2 > 0$ is the penalty parameter whose characteristics are similar to that of $\rho_1$ and the Huber function is given by [29]

$$f^{\text{Hub}}(x) = \begin{cases} x^2/2, & |x| \le 1, \\ |x| - 1/2, & |x| > 1. \end{cases}$$

As a result, $\mathbf{e}$-updates for estimating $\mathbf{w}$ involves the proximity operator of the Huber function, that is,

$$\begin{aligned}\mathbf{e}^{k+1} &= \frac{\rho_2}{1+\rho_2}\mathbf{P}_t(\mathbf{U}_{t-1}\mathbf{w}^{k+1} + \mathbf{s} - \mathbf{x}_t) \\ &\quad + \frac{1}{1+\rho_2}S_{1+\frac{1}{\rho_2}}(\mathbf{P}_t(\mathbf{U}_{t-1}\mathbf{w}^{k+1} + \mathbf{s} - \mathbf{x}_t)).\end{aligned}$$

Hence, at the $(k+1)$-th iteration, $\mathbf{w}^{k+1}$ can be updated using the following closed-form solution of the convex quadratic function:

$$\mathbf{w}^{k+1} = (\mathbf{P}_t\mathbf{U}_{t-1})^{\#}\mathbf{P}_t(\mathbf{x}_t - \mathbf{s} + \mathbf{e}^k).$$

[4]It is referred to as the penalty parameter. Although the convergence rate of the proposed algorithm depends on a specific chosen value, our convergence analysis indicates that the ADMM solver can converge for any positive fixed penalty parameters. However, varying penalty parameters can give superior convergence in practice [29]–[32]

[5]Due to the natural $\ell_2$-ball behavior of the noise (i.e., normal distributed vector) and the sparsity of some unremoved parts of outliers, Huber fitting can be a reasonable choice. The Huber function consists of square and linear terms, so it is less sensitive to variables which have a strong effect on the function $\ell_2$-norm, but also does not encourage the sparsity like $\ell_1$-norm.

**Algorithm 3:** Improved PETRELS for Updating $\mathbf{U}_t$.

**Input:** Observed signals $\{\mathbf{x}_i\}_{i=1}^t$, observation mask $\widetilde{\mathbf{P}}_t$, the previous estimate $\mathbf{U}_{t-1}$, forgetting factor $\lambda$, regularization parameter $\alpha$, the step size $\eta$, the previous matrix $\mathbf{H}_{t-1}$.
**Output:** $\mathbf{U}_t$

| **Procedure:** | **Cost** |
|---|---|
| $x_t = \dfrac{\|\widetilde{\mathbf{P}}_t\mathbf{x}_t - \widetilde{\mathbf{P}}_t\mathbf{U}_{t-1}\mathbf{w}_t\|_2}{\|\mathbf{w}_t\|_2}$ | $\Omega_t r$ |
| $\eta_t = \dfrac{x_t}{\sqrt{x_t^2+1}}$ | $\mathcal{O}(1)$ |
| **if** $\eta_t > \eta$ **then** $\eta_t = 1$ **end if** | $\mathcal{O}(1)$ |
| **for** $m = 1$ to $n$ **do** | |
| $\mathbf{R}_t^m = \lambda_t \mathbf{R}_{t-1}^m + \widetilde{\mathbf{P}}_t(m,m)\mathbf{w}_t\mathbf{w}_t^\top$ | $r^2$ |
| $\mathbf{H}_t^m = \mathbf{R}_t^m + \frac{\alpha}{2}\mathbf{I}$ | $r$ |
| $\mathbf{a}_t = (\mathbf{H}_t^m)^{-1}\mathbf{w}_t$ | $\mathcal{O}(r^2)$ |
| $\mathbf{u}_t^m = \mathbf{u}_{t-1}^m + \eta_t\beta_t\widetilde{\mathbf{P}}_t(m,m)(\mathbf{x}_t^{\text{re}}(m) - \mathbf{w}_t^\top\mathbf{u}_{t-1}^m)\mathbf{a}_t$ | $r$ |
| **end for** | |

To sum up, the rule for updating $\mathbf{w}_t$ can be given by

$$\mathbf{w}^{k+1} = (\mathbf{P}_t\mathbf{U}_{t-1})^{\#}\mathbf{P}_t(\mathbf{x}_t - \mathbf{s} + \mathbf{e}^k), \tag{22}$$

$$\mathbf{z}^{k+1} = \mathbf{P}_t(\mathbf{U}_{t-1}\mathbf{w}^{k+1} + \mathbf{s} - \mathbf{x}_t), \tag{23}$$

$$\mathbf{e}^{k+1} = \frac{\rho_2}{1+\rho_2}\mathbf{z}^{k+1} + \frac{1}{1+\rho_2}S_{1+\frac{1}{\rho_2}}(\mathbf{z}^{k+1}). \tag{24}$$

We note that, by using the Huber fitting operator, our algorithm is better in reducing the impact of outliers than GRASTA and ROSETA which use $\ell_2$-norm regularization.

The procedure is stopped when the number of iterations reaches the maximum or the accuracy tolerance for the primal residual and dual norm has been met, i.e.,

$$\left\|\mathbf{s}^{k+1} - \mathbf{s}^k\right\|_2 < \sqrt{n}\epsilon_{\text{abs}} + \epsilon_{\text{rel}}\left\|\rho_1\mathbf{r}^{k+1}\right\|_2,$$

where $\epsilon_{\text{abs}} > 0$ and $\epsilon_{\text{rel}} > 0$ are predefined tolerances for absolute and relative part respectively. A reasonable range for the absolute tolerance may be $[10^{-6}, 10^{-3}]$, while $[10^{-4}, 10^{-2}]$ is good for the relative tolerance, see [29] for further details of the stopping criterion. The main steps of the outlier detection are summarized as Algorithm 2.

### *B. Improved PETRELS for Subspace Estimation*

Having estimated $\mathbf{s}_t$, we optimize the following minimization

$$\mathbf{U}_t := \operatorname{argmin}\tilde{g}_t(\mathbf{U}) \text{ with}$$

$$\tilde{g}_t(\mathbf{U}) = \frac{1}{t}\sum_{i=1}^t \lambda^{t-i}\frac{\operatorname{tr}(\widetilde{\mathbf{P}}_i)}{n}\left\|\widetilde{\mathbf{P}}_i(\mathbf{x}_i - \mathbf{U}\mathbf{w}_i)\right\|_2^2 + \frac{\alpha}{2t}\|\mathbf{U}\|_{2,\infty}^2, \tag{25}$$

where the observation mask $\widetilde{\mathbf{P}}_i$ is computed by (10).

Thanks to the parallel scheme of PETRELS [16], the optimal solution of the problem (25) can be obtained by solving its subproblems at each row $\mathbf{u}^m$ of $\mathbf{U}$, $m = 1, 2, \ldots, n$, that is,

$$\min_{\mathbf{u}^m}\frac{1}{t}\sum_{i=1}^t \lambda^{t-i}\beta_i\widetilde{\mathbf{P}}_i(m,m)\left(\mathbf{x}_i(m) - \mathbf{w}_i^\top\mathbf{u}^m\right)^2 + \frac{\alpha}{2t}\|\mathbf{u}^m\|_2^2,$$

where $\beta_i = \frac{\operatorname{tr}(\widetilde{\mathbf{P}}_i)}{n}$. In this way, we can speed up the subspace update by ignoring the $\mathbf{u}^m$ if the $m$-th entry of $\mathbf{x}_t$ is labeled as missing observation or outlier.

Thanks to Newton's method, we can update each row of the subspace by the following rule:

$$\mathbf{u}_t^m = \mathbf{u}_{t-1}^m - \left(\mathbf{H}_t(\mathbf{u}^m)\right)^{-1}\frac{\partial\tilde{g}_t(\mathbf{U})}{\partial\mathbf{u}^m}\bigg|_{\mathbf{u}^m=\mathbf{u}_{t-1}^m}, \tag{26}$$

where the first derivative of $\tilde{g}_t$ is given by

$$\frac{\partial\tilde{g}_t(\mathbf{U})}{\partial\mathbf{u}^m} = \frac{-2}{t}\sum_{i=1}^t \lambda^{t-i}\beta_i\widetilde{\mathbf{P}}_i(m,m)\left(\mathbf{x}_i(m) - \mathbf{w}_i^\top\mathbf{u}^m\right)\mathbf{w}_i^\top + \frac{\alpha}{t}\mathbf{u}^m,$$

and the second derivative of $\tilde{g}_t$, Hessian matrix, is given by

$$\mathbf{H}_t(\mathbf{u}^m) = \frac{2}{t}\sum_{i=1}^t \lambda^{t-i}\beta_i\widetilde{\mathbf{P}}_i(m,m)\mathbf{w}_i\mathbf{w}_i^\top + \frac{\alpha}{t}\mathbf{I}.$$

Specifically, the partial derivative $\frac{\partial\tilde{g}_t(\mathbf{U})}{\partial\mathbf{u}^m}$ at $\mathbf{u}_{t-1}^m$ can be expressed by

$$\frac{\partial\tilde{g}_t(\mathbf{U})}{\partial\mathbf{u}^m}\bigg|_{\mathbf{u}^m=\mathbf{u}_{t-1}^m} = \frac{\partial\tilde{g}_{t-1}(\mathbf{U})}{\partial\mathbf{u}^m}\bigg|_{\mathbf{u}^m=\mathbf{u}_{t-1}^m} + \frac{\alpha}{t}\left(\mathbf{u}_{t-1}^m - \mathbf{u}_{t-2}^m\right) - \frac{2}{t}\beta_t\widetilde{\mathbf{P}}_t(m,m)\left(\mathbf{x}_t(m) - \mathbf{w}_t^\top\mathbf{u}_{t-1}^m\right)\mathbf{w}_t^\top.$$

Since $\mathbf{u}_{t-1}^m = \operatorname{argmin}\frac{\partial\tilde{g}_{t-1}(\mathbf{U})}{\partial\mathbf{u}^m}$ and the regularization parameter $\alpha/t$ is small, so $\frac{\partial\tilde{g}_{t-1}(\mathbf{U})}{\partial\mathbf{u}^m}\big|_{\mathbf{u}^m=\mathbf{u}_{t-1}^m} = \mathbf{0}$ and then

$$\frac{\partial\tilde{g}_t(\mathbf{U})}{\partial\mathbf{u}^m}\bigg|_{\mathbf{u}^m=\mathbf{u}_{t-1}^m} \approx \frac{-2}{t}\beta_t\widetilde{\mathbf{P}}_t(m,m)(\mathbf{x}_t(m) - \mathbf{w}_t^\top\mathbf{u}_{t-1}^m)\mathbf{w}_t^\top.$$

Let us denote $\mathbf{R}_t^m = \sum_{i=1}^t \lambda_i^{t-i}\beta_i\widetilde{\mathbf{P}}_t(m,m)\mathbf{w}_i\mathbf{w}_i^\top$, the Hessian matrix can be rewritten by

$$\mathbf{H}_t(\mathbf{u}_{t-1}^m) = \frac{2}{t}\left(\mathbf{R}_t^m + \frac{\alpha}{2}\mathbf{I}\right).$$

Therefore, a relaxed approximation of the recursive update (26) can be given by

$$\mathbf{u}_t^m \approx \mathbf{u}_{t-1}^m + \eta_t\beta_t\widetilde{\mathbf{P}}_t(m,m)\left(\mathbf{x}_t(m) - \mathbf{w}_t^\top\mathbf{u}_{t-1}^m\right)\mathbf{a}_t^\top, \tag{27}$$

where $\mathbf{H}_t^m = \mathbf{R}_t^m + \frac{\alpha}{2}\mathbf{I}$[6], $\mathbf{a}_t = (\mathbf{H}_t^m)^{-1}\mathbf{w}_t$ and $\eta_t$ denotes the adaptive step size $\eta_t \in [0,1]$ at each time instant $t$, instead of a constant as in the original PETRELS [16]. We here determine the adaptive step size $\eta_t$ as follows

$$\eta_t = \frac{x_t}{\sqrt{x_t^2+1}} \text{ with } x_t = \frac{\|\mathbf{e}_t\|_2}{\|\mathbf{w}_t\|_2}, \tag{28}$$

where the residual error $\mathbf{e}_t$ is computed by $\mathbf{e}_t = \widetilde{\mathbf{P}}_t\mathbf{x}_t - \widetilde{\mathbf{P}}_t\mathbf{U}_{t-1}\mathbf{w}_t$. Note that, the adaptive step size $\eta_t$ can be expressed by $\eta_t = \sin(\theta_t)$, see Fig. 1. The smaller angle $\theta_t$ is, the closer

[6] $\mathbf{H}_t^m \in \mathbb{R}^{r\times r}$ is a matrix of rank-one updates, so its inverse matrix can be efficiently computed recursively, thanks to Sherman-Morrison formula [34]. Also, the small regularization parameter $\alpha > 0$ can help the recursive update having a better numerical stability. The computational complexity is of order $\mathcal{O}(r^2)$.

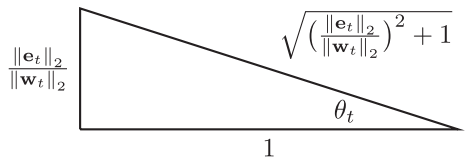


Fig. 1. Adaptive step size $\eta_t$.

to the true subspace we are, the smaller step size is needed. The update is summarized in Algorithm 3.

### C. Computational Complexity Analysis

The number of floating-point operations (flop) is used to measure the computational complexity of the proposed PETRELS-ADMM. At the $k$-th iteration in the outlier detection phase, our method requires $\mathcal{O}(\Omega r^2)$ flops where $\Omega$ is average number of observed entries at each time instant ($\Omega \leq n$). It is practically stated that the ADMM solver can converge within a few tens of iterations [29] (also see Fig. 3). Therefore, the removal of outliers costs the averaged $\mathcal{O}(\Omega r^2)$. The complexity of the subspace estimation phase is also $\mathcal{O}(\Omega r^2)$ as the original PETRELS [16]. The overall computational complexity of PETRELS-ADMM is of order $\mathcal{O}(\Omega r^2)$ flops.

## IV. Performance Analysis

In this section, we provide a convergence analysis for the proposed PETRELS-ADMM algorithm. Inspired by the results of convergence of empirical processes for online sparse coding in [35] and online robust PCA in [36], [37], we derive a theoretical approach to analyze the convergence of values of the objective function $\{f_t(\mathbf{U}_t)\}_{t=1}^{\infty}$ as well as the solutions $\{\mathbf{U}_t\}_{t=1}^{\infty}$ generated by PETRELS-ADMM.

Given assumptions defined in Section II-B, our main theoretical result can be stated by the following theorem:

*Theorem 1:* (Convergence of PETRELS-ADMM): In the stationary context, let $\{\mathbf{U}_t\}_{t=1}^{\infty}$ be the sequence of solutions generated by PETRELS-ADMM, then the sequence converges to a stationary point of the expected loss function $f(\mathbf{U})$ when $t \to \infty$.

*Proof:* Our proof can be divided into three main stages as follows: We first prove that the solutions $\{\mathbf{U}_t, \mathbf{s}_t\}_{t\geq 1}$ generated by the PETRELS-ADMM algorithm are optimal w.r.t. the cost function in (7). We then prove that a nonnegative sequence $\{g_t(\mathbf{U}_t)\}_{t=1}^{\infty}$ converges almost surely where $\{\mathbf{U}_t\}_{t=1}^{\infty}$ is the sequence of optimal solutions generated by the PETRELS-ADMM algorithm. After that, we prove that the surrogate $\{g_t(\mathbf{U}_t)\}_{t=1}^{\infty}$ converges almost surely to the empirical loss function $\{f_t(\mathbf{U}_t)\}_{t=1}^{\infty}$ as well as the true loss function, i.e., $g_t(\mathbf{U}_t) \overset{a.s.}{\to} f_t(\mathbf{U}_t) \overset{a.s.}{\to} f(\mathbf{U}_t)$, thanks to the central limit theorem.

Due to space limitation, we here present key results and report their proof sketch. The details of their proofs are provided in our supplemental material.

*Lemma 1:* (Convergence of Algorithm 2): At each time instant $t$, let $\{\mathbf{s}^k, \mathbf{u}^k, \mathbf{r}^k, \mathbf{w}^k, \mathbf{e}^k\}_{k=1}^{\infty}$ be a sequence generated by Algorithm 2 for outlier detection, there always exists a set of positive numbers $\{c_u, c_s, c_r, c_w, c_e\}$ such that, at each iteration, the minimizers satisfy

$$\begin{aligned}&\mathcal{L}(\mathbf{s}^{k+1}, \mathbf{u}^{k+1}, \mathbf{r}^{k+1}, \mathbf{w}^{k+1}, \mathbf{e}^{k+1})\\ &\leq \mathcal{L}(\mathbf{s}^{k}, \mathbf{u}^{k}, \mathbf{r}^{k}, \mathbf{w}^{k}, \mathbf{e}^{k}) - c_u\left\|\mathbf{u}^k - \mathbf{u}^{k+1}\right\|_2^2 - c_s\left\|\mathbf{s}^k - \mathbf{s}^{k+1}\right\|_2^2\\ &- c_r\left\|\mathbf{r}^k - \mathbf{r}^{k+1}\right\|_2^2 - c_w\left\|\mathbf{w}^k - \mathbf{w}^{k+1}\right\|_2^2 - c_e\left\|\mathbf{e}^k - \mathbf{e}^{k+1}\right\|_2^2,\end{aligned}$$

where the Lagrangian $\mathcal{L}(\mathbf{s}, \mathbf{u}, \mathbf{r}, \mathbf{w}, \mathbf{e})$ for updating these variables is a combination of two functions (13) and (21), as

$$\begin{aligned}\mathcal{L}(\mathbf{s}, \mathbf{u}, \mathbf{r}, \mathbf{w}, \mathbf{e}) &= q(\mathbf{s}) + h(\mathbf{u}) + \rho_1 \mathbf{r}^{\top}(\mathbf{u} - \mathbf{s}) + \frac{\rho_1}{2}\|\mathbf{u} - \mathbf{s}\|_2^2\\ &+ f^{\text{Hub}}(\mathbf{e}) + \frac{\rho_2}{2}\left\|\mathbf{P}_t(\mathbf{U}_{t-1}\mathbf{w} + \mathbf{s} - \mathbf{x}_t) - \mathbf{e}\right\|_2^2.\end{aligned}$$

The asymptotic variation of $\mathbf{s}^k$ (i.e., outliers) is then given by

$$\lim_{k\to\infty}\left\|\mathbf{s}^{k+1} - \mathbf{s}^k\right\|_2^2 = 0.$$

*Proof:* We state the following proposition, which is in the same line as in previous convergence analysis of ADMM algorithms [38], [39], used to prove the first part of lemma 1.

*Proposition 1:* Let $\{\mathbf{s}^k, \mathbf{u}^k, \mathbf{r}^k, \mathbf{w}^k, \mathbf{e}^k\}_{k=1}^{\infty}$ be a sequence generated by Algorithm 2 and denote $\mathbf{q}^k$ be one of these variables, the minimizer $\mathbf{q}^{k+1}$ of (13) satisfies

$$\mathcal{L}(\mathbf{q}^{k+1}, .) \leq \mathcal{L}(\mathbf{q}^k, .) - c_q\left\|\mathbf{q}^k - \mathbf{q}^{k+1}\right\|_2^2,$$

where $c_q$ is a positive number.

As a result, the cluster $\{\mathbf{s}^k, \mathbf{u}^k, \mathbf{r}^k, \mathbf{w}^k, \mathbf{e}^k\}$ converges to stationary point of $\mathcal{L}(\mathbf{s}, \mathbf{u}, \mathbf{r}, \mathbf{w}, \mathbf{e})$ when $k \to \infty$ and it also implies that the sequence $\{\mathbf{s}_k\}_{k=0}^{\infty}$ is convergent, i.e.,

$$\lim_{k\to\infty}\left\|\mathbf{s}^{k+1} - \mathbf{s}^k\right\|_2^2 = 0.$$

*Proposition 2:* (Convexity of the surrogate functions $g_t(\mathbf{U})$): Given assumptions in Section II-B, the surrogate function $g_t(\mathbf{U})$ defined in Eq. (7) is not only strongly convex, but also Lipschitz function, i.e., there always exists two positive numbers $m_1$ and $m_2$ such that

$$\begin{aligned}m_1\left\|\mathbf{U}_{t+1} - \mathbf{U}_t\right\|_F^2 &\leq |g_t(\mathbf{U}_{t+1}) - g_t(\mathbf{U}_t)|,\\ m_2\left\|\mathbf{U}_{t+1} - \mathbf{U}_t\right\|_F &\geq |g_t(\mathbf{U}_{t+1}) - g_t(\mathbf{U}_t)|.\end{aligned}$$

*Proof:* To prove that $g_t(\mathbf{U})$ is strongly convex, we state the following facts: $g_t(\mathbf{U})$ is continuous and differentiable; its second derivative is a positive semi-definite matrix (i.e., $\nabla^2_{\mathbf{U}} g_t(\mathbf{U}) \geq m\mathbf{I}$); and the domain of $g_t(\mathbf{U})$ is convex. In order to satisfy the Lipschitz condition, we show that the first derivative of $g_t(\mathbf{U})$ is bounded.

*Lemma 2:* (Convergence of Algorithm 3): Given an outlier vector $\mathbf{s}_t$ generated by Algorithm 2 at each time instant $t$, Algorithm 3 can provide a local optimal solution $\mathbf{U}_t$ for minimizing $g_t(\mathbf{U})$. Moreover, the asymptotic variation of estimated subspaces $\{\mathbf{U}_t\}_{t\geq 1}$ is given by

$$\left\|\mathbf{U}_t - \mathbf{U}_{t+1}\right\|_F \overset{a.s.}{\to} \mathcal{O}\left(\frac{1}{t}\right).$$

*Proof:* To establish the convergence, we exploit the fact that our modification can be seen as an approximate of the Newton

method,

$$\mathbf{U}_t \cong \mathbf{U}_{t-1} - \eta_t \left[\mathbf{H}_t(\mathbf{U}_{t-1})\right]^{-1} \nabla \tilde{g}_t(\mathbf{U}_{t-1}),$$

where $\mathbf{H}_t(\mathbf{U}_{t-1})$ and $\nabla\tilde{g}_t(\mathbf{U}_{t-1})$ are the Hessian matrix and gradient of the function $\tilde{g}_t(\mathbf{U})$ at $\mathbf{U}_{t-1}$, as shown in Section III-B. It implies that the estimated $\mathbf{U}_t$ converges to the stationary point of $g_t(\mathbf{U})$.

Furthermore, since $g_t(\mathbf{U})$ is strongly convex and Lipschitz function w.r.t the variable $\mathbf{U}$ as shown in Proposition 2, we have the following inequality

$$\begin{aligned} m_1 \left\|\mathbf{U}_{t+1} - \mathbf{U}_t\right\|_F^2 &\le \left|g_t(\mathbf{U}_{t+1}) - g_t(\mathbf{U}_t)\right| \\ &\le m_2 \left\|\mathbf{U}_{t+1} - \mathbf{U}_t\right\|_F \\ &\Leftrightarrow \left\|\mathbf{U}_t - \mathbf{U}_{t+1}\right\|_F \le \frac{m_2}{m_1} = \mathcal{O}\left(\frac{1}{t}\right). \end{aligned}$$

Note that the positive number $m_2 = \mathcal{O}(1/t)$ is already given in the proof of Proposition 2 in the supplemental material, while $m_1$ is a constant. ■

*Lemma 3:* (Convergence of the surrogate function $g_t(\mathbf{U})$): Without discounting past observations, let $\{\mathbf{U}_t\}_{t=1}^{\infty}$ be a sequence of solutions generated by Algorithm 1 at each time instant $t$, the sequence $\{g_t(\mathbf{U}_t)\}_{t=1}^{\infty}$ converges almost surely, i.e.,

$$\sum_{t=1}^{\infty} \left|\mathbb{E}[g_{t+1}(\mathbf{U}_{t+1}) - g_t(\mathbf{U}_t)|\mathcal{F}_t]\right| < +\infty \; a.s.,$$

where $\{\mathcal{F}_t\}_{t>0}$ is the filtration of the past estimations at time instant $t$.

*Proof:* Let us define the indicator function $\delta_t$ as follows

$$\delta_t \triangleq \begin{cases} 1 & \text{if } \mathbb{E}[g_{t+1}(\mathbf{U}_{t+1}) - g_t(\mathbf{U}_t)|\mathcal{F}_t] > 0, \\ 0 & \text{otherwise.} \end{cases}$$

According to the quasi-martingale convergence theorem [40, Section 4.4], in order to show the convergence of the nonnegative stochastic process $\{g_t(\mathbf{U}_t)\}_{t=1}^{\infty}$, we will prove

$$\sum_{t=0}^{\infty} \mathbb{E}\left[\delta \mathbb{E}[g_{t+1}(\mathbf{U}_{t+1}) - g_t(\mathbf{U}_t)|\mathcal{F}_t]\right] < \infty.$$

In particular, we first indicate the following inequality:

$$g_{t+1}(\mathbf{U}_{t+1}) - g_t(\mathbf{U}_t) \le \frac{\ell(\mathbf{U}_t, \mathbf{P}_{t+1}, \mathbf{x}_{t+1}) - f_t(\mathbf{U}_t)}{t+1}.$$

Since $\mathbb{E}[\ell(\mathbf{U}_t, \mathbf{P}_{t+1}, \mathbf{x}_t)] = f(\mathbf{U}_t)$, we have a nice property:

$$\begin{aligned} &\mathbb{E}[g_{t+1}(\mathbf{U}_{t+1}) - g_t(\mathbf{U}_t)|\mathcal{F}_t] \\ &\le \frac{\mathbb{E}[\ell(\mathbf{U}_t, \mathbf{P}_{t+1}, \mathbf{x}_{t+1}) - f_t(\mathbf{U}_t)|\mathcal{F}_t]}{t+1} \\ &= \frac{f(\mathbf{U}_t) - f_t(\mathbf{U}_t)}{t+1}. \end{aligned}$$

We then have

$$\begin{aligned} &\mathbb{E}\left[\delta \mathbb{E}[g_{t+1}(\mathbf{U}_{t+1}) - g_t(\mathbf{U}_t)|\mathcal{F}_t]\right] \\ &\le \mathbb{E}[\sqrt{t}(f(\mathbf{U}_t) - f_t(\mathbf{U}_t))] \frac{1}{\sqrt{t}(t+1)}. \end{aligned}$$

Under the given assumptions, we exploit the fact that the set of measurable functions $\{\ell(\mathbf{U}_i, \mathbf{P}, \mathbf{x})\}_{i\ge 1}$ defined in (2) is $\mathbb{P}$-Donsker. Therefore, the centered and scaled version of the empirical function $f_t(\mathbf{U}_t)$ satisfies the following proposition:

$$\mathbb{E}[\sqrt{t}(f(\mathbf{U}_t) - f_t(\mathbf{U}_t))] = \mathcal{O}(1),$$

thanks to Donsker theorem [41, Sec 19.2]. Furthermore, we also indicate that the sum $\sum_{t=1}^{\infty} 1/(\sqrt{t}(t+1))$ converges. The two facts result in

$$\sum_{t=0}^{\infty} \mathbb{E}\left[\delta \mathbb{E}[g_{t+1}(\mathbf{U}_{t+1}) - g_t(\mathbf{U}_t)|\mathcal{F}_t]\right] < \infty.$$

Since $g_t(\mathbf{U}_t) > 0$, we can conclude that $\{g_t(\mathbf{U}_t)\}_{t>0}$ is quasi-martingale and converges almost surely.

*Lemma 4:* (Convergence of the empirical loss function $f_t(\mathbf{U})$): The empirical loss functions $f_t(\mathbf{U}_t)$ and its surrogate $g_t(\mathbf{U}_t)$ converge to the same limit, i.e.,

$$g_t(\mathbf{U}_t) \xrightarrow{a.s.} f_t(\mathbf{U}_t).$$

*Proof:* We begin the proof with providing the following inequality:

$$\frac{g_t(\mathbf{U}_t) - f_t(\mathbf{U}_t)}{t+1} \le \underbrace{u_t - u_{t+1}}_{(S-1)} + \underbrace{\frac{\ell(\mathbf{U}_t, \mathbf{P}_{t+1}, \mathbf{x}_{t+1}) - f_t(\mathbf{U}_t)}{t+1}}_{(S-2)},$$

where $u_t \triangleq g_t(\mathbf{U}_t)$. We then prove that the two sequences (S-1)-(S-2) converge almost surely. As a result, the sequence $\{(g_t(\mathbf{U}_t) - f_t(\mathbf{U}_t))\frac{1}{t+1}\}$ also convergence almost surely, i.e.,

$$\sum_{t=0}^{\infty} \left(g_t(\mathbf{U}_t) - f_t(\mathbf{U}_t)\right) \frac{1}{t+1} < \infty.$$

In parallel, we exploit that the real sequence $\{\frac{1}{t+1}\}_{t\ge 0}$ diverges, i.e., $\sum_{t=1}^{\infty} \frac{1}{t+1} = \infty$. It implies that $g_t(\mathbf{U}_t) - f_t(\mathbf{U}_t)$ converges.

*Corollary 1:* The expected loss function $\{f(\mathbf{U}_t)\}_{t=1}^{\infty}$ converges almost surely when $t \to \infty$.

*Proof:* Since $f_t(\mathbf{U}_t) \xrightarrow{a.s.} f(\mathbf{U}_t)$ and $g_t(\mathbf{U}_t) \xrightarrow{a.s.} f_t(\mathbf{U}_t)$, then $g_t(\mathbf{U}_t) \xrightarrow{a.s.} f(\mathbf{U}_t)$. Since $g_t(\mathbf{U}_t)$ converges almost surely, $f(\mathbf{U}_t)$ also converges almost surely when $t \to \infty$. ■

*Corollary 2:* When $t \to \infty$, let $\mathbf{U}_t = \underset{\mathbf{U}\in\mathbb{R}^{n\times r}}{\operatorname{argmin}} g_t(\mathbf{U})$, we have

$$f_t(\mathbf{U}_t) \le f_t(\mathbf{U}) + \frac{L}{2}\|\mathbf{U} - \mathbf{U}_t\|_F^2, \forall\, \mathbf{U} \in \mathbb{R}^{n\times r},$$

where $L$ is a positive constant. In other words, $\mathbf{U}_t$ is the minimum point of $f(\mathbf{U})$.

*Proof:* Let us denote the error function $e_t(\mathbf{U}) = g_t(\mathbf{U}) - f_t(\mathbf{U})$.

Due to $g_t(\mathbf{U}_t) \xrightarrow{a.s.} f_t(\mathbf{U}_t)$ when $t \to \infty$, we have $\nabla e_t(\mathbf{U}_t) = \mathbf{0}$ and hence the following inequality

$$\|\nabla e_t(\mathbf{U})\| \le \frac{L}{2}\|\mathbf{U} - \mathbf{U}_t\|_F.$$

It is therefore that

$$\frac{|e_t(\mathbf{U}) - e_t(\mathbf{U}_t)|}{\|\mathbf{U} - \mathbf{U}_t\|_F} \le \frac{L}{2}\|\mathbf{U} - \mathbf{U}_t\|_F,$$

thanks to the mean value theorem. In other word, we have $|e_t(\mathbf{U})| \leq \frac{L}{2}\|\mathbf{U}-\mathbf{U}_t\|_F^2$ because of $e_t(\mathbf{U}_t) \overset{a.s.}{\to} 0$.

In addition, for all $\mathbf{U} \in \mathbb{R}^{n\times r}$, we always have $f_t(\mathbf{U}_t) \leq g_t(\mathbf{U})$. Therefore, we can conclude the corollary as follows

$$\begin{aligned} f_t(\mathbf{U}_t) &\leq g_t(\mathbf{U}_t) = f_t(\mathbf{U}) + e_t(\mathbf{U}) \\ &\leq f_t(\mathbf{U}) + \frac{L}{2}\|\mathbf{U}-\mathbf{U}_t\|_F^2. \end{aligned}$$

It ends the proof.

## V. Experiments

In this section, we evaluate the performance of the proposed algorithm by comparing it to the state-of-the-art in three scenarios relative to: robust subspace tracking, robust matrix completion and video background-foreground separation respectively. In particular, extensive experiments on simulated data are conducted to demonstrate the convergence and robustness of our PETRELS-ADMM algorithm for subspace tracking and matrix completion. While four real video sequences are used to illustrate the effectiveness of PETRELS-ADMM for background-foreground separation.

### A. Robust Subspace Tracking

In the following experiments, data $\mathbf{x}_t$ at each time $t$ is generated randomly using the standard signal model as in (1)

$$\mathbf{x}_t = \mathbf{P}_t(\mathbf{U}\boldsymbol{\omega}_t + \mathbf{n}_t + \mathbf{s}_t),$$

where $\mathbf{U} \in \mathbb{R}^{n\times r}$ denotes a mixing matrix, $\boldsymbol{\omega}_t$ is a random vector living on $\mathbb{R}^r$ space (i.e., $\boldsymbol{\ell}_t = \mathbf{U}\boldsymbol{\omega}_t$) and they are Gaussian i.i.d. of pdf $\mathcal{N}(0,1)$; $\mathbf{n}_t$ represents the white Gaussian noise $\mathcal{N}(0,\sigma^2)$, with $\text{SNR} = -10\log_{10}(\sigma^2)$ is the signal-to-noise ratio to control the impact of noise on algorithm performance; and $\mathbf{s}_t$ is uniform i.i.d. over $[0, \text{fac-outlier}]$ given the magnitude fac-outlier of outliers that aim to create a space for outliers. Indices of missing entries and outliers are generated randomly using the Bernoulli model with the probability $\omega_{\text{missing}}$ and $\omega_{\text{outlier}}$ respectively. The two probabilities represent the density of missing entries and outliers in the data.

In order to evaluate the subspace estimation accuracy, we use the subspace estimation performance (SEP) [19] metric

$$\text{SEP} = \frac{1}{L}\sum_{i=1}^{L} \frac{\text{tr}\left\{\mathbf{U}_{\text{es-i}}^{\#}(\mathbf{I}-\mathbf{U}_{\text{ex}}\mathbf{U}_{\text{ex}}^{\#})\mathbf{U}_{\text{es-i}}\right\}}{\text{tr}\left\{\mathbf{U}_{\text{es-i}}^{\#}(\mathbf{U}_{\text{ex}}\mathbf{U}_{\text{ex}}^{\#})\mathbf{U}_{\text{es-i}}\right\}},$$

where $L$ is the number of independent runs, $\mathbf{U}_{\text{ex}}$ and $\mathbf{U}_{\text{es-i}}$ are the true and the estimated subspaces at the $i$-th run respectively. Particularly, the denominator measures the sum of the squares of the cosines of the principal angles between $\mathbf{U}_{\text{es-i}}$ and $\mathbf{U}_{\text{ex}}$, while the numerator evaluates the similar sum but for the two subspaces $\mathbf{U}_{\text{es-i}}$ and the orthogonal complement $\mathbf{U}_{\text{ex}}^{\perp}$. Accordingly, the lower SEP is, the better the algorithm performance is.

State-of-the-art algorithms for comparison are: GRASTA [15], ROSETA [18] and PETRELS-CFAR [19], ReProCS [20] and NORST [21]. Throughout our experiments, their algorithm parameters are set by default as mentioned in the algorithms. In particular, we set a penalty parameter $\rho = 1.8$ and a constant step-size scale $C = 2$ in GRASTA. An adaptive step size of ROSETA is initialized at $\mu_0 = \frac{C}{1+\eta_0}$ with $C = 8$ and $\eta_0 = 99$, while two thresholds for controlling the step size are set at $\eta_{\text{low}} = 50$ and $\eta_{\text{high}} = 100$. PETRELS-CFAR includes a forgetting factor set at $\lambda = 0.999$, a window size $N_w = 150$ and a false alarm probability $P_{\text{fa}}$ varied from $[0.1, 0.7]$ depended on the outlier intensity. Both ReProCS and NORST require several predefined parameters, including $t_{\text{train}} = 200$ data samples, $\alpha = 60, K = 33$ and $\omega_{eval} = 7.8\times 10^{-4}$. For our algorithm, we set the penalty parameters at 1.5, the regularization parameter $\alpha = 0.1$ and the step-size threshold $\eta = \sin(\pi/3)$, while the maximum number of iterations for outlier detection phase is fixed at $K = 50$. Matlab codes are available online.[7] The experimental results are averaged over 100 independent runs.

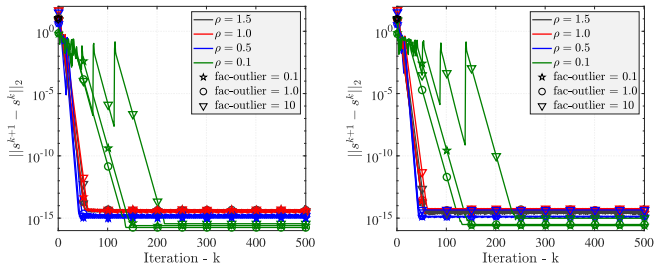


(a) SNR $= 0$ dB. (b) SNR $= 10$ dB.

Fig. 2. Convergence of PETRELS-ADMM in terms of the variation $\|\mathbf{s}^{k+1} - \mathbf{s}^k\|_2$: $n = 50, r = 2$, 90% entries observed, and outlier density $\omega_{\text{outlier}} = 0.1$.

*1) Convergence of PETRELS-ADMM:* To demonstrate the convergence of our algorithm, we use a synthetic data whose number of row $n = 50$, rank $r = 2$, and 5000 vector samples with 90% entries observed on average. Specifically, the outlier density $\omega_{\text{outlier}}$ is varied from 0.05 to 0.4, while the outlier intensity is set at three values representing a low, medium and high level (i.e., fac-outlier $= 0.1, 1$ and 10 respectively). The penalty parameter $\rho$ varies in the range [0.1,1.5]. Also, two noise levels are considered, with SNR $\in \{0, 10\}$ dB. The results are shown as in Fig. 2 and Fig. 3.

Fig. 2 shows the convergence behavior of PETRELS-ADMM w.r.t the two variables: fac-outlier and the weight $\rho$. We can see that, the variation of $\{\mathbf{s}^k\}_{k\geq 1}$ always converges in all testing cases. When the penalty parameter $\rho \geq 0.5$, the convergence rate is fast, i.e. the variation $\|\mathbf{s}^{k+1} - \mathbf{s}^k\|_2$ can converge in 50 iterations in both low- and high-noise cases. The results are practical evidences of Lemma 1. Similarly, Fig. 3 shows that the convergence of the variations of the sequence $\{\mathbf{U}_t\}_{t\geq 0}$, generated by PETRELS- ADMM follows the theoretical behavior proved in Lemma 2, that is, $\|\mathbf{U}_t - \mathbf{U}_{t+1}\|_F \overset{a.s.}{\to} \mathcal{O}(\frac{1}{t})$ almost surely.

[7] GRASTA: https://sites.google.com/site/hejunzz/grasta ROSETA: http://www.merl.com/research/license#ROSETA ReProCS: https://github.com/praneethmurthy/ReProCS Our code: https://avitech.uet.vnu.edu.vn/en/petrels-admm

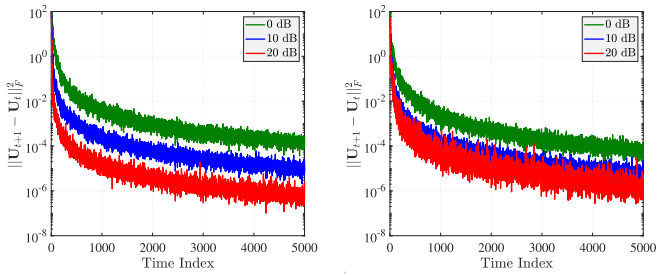


(a) Outlier density $\omega_{\text{outlier}} = 0.05$. (b) Outlier density $\omega_{\text{outlier}} = 0.4$.

Fig. 3. Convergence of PETRELS-ADMM in terms of the variation $\|\mathbf{U}_{t+1} - \mathbf{U}_t\|_F$: $n = 50, r = 2$, 90% entries observed and outlier intensity fac-outlier $= 10$.

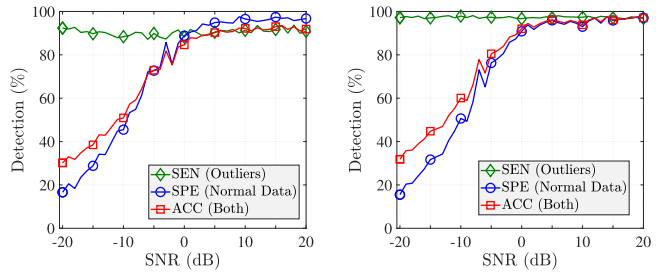


(a) fac-outlier $= 1$. (b) fac-outlier $= 10$.

Fig. 4. Outlier detection accuracy versus the noise level: $n = 50, r = 2, 80\%$ entries observed, and 20% outliers.

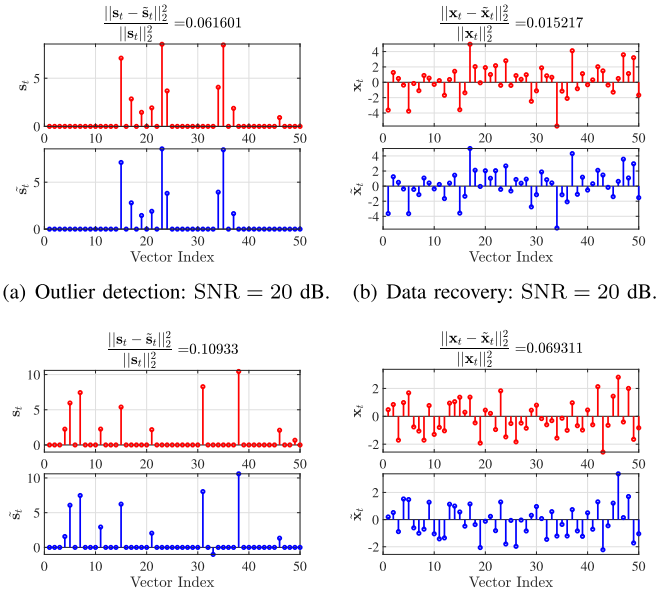


(a) Outlier detection: SNR $= 20$ dB. (b) Data recovery: SNR $= 20$ dB.

(c) Outlier detection: SNR $= 10$ dB. (d) Data recovery: SNR $= 10$ dB.

Fig. 5. Outlier detection and data reconstruction: $n = 50, r = 2, 90\%$ entries observed, outlier intensity fac-outlier $= 1$, and outlier density $\omega_{\text{outlier}} = 0.1$.

*2) Outlier Detection:* Following the above experiment, we next assess the ability of PETRELS-ADMM for outlier detection against the noise level. The three statistical metrics including Sensitivity (SEN) and Specificity (SEP) and Accuracy (ACC) are used to evaluate its outlier detection performance [42]. Particularly, SEN measures the percentage of outliers detected correctly over the total outliers in the measurement data. SEP is similar to SEN, but for normal entries and ACC indicates how the estimator makes the correct detection. We use the same data above, but 20% of the observations are missing. The outlier density $\omega_{\text{outlier}}$ is set at 0.2, while two intensity levels are considered, with fac-outlier $\in \{1, 10\}$.

Fig. 4 illustrates the outlier detection performance of PETRELS-ADMM versus the noise level SNR. As can be seen that when we increase the value of SNR from $-20$ dB to 20 dB, the detection accuracy goes up first and then converges towards a constant level. At very low SNRs (i.e., $<0$ dB), the proposed algorithm does not work well in which many normal entries are labeled as outliers, although the number of correctly detected outliers are high. When SNR $>0$ dB, PETRELS-ADMM achieves a competitive prediction accuracy with respect to all three evaluation metrics.

Fig. 5 provides more practical evidences to demonstrate the effectiveness of PETRELS-ADMM for the outlier detection. Particularly, the locations of outliers $\mathbf{s}_t$ are well detected even when the measurement data is corrupted by noise with a moderate SNR value (e.g. 10 dB). Also, amplitude of the outliers is recovered nearly correctly with a small relative error (RE $= \frac{\|\mathbf{s}_t - \tilde{\mathbf{s}}_t\|_2}{\|\mathbf{s}_t\|_2}$) in both cases (e.g. RE $= 0.0616$ at the 20 dB noise level). As a result, the corrupted signals are also well reconstructed, as illustrated in Fig. 5(b) and (d).

*3) Robustness of PETRELS-ADMM:* To investigate the robustness of PETRELS-ADMM, we vary the outlier intensity, density and missing density and then measure the SEP metric. Moreover, we also demonstrate the effectiveness of PETRELS-ADMM against noisy and time-varying environments.

*Impact of outlier intensity on algorithm performance.*

We fix $n = 50$, $r = 2$, 90% entries observed, outlier density $\omega_{\text{outlier}} = 0.1$, SNR$= 20$ dB while varying fac-outlier in the range $[0.1, 10]$. We can see from Fig. 6 that PETRELS-ADMM always outperforms other state-of-the-art algorithms in all testing cases with different fac-outlier values. At low outlier intensity (i.e., fac-outlier $\leq 1$), all algorithms yield good accuracy with fast convergences, though ROSETA and ReProCS obtain the higher SEP (i.e., $\approx 10^{-3}$) as compared to that of the four remaining algorithms. In particular, PETRELS-ADMM provides the best subspace estimation accuracy, i.e., SEP $\approx 10^{-5}$ in both cases (see Fig. 6(a)-(b)). At a high intensity level (e.g. fac-outlier $= 5$ or 10), PETRELS-ADMM again provides the best performance in terms of both convergence rate and accuracy. GRASTA performs similarly to ReProCS and slightly worse than PETRELS-CFAR (i.e., their SEP values are around $10^{-4}$). While ROSETA and NORST fail to recover the underlying subspace in the presence of strong outliers. Note that, in all four experiments above, PETRELS-ADMM always obtains the best SEP value of around $10^{-5}$ and hence is robust to outlier intensity.

*Impact of outlier density on algorithm performance.* We fix $n = 50$, $r = 2$, 90% entries observed, outlier intensity fac-outlier $= 5$, SNR $= 20$ dB while varying the outlier density

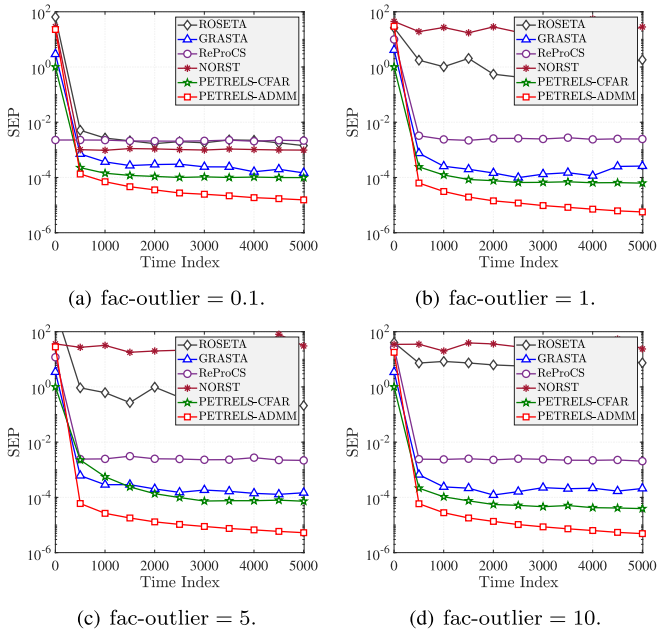


(a) fac-outlier $= 0.1$. (b) fac-outlier $= 1$. (c) fac-outlier $= 5$. (d) fac-outlier $= 10$.

Fig. 6. Impact of outlier intensity on algorithm performance: $n = 50$, $r = 2$, 90% entries observed, outlier density $\omega_{\text{outlier}} = 0.1$, and SNR $= 20$ dB.

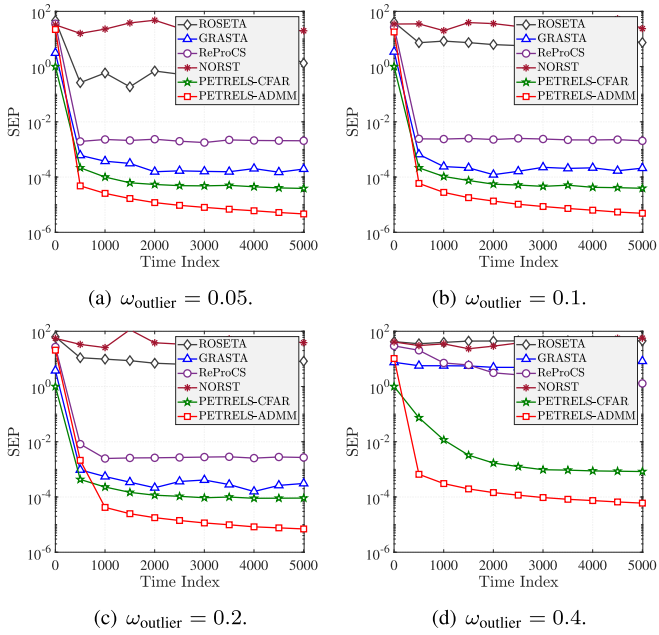


(a) $\omega_{\text{outlier}} = 0.05$. (b) $\omega_{\text{outlier}} = 0.1$. (c) $\omega_{\text{outlier}} = 0.2$. (d) $\omega_{\text{outlier}} = 0.4$.

Fig. 7. Impact of outlier density on algorithm performance: $n = 50$, $r = 2$, 90% entries observed, outlier intensity fac-outlier $= 10$, and SNR $= 20$ dB.

$\omega_{\text{outlier}}$ in the range [0.05, 0.4]. The results are shown as in Fig. 7. PETRELS-ADMM outperforms the four remaining algorithms in this context. In particular, our algorithm performs very well even when the fraction of outliers is high (e.g. $\omega_{\text{outlier}} = 0.4$). By contrast, four algorithms including GRASTA, ROSETA, ReProCS and NORST may fail to track subspace in the case of a high outlier density (see Fig. 7(d)). The PETRELS-CFAR works well but has a lower convergence rate and accuracy in terms of SEP metric as compared to PETRELS-ADMM. When the

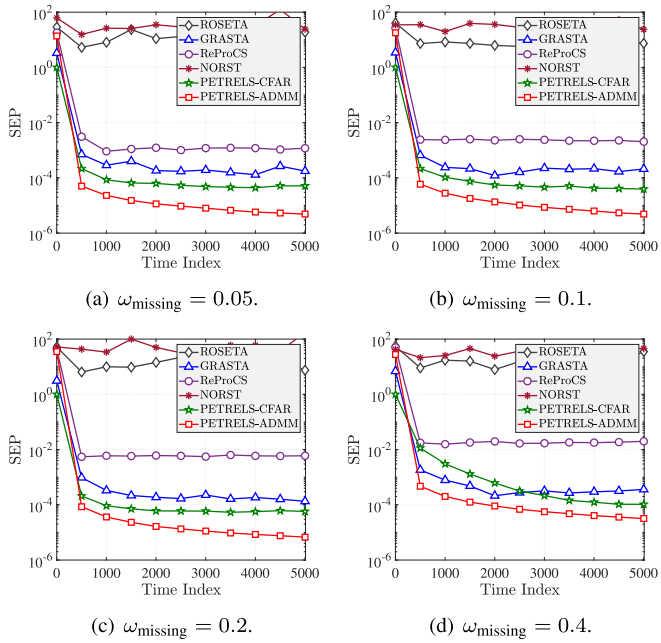


(a) $\omega_{\text{missing}} = 0.05$. (b) $\omega_{\text{missing}} = 0.1$. (c) $\omega_{\text{missing}} = 0.2$. (d) $\omega_{\text{missing}} = 0.4$.

Fig. 8. Impact of the density of missing entries on algorithm performance: $n = 50, r = 2$, outlier density $\omega_{\text{outlier}} = 0.1$, outlier intensity fac-outlier $=$ 10, and SNR $= 20$ dB.

measurement data is corrupted by a smaller number of outliers, PETRELS-ADMM still provides better performance than the others, as shown in Fig. 7 (a)-(c).

*Impact of the density of missing entries on algorithm performance*. Following the above experiments, we change the number of missing entries in the measurement data by varying the probability $\omega_{\text{missing}}$ while fixing the other attributes. The results are reported in Fig. 8 and Fig. 9. In particular, the effect of $\omega_{\text{missing}}$ on algorithm performance is presented in Fig. 8. Similarly, PETRELS-ADMM yields the best performance in four cases of missing observations. Three algorithms including PETRELS-CFAR, GRASTA and ReProCS provide good performance but with slower convergence rate and accuracy, while ROSETA and NORST have failed again in this task due to the high outlier intensity (i.e., fac-outlier $= 10$). As can be seen from Fig. 9(a)–(c) that the state-of-the-art algorithms only perform well when the number of corruptions is smaller than half the number of entries in the data measurement. While PETRELS-ADMM still obtains the reasonable subspace estimation performance in terms of SEP (i.e., $\approx 10^{-3}$) in the case of very high corruptions, see Fig. 9(d).

*Noisy and Time-Varying Environments*. We first investigate the effect of the noise on the performance of PETRELS-ADMM in comparison with the state-of-the-art algorithms. We vary the value of SNR in the range from 0 dB to 20 dB and assess their performance on the same data above. Experimental results are illustrated in Fig. 10. As can be seen that the convergence rate of PETRELS-ADMM is not affected by SNR, but only its estimation accuracy, as shown in Fig. 10(a). Specifically, when we decrease the value of SNR, the estimation error between the true subspace and the estimation increases gradually. At a

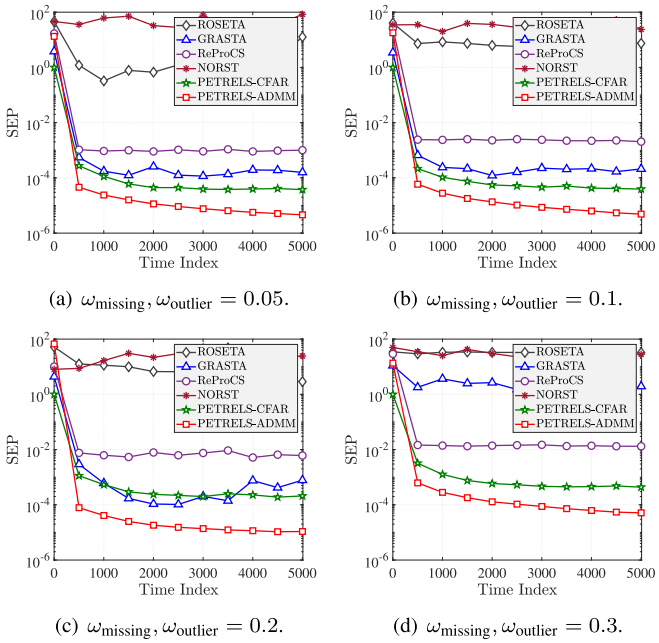


(a) $\omega_{\text{missing}}, \omega_{\text{outlier}} = 0.05$. (b) $\omega_{\text{missing}}, \omega_{\text{outlier}} = 0.1$.

(c) $\omega_{\text{missing}}, \omega_{\text{outlier}} = 0.2$. (d) $\omega_{\text{missing}}, \omega_{\text{outlier}} = 0.3$.

Fig. 9. Impact of the corruption fraction by missing data and outliers on algorithm performance: $n = 50, r = 2$ and fac-outlier $= 10$ and SNR $= 20$ dB.

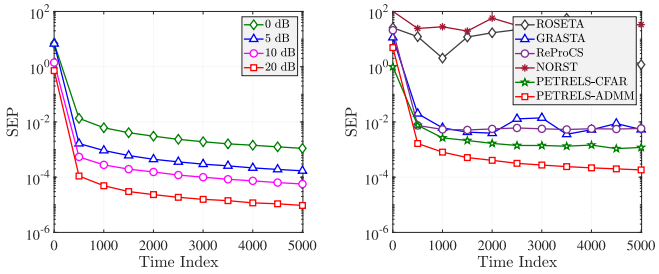


(a) PETRELS-ADMM. (b) SNR $= 5$ dB.

Fig. 10. Impact of the additive noise on algorithm performance: $n = 50, r = 2$, 90% entries observed and 10% outliers with intensity fac-outlier $= 10$.

high SNR level (e.g. 20 dB), previous experiments indicate that PETRELS-ADMM outperforms state-of-the-art algorithms, see Fig. 6-9. At a low SNR level (e.g. 5 dB), PETRELS-ADMM yields the best estimation accuracy as well as convergence rate again, as illustrated in Fig. 10(b). Similar outstanding performance of PETRELS-ADMM were also observed at lower SNR levels of 10, 5 or 0 dB (please see Figs. 8-10 of the supplementary material).

The robustness of PETRELS-ADMM is next investigated against nonstationary and time-varying environments. Particularly, the true subspace $\mathbf{U}$ is supposed to be varying with time under the model $\mathbf{U}_t = (1-\varepsilon)\mathbf{U}_{t-1} + \varepsilon \mathbf{N}_t$, where $\mathbf{N}_t \in \mathbb{R}^{n\times r}$ is a Gaussian noise matrix (zero-mean and unit-variance) and $\varepsilon$ is to control the subspace change which is chosen among $\{10^{-1}, 10^{-2}, 10^{-3}\}$. We use the same signal model as in the previous tasks and 1000 vector samples. Also, we create an abrupt change at $t = 500$ to see how fast the proposed algorithm can converge. We measure the performance of PETRELS-ADMM at

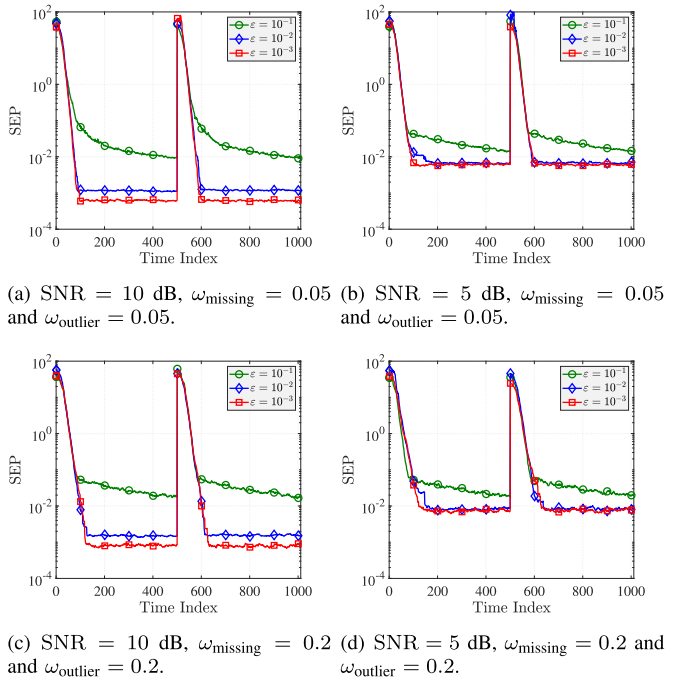


(a) SNR $= 10$ dB, $\omega_{\text{missing}} = 0.05$ and $\omega_{\text{outlier}} = 0.05$. (b) SNR $= 5$ dB, $\omega_{\text{missing}} = 0.05$ and $\omega_{\text{outlier}} = 0.05$.

(c) SNR $= 10$ dB, $\omega_{\text{missing}} = 0.2$ and $\omega_{\text{outlier}} = 0.2$. (d) SNR $= 5$ dB, $\omega_{\text{missing}} = 0.2$ and $\omega_{\text{outlier}} = 0.2$.

Fig. 11. PETRELS-ADMM in time-varying scenarios.

two noise levels (SNR $= 5$ and 10 dB) with different corruption fractions. Experimental results are illustrated in Fig. 11(a)-(d). In the same manner to the effect of the noise, the time-varying factor $\varepsilon$ does not affect the convergence rate of PETRELS-ADMM, but only its subspace estimation. Fig. 11 shows that the estimation accuracy of the proposed algorithm will decrease if the time-varying factor $\varepsilon$ increases. When the underlying subspace varies slowly (e.g. $\varepsilon \leq 10^{-2}$), the resulting values of SEP, which always converge towards an error floor, indicate that PETRELS-ADMM can be robust to slowly time-varying scenarios.

### *B. Robust Matrix Completion*

We compare here the robust matrix completion (RMC) performance using PETRELS-ADMM with GRASTA [15], LRGeomGC [43] and RPCA-GD [44].

The measurement data $\mathbf{X} = \mathbf{P} \circledast (\mathbf{UW} + \mathbf{S} + \mathbf{N})$ used for this task corresponds to the rank-2 matrices of size of $400 \times 400$, where the operator $\circledast$ denotes the Hadamard product. Particularly, we generated the mixing matrix $\mathbf{U} \in \mathbb{R}^{400\times 2}$ and the coefficient matrix $\mathbf{W} \in \mathbb{R}^{2\times 400}$ at random. Their entries were random variables that follow Gaussian distribution with zero mean and unit variance. The measurement data $\mathbf{X}$ was corrupted by a white Gaussian noise $\mathbf{N} \in \mathbb{R}^{400\times 400}$ whose SNR is fixed at 40 dB. In the literature, the SNR value of around 40 dB is used for performance evaluation of completion algorithms due to missing observations and/or outliers at low-noise conditions [45]. The data matrix was affected by different percentages of missing ($\mathbf{P}$) and outliers ($\mathbf{S}$) from $0\% - 90\%$. The location and value of corrupted entries (including missing and outliers) were uniformly distributed.

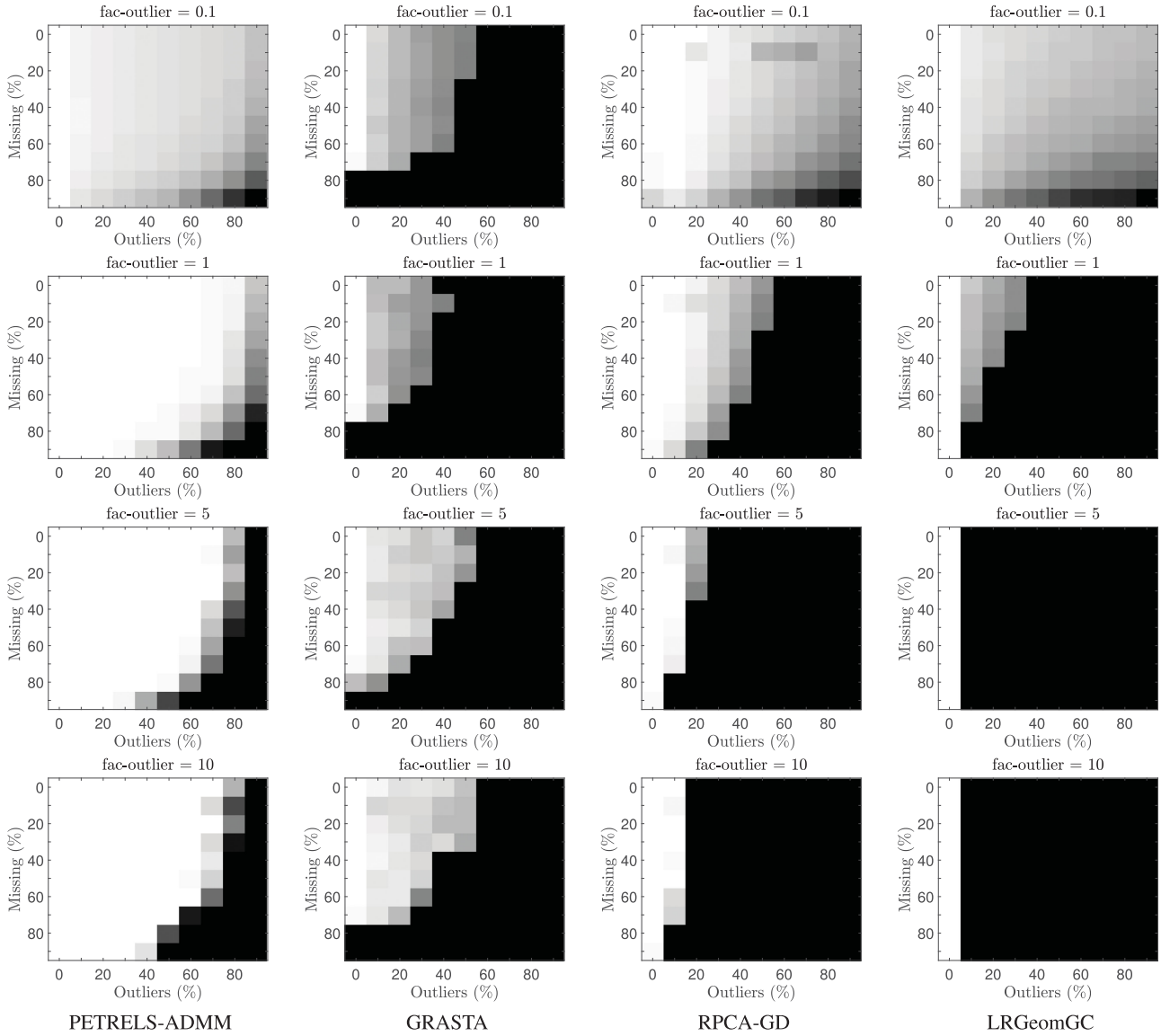


Fig. 12. Effect of outlier intensity on robust matrix completion performance. White color denotes perfect recovery, black color denotes failure and gray colour is in between.

Fig. 12 shows that the proposed algorithm of PETRELS-ADMM based RMC outperforms GRASTA, LRGeomGC and RPCA-GD. At low outlier intensity (i.e., fac-outlier $= 0.1$), PETRELS-ADMM based RMC, LRGeomGC and RCPA-GD provide excellent performance even when the data is corrupted by a very high corruption fraction. At high outlier intensity (i.e., fac-outlier $\geq 1$), PETRELS-ADMM based RMC provides the best matrix reconstruction error performance, GRASTA still retain good performance, while RPCA-GD and LRGeomGC fail to recover corrupted entries.

### C. Video Background/Foreground Separation

We further illustrate the effectiveness of the proposed PETRELS-ADMM algorithm in the application of RST for video background/foreground separation, and compare with GRASTA and PETRELS-CFAR. We use four real video sequences for this task, including `Hall`, `Lobby`, `Sidewalk` and `Highway` datasets. In particular, the two former datasets are from GRASTA's homepage,[8] while the two latter datasets are from `CD.net2012`[9] [46]. The `Hall` dataset consists of 3584 frames of size $174 \times 144$ pixels, while the `Lobby` dataset has 1546 frames of size $144 \times 176$ pixels. The `Sidewalk` dataset includes 1200 frames of size $240 \times 352$ pixels. `Highway dataset` has 1700 frames of size $240 \times 320$ pixels. We can see from Fig. 13, PETRELS-ADMM is capable of detecting objects in video and provides competitive performance as compared to GRASTA and PETRELS-CFAR.

[8]Online. [Available]: https://sites.google.com/site/hejunzz/grasta
[9]Online. [Available]: http://jacarini.dinf.usherbrooke.ca/dataset2012

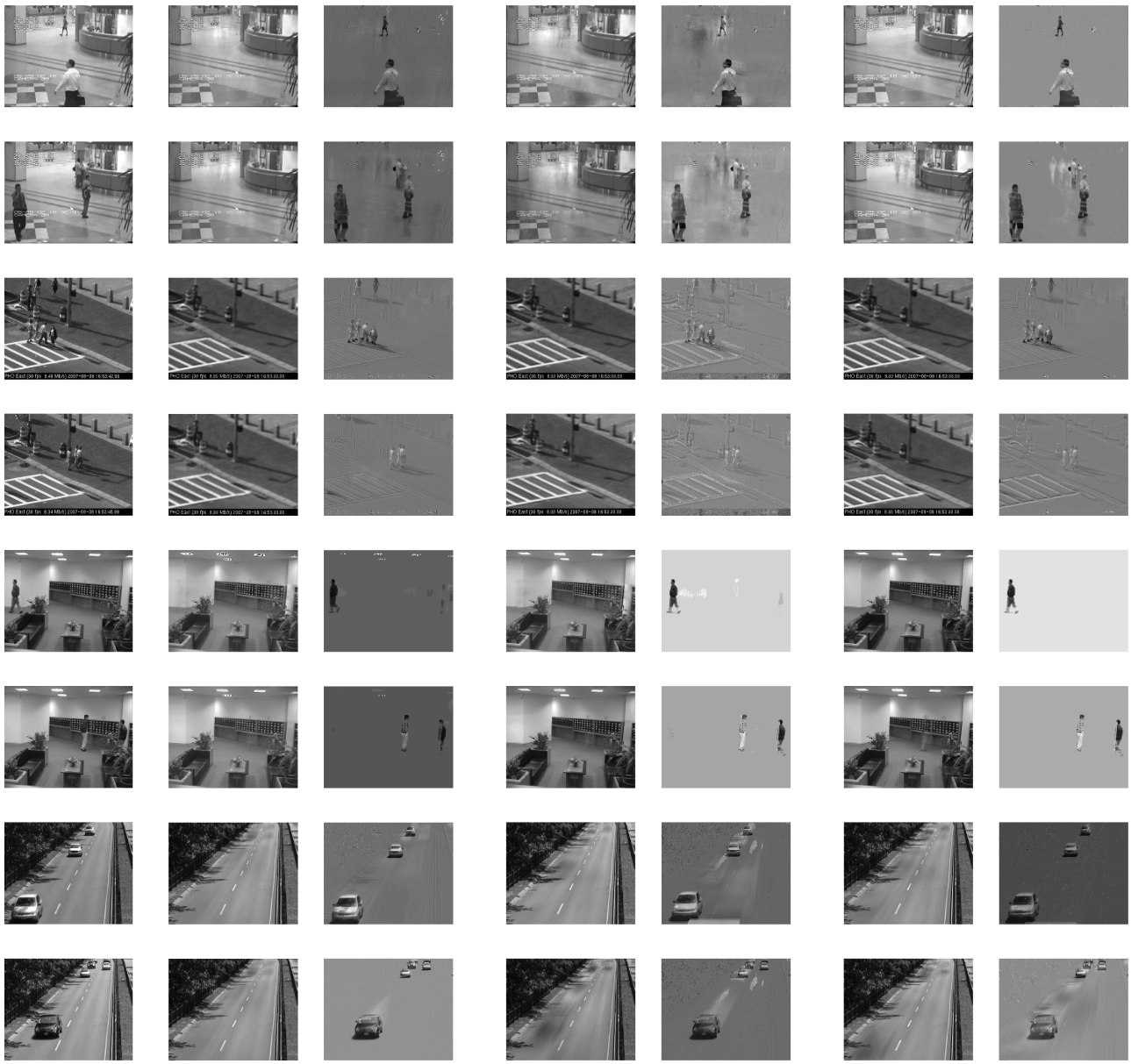


Fig. 13. Qualitative illustration of video background-foreground separation application.

## VI. Conclusion

In this paper, we have proposed an efficient algorithm, namely PETRELS-ADMM, for the robust subspace tracking problem to handle missing data in the presence of outliers. By converting the original RST problem to a surrogate one, which facilitates the tracking ability, we have derived an online implementation for outlier rejection with a low computational complexity and a fast convergence rate while still retaining a high subspace estimation performance. We have established a theoretical convergence which guarantees that the solutions generated by PETRELS-ADMM will converge to a stationary point asymptotically. The simulation results have suggested that our algorithm is more effective than the state-of-the-art algorithms for robust subspace tracking and robust matrix completion. The effectiveness of PETRELS-ADMM was also verified for the problem of video background-foreground separation.

## References

[1] A. Tulay and H. Simon, *Adaptive Signal Processing: Next Generation Solutions*. Hoboken, NJ, USA: John Wiley Sons, 2010.

[2] N. Vaswani, Y. Chi, and T. Bouwmans, "Rethinking PCA for modern data sets: Theory, algorithms, and applications," *Proc. IEEE*, vol. 106, no. 8, pp. 1274–1276, Aug. 2018.

[3] G. H. Golub and C. F. Van Loan, *Matrix Computations*. Baltimore, MD, USA: JHU Press, 2012.

[4] P. Comon and G. H. Golub, "Tracking a few extreme singular values and vectors in signal processing," *Proc. IEEE*, vol. 78, no. 8, pp. 1327–1343, Aug. 1990.

[5] I. T. Jolliffe and J. Cadima, "Principal component analysis: A review and recent developments," *Philos. Trans. Roy. Soc. A*, vol. 374, no. 2065, 2016, Art. no. 20150202.

[6] C. Wang, Y. C. Eldar, and Y. M. Lu, "Subspace estimation from incomplete observations: A high-dimensional analysis," *IEEE J. Sel. Top. Signal Process.*, vol. 12, no. 6, pp. 1240–1252, Dec. 2018.

[7] L. Balzano, Y. Chi, and Y. M. Lu, "Streaming PCA and subspace tracking: The missing data case," *Proc. IEEE*, vol. 106, no. 8, pp. 1293–1310, Aug. 2018.

[8] N. Vaswani, T. Bouwmans, S. Javed, and P. Narayanamurthy, "Robust subspace learning: Robust PCA, robust subspace tracking, and robust subspace recovery," *IEEE Signal Process. Mag.*, vol. 35, no. 4, pp. 32–55, Jul. 2018.

[9] M. Mardani, G. Mateos, and G. B. Giannakis, "Subspace learning and imputation for streaming big data matrices and tensors," *IEEE Trans. Signal Process.*, vol. 63, no. 10, pp. 2663–2677, May 2015.

[10] V. Nguyen, K. Abed-Meraim, N. Linh-Trung, and R. Weber, "Generalized minimum noise subspace for array processing," *IEEE Trans. Signal Process.*, vol. 65, no. 14, pp. 3789–3802, Jul. 2017.

[11] S. Haghighatshoar and G. Caire, "Low-complexity massive MIMO subspace estimation and tracking from low-dimensional projections," *IEEE Trans. Signal Process.*, vol. 66, no. 7, pp. 1832–1844, Apr. 2018.

[12] S. Buzzi and C. D'Andrea, "Subspace tracking and least squares approaches to channel estimation in millimeter wave multiuser MIMO," *IEEE Trans. Commun.*, vol. 67, no. 10, pp. 6766–6780, Oct. 2019.

[13] L. Balzano, R. Nowak, and B. Recht, "Online identification and tracking of subspaces from highly incomplete information," in *Proc. Ann. Allerton Conf. Commun., Cont. Comput.*, 2010, pp. 704–711.

[14] D. Zhang and L. Balzano, "Global convergence of a grassmannian gradient descent algorithm for subspace estimation." in *Proc. Int. Conf. Art. Intel. Stat.*, Cadiz, Spain, 2016, pp. 1460–1468.

[15] J. He, L. Balzano, and A. Szlam, "Incremental gradient on the grassmannian for online foreground and background separation in subsampled video," in *Proc. IEEE Comput. Soc. Conf. Comput. Vis. Pattern Recognit.*, 2012, pp. 1568–1575.

[16] Y. Chi, Y. C. Eldar, and R. Calderbank, "PETRELS: Parallel subspace estimation and tracking by recursive least squares from partial observations," *IEEE Trans. Signal Process.*, vol. 61, no. 23, pp. 5947–5959, Dec. 2013.

[17] B. Yang, "Projection approximation subspace tracking," *IEEE Trans. Signal Process.*, vol. 43, no. 1, pp. 95–107, Jan. 1995.

[18] H. Mansour and X. Jiang, "A robust online subspace estimation and tracking algorithm," in *Proc. IEEE Int. Conf. Acoust. Speech Signal Process.*, 2015, pp. 4065–4069.

[19] N. Linh-Trung, V. D. Nguyen, M. Thameri, T. Minh-Chinh, and K. Abed-Meraim, "Low-complexity adaptive algorithms for robust subspace tracking," *IEEE J. Sel. Top. Signal Process.*, vol. 12, no. 6, pp. 1197–1212, Dec. 2018.

[20] P. Narayanamurthy and N. Vaswani, "Provable dynamic robust PCA or robust subspace tracking," *IEEE Trans. Inf. Theory*, vol. 65, no. 3, pp. 1547–1577, Mar. 2019.

[21] P. Narayanamurthy, V. Daneshpajooh, and N. Vaswani, "Provable subspace tracking from missing data and matrix completion," *IEEE Trans. Signal Process.*, vol. 67, no. 16, pp. 4245–4260, Aug. 2019.

[22] C. Hage and M. Kleinsteuber, "Robust PCA and subspace tracking from incomplete observations using $\ell_0$-surrogates," *Comput. Stat.*, vol. 29, no. 3-4, pp. 467–487, 2014.

[23] S. Chouvardas, Y. Kopsinis, and S. Theodoridis, "Robust subspace tracking with missing entries: The set-theoretic approach," *IEEE Trans. Signal Process.*, vol. 63, no. 19, pp. 5060–5070, Oct. 2015.

[24] A. Gonen, D. Rosenbaum, Y. C. Eldar, and S. Shalev-Shwartz, "Subspace learning with partial information," *J. Mach. Learn. Res.*, vol. 17, no. 1, pp. 1821–1841, 2016.

[25] P. V. Giampouras, A. A. Rontogiannis, K. E. Themelis, and K. D. Koutroumbas, "Online sparse and low-rank subspace learning from incomplete data: A Bayesian view," *Signal Process.*, vol. 137, pp. 199–212, 2017.

[26] L. T. Thanh, V.-D. Nguyen, N. Linh-Trung, and K. Abed-Meraim, "Robust subspace tracking with missing data and outliers via ADMM," *in Eur. Signal Process. Conf.*, 2019, pp. 1–5.

[27] M. Shor and N. Levanon, "Performances of order statistics CFAR," *IEEE Trans. Aerosp. Electron. Syst.*, vol. 27, no. 2, pp. 214–224, Mar. 1991.

[28] J. A. Tropp, "Just relax: Convex programming methods for identifying sparse signals in noise," *IEEE Trans. Inf. Theory*, vol. 52, no. 3, pp. 1030–1051, Mar. 2006.

[29] S. Boyd *et al.*, "Distributed optimization and statistical learning via the alternating direction method of multipliers," *Found. Trends Mach. Learn.*, vol. 3, no. 1, pp. 1–122, 2011.

[30] E. Ghadimi, A. Teixeira, I. Shames, and M. Johansson, "Optimal parameter selection for the alternating direction method of multipliers (ADMM): Quadratic problems," *IEEE Trans. Auto. Cont.*, vol. 60, no. 3, pp. 644–658, Mar. 2015.

[31] Y. Xu, M. Liu, Q. Lin, and T. Yang, "ADMM without a fixed penalty parameter: Faster convergence with new adaptive penalization," in *Proc. Adv. Neural Inf. Process. Syst.*, 2017, pp. 1267–1277.

[32] W. Tian and X. Yuan, "An alternating direction method of multipliers with a worst-case $\mathcal{O}(1/n^2)$ convergence rate," *Math. Comput.*, vol. 88, no. 318, pp. 1685–1713, 2019.

[33] N. Parikh *et al.*, "Proximal algorithms," *Found. Trends Optim.*, vol. 1, no. 3, pp. 127–239, 2014.

[34] W. W. Hager, "Updating the inverse of a matrix," *SIAM Rev.*, vol. 31, no. 2, pp. 221–239, 1989.

[35] J. Mairal, F. Bach, J. Ponce, and G. Sapiro, "Online learning for matrix factorization and sparse coding," *J. Mach. Learn. Res.*, vol. 11, no. Jan, pp. 19–60, 2010.

[36] J. Feng, H. Xu, and S. Yan, "Online robust PCA via stochastic optimization," in *Proc. Adv. Neural Inf. Process. Syst.*, 2013, pp. 404–412.

[37] J. Shen, H. Xu, and P. Li, "Online optimization for max-norm regularization," *Machi. Learn.*, vol. 106, no. 3, pp. 419–457, 2017.

[38] G. Li and T. K. Pong, "Global convergence of splitting methods for nonconvex composite optimization," *SIAM J. Optim.*, vol. 25, no. 4, pp. 2434–2460, 2015.

[39] Y. Wang, W. Yin, and J. Zeng, "Global convergence of ADMM in nonconvex nonsmooth optimization," *J. Sci. Comput.*, vol. 78, no. 1, pp. 29–63, 2019.

[40] L. Bottou, *On-Line Learning and Stochastic Approximations*. Cambridge, U.K.: Cambridge Univ. Press, 1999.

[41] A. W. Van der Vaart, *Asymptotic Statistics*. Cambridge, U.K.: Cambridge Univ. Press, 2000.

[42] D. M. Powers, "Evaluation: From precision, recall and f-measure to ROC, informedness, markedness and correlation," *J. Mach. Learn. Tech.*, vol. 2, no. 1, pp. 37–63, 2011.

[43] B. Vandereycken, "Low-rank matrix completion by riemannian optimization," *SIAM J. Optim.*, vol. 23, no. 2, pp. 1214–1236, 2013.

[44] X. Yi, D. Park, Y. Chen, and C. Caramanis, "Fast algorithms for robust PCA via gradient descent," in *Proc. Adv. Neural Inf. Process. Syst.*, 2016, pp. 4152–4160.

[45] L. T. Nguyen, J. Kim, and B. Shim, "Low-rank matrix completion: A contemporary survey," *IEEE Access*, vol. 7, pp. 94 215–94 237, 2019.

[46] N. Goyette, P. Jodoin, F. Porikli, J. Konrad, and P. Ishwar, "Changedetection.net: A. new change detection benchmark dataset," in *Proc. IEEE Conf. Comput. Vis. Pattern Recognit.*, 2012, pp. 1–8.


**Le Trung Thanh** received the B.Sc. and M.Sc. degrees in electronics and telecommunications from VNU University of Engineering and Technology, Vietnam National University, Hanoi (VNU), Vietnam, in 2016 and 2018, respectively. He is currently working toward the Ph.D. degree with the University of Orleans, Orléans, France.

His research interests include signal processing, subspace tracking, tensor analysis, and system identification.

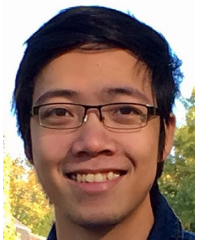

**Nguyen Viet Dung** (Member, IEEE) received the B.Sc. degree in electronics and telecommunication engineering from VNU University of Engineering and Technology, Vietnam National University, Hanoi (VNU) in 2009, the M.Sc. degree in networks and telecommunications from École Normale Supérieure de Cachan, Université Paris XI (currently, University of Paris-Saclay, France), Orsay, France, in 2012, and the Ph.D. degree in signal processing from the University of Orleans, Orléans, France, in 2016.

From 2017 to 2018, he was a Postdoc with CentraleSupélec, University of Paris-Saclay. Since 2019, he has been a Research Engineer with Lab-STICC, UMR 6285 CNRS ENSTA Bretagne, Brest, France. His research interests include channel modelling in array signal processing, adaptive matrix and tensor analysis, blind source separation, and statistical performance analysis.

**Nguyen Linh Trung** (Senior Member, IEEE) received the B.Eng. and Ph.D. degrees in electrical engineering from the Queensland University of Technology, Brisbane, QLD, Australia, in 1998 and 2005, respectively.

Since 2006, he has been with the Faculty of VNU University of Engineering and Technology, Vietnam National University, Hanoi (VNU), where he is currently an Associate Professor of electronic engineering with the Faculty of Electronics and Telecommunications and the Director of the Advanced Institute of Engineering and Technology. His research focuses on signal processing methods, including time-frequency signal analysis, blind processing, adaptive filtering, compressive sampling, tensor-based signal analysis, graph signal processing, and apply them to wireless communication, networking, and biomedical engineering.

**Karim Abed-Meraim** (Fellow, IEEE) was born in 1967. He received the State Engineering degree from Ecole Polytechnique, Palaiseau, France, in 1990, the State Engineering degree from Ecole Nationale Supérieure des Télécommunications (ENST), Paris, France, in 1992, the M.Sc. degree from Paris XI University, Orsay, France, in 1992, and the Ph.D. degree from the ENST in 1995 in the field of signal processing and communications.

From 1995 to 1998, he was a Research Staff with the Electrical Engineering Department of the University of Melbourne, Melbourne, VIC, Australia, where he worked on several research project related to "Blind System Identification for Wireless Communications," "Blind Source Separation," and "Array Processing for Communications,". From 1998 to 2012, he has been an Assistant and Associate Professor with the Signal and Image Processing Department of Telecom-ParisTech. He is the author of more than 450 scientific publications including book chapters, international journal and conference papers and patents. His research interests include signal processing for communications, adaptive filtering and tracking, array processing, and statistical performance analysis. In September 2012, he joined the PRISME Laboratory, University of Orleans, Orleans, France, as a Full Professor.

Prof. Abed-Meraim is an IEEE SAM-TC member and the Past Associate Editor for the IEEE TRANSACTIONS ON SIGNAL PROCESSING.

# Supplementary Material to "Robust Subspace Tracking with Missing Data and Outliers: Novel Algorithm with Convergence Guarantee"

Le Trung Thanh, Nguyen Viet Dung, *Member, IEEE*, Nguyen Linh Trung, *Senior Member, IEEE* and Karim Abed-Meraim, *Fellow, IEEE*

## I. Proof of Lemma 1

Follow the line as in previous convergence analysis of ADMM algorithms [1], [2], we can derive the proof of Lemma 1 as follows:

(P-1) The minimizer $\mathbf{u}^{k+1}$ defined in (15) in the main manuscript satisfies

$$\mathcal{L}(\mathbf{s}^k, \mathbf{u}^{k+1}, \mathbf{r}^k, \mathbf{w}^k, \mathbf{e}^k) \leq \mathcal{L}(\mathbf{s}^k, \mathbf{u}^k, \mathbf{r}^k, \mathbf{w}^k, \mathbf{e}^k) - \frac{1+\rho_1}{2}\|\mathbf{u}^k - \mathbf{u}^{k+1}\|_2^2. \tag{1}$$

In particular, the $\mathbf{u}$-update in fact minimizes the following objective function at the $k$-th iteration, as

$$\mathbf{u}^{k+1} \triangleq \underset{\mathbf{u}}{\operatorname{argmin}}\, \mathcal{L}_{\mathbf{u},k}(\mathbf{u}, .) = \frac{1+\rho_1}{2}\,\|\mathbf{u}\|_2^2 - [\mathbf{P}_t(\mathbf{x}_t - \mathbf{U}_{t-1}\mathbf{w}) - \rho_1(\mathbf{s}^k - \mathbf{r}^k)]^\top \mathbf{u}. \tag{2}$$

The function $\mathcal{L}_{\mathbf{u},k}(\mathbf{u}, .)$ w.r.t the variable $\mathbf{u}$ in (2) is strongly convex with a positive constant $(1+\rho_1)$, i.e., the Hessian of $\mathcal{L}_{\mathbf{u},k}(\mathbf{u}, .)$ is given by

$$\nabla^2 \mathcal{L}_{\mathbf{u},k}(\mathbf{u}, .) = (1+\rho_1)\mathbf{I}.$$

Since $\mathbf{u}^{k+1} = \underset{\mathbf{u}}{\operatorname{argmin}}\, \mathcal{L}_{\mathbf{u},k}(\mathbf{u}, .)$, we have the fact $\mathcal{L}_{\mathbf{u},k}(\mathbf{u}^{k+1}, .) \leq \mathcal{L}_{\mathbf{u},k}(\mathbf{u}^k, .)$. Therefore, we obtain the following inequality

$$\mathcal{L}_{\mathbf{u},k}(\mathbf{u}^{k+1}, .) \leq \mathcal{L}_{\mathbf{u},k}(\mathbf{u}^k, .) - \frac{1+\rho_1}{2}\|\mathbf{u}^{k+1} - \mathbf{u}^k\|_2^2. \tag{3}$$

(P-2) The minimizer $\mathbf{s}^{k+1}$ defined in (16) in the main manuscript satisfies

$$\mathcal{L}(\mathbf{s}^{k+1}, \mathbf{u}^{k+1}, \mathbf{r}^k, \mathbf{w}^k, \mathbf{e}^k) \leq \mathcal{L}(\mathbf{s}^k, \mathbf{u}^{k+1}, \mathbf{r}^k, \mathbf{w}^k, \mathbf{e}^k) - c_s\|\mathbf{s}^k - \mathbf{s}^{k+1}\|_2^2, \tag{4}$$

with a positive constant $c_s$.

In particular, at the $k$-th iteration, the variable $\mathbf{s}$ is updated by minimizing the objective function $\mathcal{L}_{\mathbf{s},k}(\mathbf{s}, .)$ as

$$\mathbf{s}^{k+1} \triangleq \underset{\mathbf{s}}{\operatorname{argmin}}\, \mathcal{L}_{\mathbf{s},k}(\mathbf{s}, .) = \rho\,\|\mathbf{s}\|_1 + \frac{\rho_1}{2}\|\mathbf{s} - (\mathbf{u}^{k+1} + \mathbf{r}^k)\|_2^2. \tag{5}$$

Le Trung Thanh is with the University of Engineering and Technology, Vietnam National University, Hanoi, Vietnam, and the PRISME Laboratory, University of Orléans, Orléans, France. Email: thanhletrung@vnu.edu.vn, trung-thanh.le@univ-orleans.fr.

Nguyen Viet Dung is with the University of Engineering and Technology, Vietnam National University, Hanoi and the National Institute of Advanced Technologies of Brittany (ENSTA Bretagne), Brest, France. Email: dungnv@vnu.edu.vn, viet.nguyen@ensta-bretagne.fr.

Nguyen Linh Trung (corresponding author) is with the University of Engineering and Technology, Vietnam National University, Hanoi. E-mail: linhtrung@vnu.edu.vn.

Karim Abed-Meraim is with the PRISME Laboratory, University of Orléans, France. Email: karim.abed-meraim@univ-orleans.fr.

This work was funded by the National Foundation for Science and Technology Development (NAFOSTED) of Vietnam under grant number 102.04-2019.14.

Because the two functions of the $\ell_1$-norm $\|\mathbf{s}\|_1$ and $\ell_2$-norm $\left\|\mathbf{s}-(\mathbf{u}^{k+1}+\mathbf{r}^k)\right\|_2^2$ are convex, so the $\mathcal{L}_{\mathbf{s},k}(\mathbf{s},.)$ in (5) w.r.t. $\mathbf{s}$ is also convex. It is therefore that for any $\mathbf{s}^k, \mathbf{s}^{k+1} \in \mathbf{R}^n$, we always have

$$\mathcal{L}_{\mathbf{s},k}(\mathbf{s}^k,.) \geq \mathcal{L}_{\mathbf{s},k}(\mathbf{s}^{k+1},.) + \langle \mathbf{s}^k - \mathbf{s}^{k+1}, \nabla\mathcal{L}_{\mathbf{s},k}(\mathbf{s}^{k+1},.)\rangle + \frac{1}{2}\|\mathbf{s}^{k+1}-\mathbf{s}^k\|_2^2. \tag{6}$$

Since $\mathbf{s}^{k+1} = \underset{\mathbf{s}}{\operatorname{argmin}}\, \mathcal{L}_{\mathbf{s},k}(\mathbf{s},.)$, the first derivative $\nabla\mathcal{L}_{\mathbf{s},k}(\mathbf{s}^{k+1},.) = \mathbf{0}$, and hence the inequality

$$\mathcal{L}_{\mathbf{s},k}(\mathbf{s}^{k+1},.) \leq \mathcal{L}_{\mathbf{s},k}(\mathbf{s}^k,.) - \frac{1}{2}\|\mathbf{s}^{k+1}-\mathbf{s}^k\|_2^2.$$

As a result, we have

$$\sum_{k=1}^{K}\frac{1}{2}\|\mathbf{s}^{k+1}-\mathbf{s}^k\|_2^2 \leq \sum_{i=1}^{K}\mathcal{L}_{\mathbf{s},k}(\mathbf{s}^k,.) - \mathcal{L}_{\mathbf{s},k}(\mathbf{s}^{k+1},.) = \mathcal{L}_{\mathbf{s},k}(\mathbf{s}^1,.) - \mathcal{L}_{\mathbf{s},k}(\mathbf{s}^{K+1},.). \tag{7}$$

Let $K \to \infty$, we then have

$$\sum_{k=1}^{\infty}\|\mathbf{s}^{k+1}-\mathbf{s}^k\|_2^2 < \infty. \tag{8}$$

It ends the proof of (P-2).

(P-3) The minimizer $\mathbf{r}^{k+1}$ defined in (14) satisfies

$$\mathcal{L}(\mathbf{s}^{k+1},\mathbf{u}^{k+1},\mathbf{r}^{k+1},\mathbf{w}^k,\mathbf{e}^k) \leq \mathcal{L}(\mathbf{s}^{k+1},\mathbf{u}^{k+1},\mathbf{r}^k,\mathbf{w}^k,\mathbf{e}^k) - c_r\|\mathbf{r}^k-\mathbf{r}^{k+1}\|_2^2. \tag{9}$$

Follow the $\mathbf{r}$-update in (14), it is easy to verify that

$$\begin{aligned}\mathcal{L}(\mathbf{s}^{k+1},\mathbf{u}^{k+1},\mathbf{r}^{k+1},\mathbf{w}^k,\mathbf{e}^k) &= \rho_1(\mathbf{r}^k-\mathbf{s}^{k+1}+\mathbf{u}^{k+1})^\top(\mathbf{u}^{k+1}-\mathbf{s}^{k+1}) + A\\ &= \rho_1(\mathbf{r}^k)^\top(\mathbf{u}^{k+1}-\mathbf{s}^{k+1}) - \rho_1\|\mathbf{u}^{k+1}-\mathbf{s}^{k+1}\|_2^2 + A\\ &= \mathcal{L}(\mathbf{s}^{k+1},\mathbf{u}^{k+1},\mathbf{r}^k,\mathbf{w}^k,\mathbf{e}^k) - \rho_1\|\mathbf{r}^{k+1}-\mathbf{r}^k\|_2^2,\end{aligned}$$

where $A = g(\mathbf{s}^{k+1}) + h(\mathbf{u}^{k+1}) + \frac{\rho_1}{2}\|\mathbf{u}^{k+1}-\mathbf{s}^{k+1}\|$. It results in (P-3).

(P-4) The minimizer $\mathbf{w}^{k+1}$ defined in (20) satisfies

$$\mathcal{L}(\mathbf{s}^{k+1},\mathbf{u}^{k+1},\mathbf{r}^{k+1},\mathbf{w}^{k+1},\mathbf{e}^k) \leq \mathcal{L}(\mathbf{s}^{k+1},\mathbf{u}^{k+1},\mathbf{r}^{k+1},\mathbf{w}^k,\mathbf{e}^k) - c_w\|\mathbf{w}^k-\mathbf{w}^{k+1}\|_2^2. \tag{10}$$

The $\mathbf{w}$-update minimizes the following objective function

$$\mathbf{w}^{k+1} \triangleq \mathcal{L}_{\mathbf{w},k}(\mathbf{w},.) = \frac{\rho_2}{2}\|\mathbf{P}_t(\mathbf{U}_t\mathbf{w}+\mathbf{s}^{k+1}-\mathbf{x}_t)-\mathbf{e}^k\|_2^2$$

Since $\mathcal{L}_{\mathbf{z},k}(\mathbf{w},.)$ is strongly convex, it implies (P-4) that

$$\mathcal{L}(\mathbf{s}^{k+1},\mathbf{u}^{k+1},\mathbf{r}^{k+1},\mathbf{w}^{k+1},\mathbf{e}^k) \leq \mathcal{L}(\mathbf{s}^{k+1},\mathbf{u}^{k+1},\mathbf{r}^{k+1},\mathbf{w}^k,\mathbf{e}^k) - c_w\|\mathbf{w}^k-\mathbf{w}^{k+1}\|_2^2.$$

with a positive number $c_w$.

(P-5) The minimizer $\mathbf{e}^{k+1}$ defined in (22) satisfies

$$\mathcal{L}(\mathbf{s}^{k+1},\mathbf{u}^{k+1},\mathbf{r}^{k+1},\mathbf{w}^{k+1},\mathbf{e}^{k+1}) \leq \mathcal{L}(\mathbf{s}^{k+1},\mathbf{u}^{k+1},\mathbf{r}^{k+1},\mathbf{w}^{k+1},\mathbf{e}^k) - c_e\|\mathbf{e}^k-\mathbf{e}^{k+1}\|_2^2. \tag{11}$$

Similarly, the Hessian matrix of $\mathcal{L}_{\mathbf{e},k}(\mathbf{e},.)$ is a positive-define matrix, as

$$\nabla^2\mathcal{L}_{\mathbf{e},k}(\mathbf{e},.) = \operatorname{diag}\left(\left[(\mathbf{e}(1)^2+1)^{-3/2},\ldots,(\mathbf{e}(n))^2+1)^{-3/2}\right]\right) + \frac{\rho_2}{2}\mathbf{I}. \tag{12}$$

From the Proposition 2, we have

$$\mathcal{L}_{\mathbf{e},k}(\mathbf{e}^{k+1},.) \leq \mathcal{L}_{\mathbf{e},k}(\mathbf{e}^k,.) - \frac{\rho_2}{2}\left\|\mathbf{e}^{k+1}-\mathbf{e}^k\right\|_2^2. \tag{13}$$

It ends the proof.

## II. Proof of Proposition 2

To prove that $g_t(\mathbf{U})$ is strongly convex, we state the following facts: $g_t(\mathbf{U})$ is continuous and differentiable; its second derivative is a positive semi-definite matrix (i.e., $\nabla^2_{\mathbf{U}} g_t(\mathbf{U}) \geq m\mathbf{I}$); and the domain of $g_t(\mathbf{U})$ is convex. In order to satisfy the Lipschitz condition, we show that the first derivative of $g_t(\mathbf{U})$ is bounded.

*Stage I: Prove that $g_t$ is a strong convex function.*

We show that there exists a positive number $m$ such that

$$|g_t(\mathbf{U}_{t+1}) - g_t(\mathbf{U}_t)| \geq m_1 \left\|\mathbf{U}_{t+1} - \mathbf{U}_t\right\|_F^2. \tag{14}$$

In particular, we state the two claims as follows:

(C-1) $g_t(\mathbf{U})$ is continuous and differentiable.

*Proof.* Given two variables $\mathbf{A}, \mathbf{B} \in \mathcal{U}$ such that $\|\mathbf{A} - \mathbf{B}\|_F^2 < \gamma$ for some positive constant $\gamma$. It is easy to verify that there exists a positive number $\theta$ such that $|g_t(\mathbf{A}) - g_t(\mathbf{B})| < \theta$.
Under the given assumptions, we have the following inequality:

$$\begin{aligned}
|g_t(\mathbf{A}) - g_t(\mathbf{B})| =& \frac{1}{t}\left| \sum_{i=1}^{t} \lambda_i^{t-i} \left\|\mathbf{P}_i(\mathbf{A}\mathbf{w}_i + \mathbf{s}_i - \mathbf{x}_i)\right\|_2^2 - \sum_{i=1}^{t} \lambda_i^{t-i} \left\|\mathbf{P}_i(\mathbf{B}\mathbf{w}_i + \mathbf{s}_i - \mathbf{x}_i)\right\|_2^2 \right| \\
&\leq \frac{1}{t} \sum_{i=1}^{t} \lambda_i^{t-i} \left\|\mathbf{P}_i(\mathbf{A} - \mathbf{B})\mathbf{w}_i\right\|_2 \left\|\mathbf{P}_i(\mathbf{A} + \mathbf{B})\mathbf{w}_i + 2(\mathbf{s}_i - \mathbf{x}_i)\right\|_2 \\
&\leq \frac{1}{t} \sum_{i=1}^{t} 2\lambda_i^{t-i} \left\|\mathbf{w}_i\right\|_2^2 \left\|(\mathbf{A} - \mathbf{B})\right\|_F \left\|(\mathbf{A} + \mathbf{B})\right\|_F \left\|\mathbf{s}_i - \mathbf{x}_i\right\|_2 = \theta,
\end{aligned}$$

where $\lambda_i = \lambda(\mathrm{tr}(\mathbf{P}_i)/n)^{1/t-i}$, thanks to the triangle inequality. It is therefore that the set of functions $\{g_t(\mathbf{U})\}_{t=1}^{\infty}$ is continuous on $\mathcal{U}$.
Furthermore, for any $\mathbf{U}^*, \boldsymbol{\Delta} \in \mathcal{U}$, we show that the following limit exists:

$$\begin{aligned}
\lim_{\|\boldsymbol{\Delta}\|\to 0} \frac{|g_t(\mathbf{U}^* + \boldsymbol{\Delta}) - g_t(\mathbf{U}^*)|}{\|\boldsymbol{\Delta}\|} = \lim_{\|\boldsymbol{\Delta}\|\to 0} \frac{1}{t\|\boldsymbol{\Delta}\|} \sum_{i=1}^{t} \lambda_i^{t-i} \Bigg( & \left\|\mathbf{P}_i((\mathbf{U}^* + \boldsymbol{\Delta})\mathbf{w}_i + \mathbf{s}_i - \mathbf{x}_i)\right\|_2^2 \\
& - \left\|\mathbf{P}_i(\mathbf{U}^*\mathbf{w}_i + \mathbf{s}_i - \mathbf{x}_i)\right\|_2^2 \Bigg).
\end{aligned} \tag{15}$$

Specifically, let us denote $\mathbf{y}_i = \mathbf{P}_i(\mathbf{U}^*\mathbf{w}_i + \mathbf{s}_i - \mathbf{x}_i)$, the limit can be written as follows:

$$\begin{aligned}
\lim_{\|\boldsymbol{\Delta}\|\to 0} \frac{|g_t(\mathbf{U}^* + \boldsymbol{\Delta}) - g_t(\mathbf{U}^*)|}{\|\boldsymbol{\Delta}\|} &= \lim_{\|\boldsymbol{\Delta}\|\to 0} \frac{1}{t\|\boldsymbol{\Delta}\|} \sum_{i=1}^{t} \lambda_i^{t-i} \big( \left\|\mathbf{y}_i - \mathbf{P}_i\boldsymbol{\Delta}\mathbf{w}_i\right\|_2^2 - \left\|\mathbf{y}_i\right\|_2^2 \big) \\
&= \lim_{\|\boldsymbol{\Delta}\|\to 0} \frac{1}{t\|\boldsymbol{\Delta}\|} \sum_{i=1}^{t} \lambda_i^{t-i} \big( \left\|\mathbf{P}_i\boldsymbol{\Delta}\mathbf{w}_i\right\|_2^2 - 2\langle \mathbf{y}_i, \mathbf{P}_i\boldsymbol{\Delta}\mathbf{w}_i \rangle \big) \\
&= -\frac{2}{t} \sum_{i=1}^{t} \lambda_i^{t-i} \|\mathbf{y}_i\|_2 \cos(\mathbf{y}_i, \mathbf{P}_i\boldsymbol{\Delta}\mathbf{w}_i) < \infty.
\end{aligned} \tag{16}$$

As a result, the function $g_t(\mathbf{U})$ is differentiable and its first derivative $\nabla g_t(\mathbf{U})$ can be given by

$$\nabla g_t(\mathbf{U}) = \frac{2}{t} \sum_{i=1}^{t} \lambda_i^{t-i} \mathbf{P}_i(\mathbf{U}\mathbf{w}_i + \mathbf{s}_i - \mathbf{x}_i)\mathbf{w}_i^{\top}. \tag{17}$$

In the similar way, it is easy to verify that $\nabla g_t(\mathbf{U})$ is also continuous and the second derivative $\nabla^2 g_t(\mathbf{U})$ is given by

$$\nabla^2 g_t(\mathbf{U}) = \frac{2}{t}\sum_{i=1}^{t} \lambda_i^{t-i}\mathbf{P}_i\mathbf{w}_i\mathbf{w}_i^\top. \tag{18}$$

□

(C-2) The second derivative $\nabla^2 g_t(\mathbf{U})$ is a positive-define matrix. For all $\mathbf{x} \in \mathbb{R}^{p\times 1}$, we have

$$\mathbf{x}^\top\nabla^2 g_t(\mathbf{U})\mathbf{x} = \frac{2}{t}\sum_{i=1}^{t} \lambda_i^{t-i}\mathbf{P}_i(\mathbf{w}_i^\top\mathbf{x})^\top(\mathbf{w}_i^\top\mathbf{x}) = \frac{2}{t}\sum_{i=1}^{t} \lambda_i^{t-i}\mathbf{P}_i(\mathbf{w}_i^\top\mathbf{x})^2 > 0, \quad \forall\lambda, t > 0. \tag{19}$$

It implies that there always exist a positive constant $m$ such that $\nabla^2 g_t(\mathbf{U}) \geq m\mathbf{I}$.

It follows to the claims (C-1), (C-2) and the assumptions showing that the domain of $g_t(\mathbf{U})$ is a convex set that $g_t(\mathbf{U}_t)$ is strongly convex [3, Section 3.1.4].

*Stage II: Prove that $g_t(\mathbf{U})$ is also a Lipschitz function:*

$$|g_t(\mathbf{U}_{t+1}) - g_t(\mathbf{U}_t)| \leq m_2 \left\|\mathbf{U}_{t+1} - \mathbf{U}_t\right\|_F. \tag{20}$$

Let us denote $d_t(\mathbf{U}) = g_t(\mathbf{U}) - g_{t+1}(\mathbf{U})$. Since $\mathbf{U}_t = \underset{\mathbf{U}}{\operatorname{argmin}}\, g_t(\mathbf{U})$, we exploit that $g_{t+1}(\mathbf{U}_{t+1}) \leq g_{t+1}(\mathbf{U}_t)$ and hence

$$\begin{aligned} g_t(\mathbf{U}_{t+1}) - g_t(\mathbf{U}_t) &= g_t(\mathbf{U}_{t+1}) - g_{t+1}(\mathbf{U}_t) + g_{t+1}(\mathbf{U}_t) - g_t(\mathbf{U}_t) \\ &\leq \big(\underbrace{g_t(\mathbf{U}_{t+1}) - g_{t+1}(\mathbf{U}_{t+1})}_{d_t(\mathbf{U}_{t+1})}\big) - \big(\underbrace{g_t(\mathbf{U}_t) - g_{t+1}(\mathbf{U}_t)}_{d_t(\mathbf{U}_t)}\big). \end{aligned} \tag{21}$$

The first derivative of $d_t(\mathbf{U}) = g_t(\mathbf{U}) - g_{t+1}(\mathbf{U})$ is given by

$$\begin{aligned} \nabla d_t(\mathbf{U}) &= \nabla g_t(\mathbf{U}) - \nabla g_{t+1}(\mathbf{U}) \\ &= \frac{1}{t}\sum_{i=1}^{t} \lambda_i^{t-i}\mathbf{P}_i(\mathbf{U}\mathbf{w}_i + \mathbf{s}_i - \mathbf{x}_i)\mathbf{w}_i^\top - \frac{1}{t+1}\sum_{i=1}^{t+1} \lambda_i^{t+1-i}\mathbf{P}_i(\mathbf{U}\mathbf{w}_i + \mathbf{s}_i - \mathbf{x}_i)\mathbf{w}_i^\top. \end{aligned} \tag{22}$$

Let $\mathbf{A}_t = \sum_{i=1}^{t} \lambda_i^{t-i}\mathbf{P}_i\mathbf{U}\mathbf{w}_i\mathbf{w}_i^\top$ and $\mathbf{B}_t = \sum_{i=1}^{t} \lambda_i^{t-i}\mathbf{P}_i(\mathbf{s}_i - \mathbf{x}_i)$, we can rewrite $\nabla d_t(\mathbf{U})$ as

$$\nabla d_t(\mathbf{U}) = \left(\frac{\mathbf{A}_t}{t} - \frac{\mathbf{A}_{t+1}}{t+1}\right) + \left(\frac{\mathbf{B}_t}{t} - \frac{\mathbf{B}_{t+1}}{t+1}\right). \tag{23}$$

Under the given assumptions, the subspace $\mathbf{U}$, outlier $\{\mathbf{s}_t\}$, signal $\{\mathbf{x}_t\}$ and subspace coefficients $\{\mathbf{w}_t\}$ are bounded, then both $\mathbf{A}_t$ and $\mathbf{B}_t$ are bounded. It is therefore that

$$\left\|\nabla d_t(\mathbf{U})\right\|_F \leq \left\|\frac{\mathbf{A}_t}{t} - \frac{\mathbf{A}_{t+1}}{t+1}\right\|_F + \left\|\frac{\mathbf{B}_t}{t} - \frac{\mathbf{B}_{t+1}}{t+1}\right\|_F \leq m_2 = \mathcal{O}(1/t). \tag{24}$$

Therefore $d_t(\mathbf{U})$ is Lipschiz with the constant $m_2$,

$$\frac{|d_t(\mathbf{U}_{t+1}) - d_t(\mathbf{U}_t)|}{\left\|\mathbf{U}_{t+1} - \mathbf{U}_t\right\|_F} \leq m_2, \text{ hence } \frac{|g_t(\mathbf{U}_{t+1}) - g_t(\mathbf{U}_t)|}{\left\|\mathbf{U}_{t+1} - \mathbf{U}_t\right\|_F} \leq m_2. \tag{25}$$

This ends the proof.

## III. Proof of the Lemma 3

Inspired of the result of convergence analysis for online sparse coding framework in [4, Proposition 2], we derive the convergence of $g_t(\mathbf{U}_t)$ in the similar way. In particular, we first denote the nonnegative stochastic process $\{u_t\}, u_t \triangleq g_t(\mathbf{U}_t) \geq 0$, and then prove that it is a quasi-martingale, i.e., we have to prove the sum of the positive difference of $\{u_t\}_{t=1}^{\infty}$ is bounded,

$$\sum_{t=1}^{\infty} \left|\mathbb{E}[u_{t+1} - u_t|\mathcal{F}_t]\right| < +\infty \quad a.s. \tag{26}$$

We can express $g_{t+1}(\mathbf{U}_t)$ with respect to $g_t(\mathbf{U}_t)$ as follows

$$\begin{aligned} g_{t+1}(\mathbf{U}_t) &= \frac{1}{t+1}\sum_{i=1}^{t+1} \lambda_i^{t+1-i} \left\|\mathbf{P}_i(\mathbf{U}_t\mathbf{w}_i + \mathbf{s}_i - \mathbf{x}_i)\right\|_2^2 + \rho\left\|\mathbf{s}_i\right\|_1 \\ &= \left(\frac{\lambda}{t+1}\sum_{i=1}^{t} \lambda_i^{t-i} \left\|\mathbf{P}_i(\mathbf{U}_t\mathbf{w}_i + \mathbf{s}_i - \mathbf{x}_i)\right\|_2^2 + \rho\left\|\mathbf{s}_i\right\|_1\right) + \left(\frac{1}{t+1}\big(\left\|\mathbf{P}_{t+1}\mathbf{U}_t + \mathbf{s}_{t+1} - \mathbf{x}_{t+1}\right\|_2^2 + \rho\left\|\mathbf{s}_{t+1}\right\|_1\big)\right) \\ &= \frac{\lambda_i t}{t+1} g_t(\mathbf{U}_t) + \frac{1}{t+1}\ell(\mathbf{U}_t, \mathbf{P}_{t+1}, \mathbf{x}_{t+1}). \end{aligned}$$

Since $\mathbf{U}_{t+1} = \underset{\mathbf{U}}{\operatorname{argmin}}\, g_{t+1}(\mathbf{U})$, we have the fact $g_{t+1}(\mathbf{U}_{t+1}) - g_{t+1}(\mathbf{U}_t) \leq 0$, $f_t(\mathbf{U}_t) \leq g_t(\mathbf{U}_t)$, and hence

$$\begin{aligned} u_{t+1} - u_t = g_{t+1}(\mathbf{U}_{t+1}) - g_t(\mathbf{U}_t) &= \underbrace{g_{t+1}(\mathbf{U}_{t+1}) - g_{t+1}(\mathbf{U}_t)}_{\leq 0} + g_{t+1}(\mathbf{U}_t) - g_t(\mathbf{U}_t) \\ &\leq g_{t+1}(\mathbf{U}_t) - g_t(\mathbf{U}_t) = \frac{1}{t+1}\ell(\mathbf{U}_t, \mathbf{P}_{t+1}, \mathbf{x}_{t+1}) - \frac{t(1-\lambda_i)+1}{t+1} g_t(\mathbf{U}_t). \end{aligned} \tag{27}$$

It is therefore that

$$\begin{aligned} \mathbb{E}[u_{t+1} - u_t|\mathcal{F}_t] &\leq \frac{\mathbb{E}[\ell(\mathbf{U}_t, \mathbf{P}_{t+1}, \mathbf{x}_{t+1}) - (t(1-\lambda_i)+1) g_t(\mathbf{U}_t)|\mathcal{F}_t]}{t+1} \\ &\leq \frac{\mathbb{E}[\ell(\mathbf{U}_t, \mathbf{P}_{t+1}, \mathbf{x}_{t+1}) - g_t(\mathbf{U}_t)|\mathcal{F}_t]}{t+1} \leq \frac{\mathbb{E}[\ell(\mathbf{U}_t, \mathbf{P}_{t+1}, \mathbf{x}_{t+1})] - f_t(\mathbf{U}_t)}{t+1} = \frac{f(\mathbf{U}_t) - f_t(\mathbf{U}_t)}{t+1} \end{aligned}$$

because of $f_t(\mathbf{U}_t) \leq g_t(\mathbf{U}_t)$ and $\mathbb{E}[\ell(\mathbf{U}_t, \mathbf{P}_{t+1}, \mathbf{x}_t)] = f(\mathbf{U}_t)$.

Let us define the indicator function $\delta_t$ as follows

$$\delta_t \triangleq \begin{cases} 1 & \text{if} \quad \mathbb{E}[g_{t+1}(\mathbf{U}_{t+1}) - g_t(\mathbf{U}_t)|\mathcal{F}_t] > 0 \\ 0 & \text{otherwise,} \end{cases}$$

we then have

$$\mathbb{E}\big[\delta\mathbb{E}[g_{t+1}(\mathbf{U}_{t+1}) - g_t(\mathbf{U}_t)|\mathcal{F}_t]\big] \leq \mathbb{E}[\sqrt{t}(f(\mathbf{U}_t) - f_t(\mathbf{U}_t))]\frac{1}{\sqrt{t}(t+1)}. \tag{28}$$

Under the given assumptions that $\{\mathbf{U}, \mathbf{w}, \mathbf{s}, \mathbf{x}\}$ are bounded, we exploit that the set of measurable functions $\{\ell(\mathbf{U}_i, \mathbf{P}, \mathbf{x})\}_{i\geq 1}$, which is composed of a quadratic norm term and $\ell_1$-norm term, is $\mathbb{P}$-Donsker. Therefore, the centered and scaled version of the empirical function $f_t(\mathbf{U}_t)$ satisfies the following proposition:

$$\mathbb{E}[\sqrt{t}(f(\mathbf{U}_t) - f_t(\mathbf{U}_t))] = \mathcal{O}(1), \tag{29}$$

thanks to Proposition 9.

Furthermore, let us consider the convergence of the sum $\sum_{t=1}^{\infty} \frac{\alpha}{\sqrt{t}(t+1)}$. We use the Cauchy-MacLaurin integral test [5] for convergence, as

$$\begin{aligned}\int_{t=1}^{+\infty} \frac{\alpha}{\sqrt{t}(t+1)} dt &= \alpha \int_{x=1}^{+\infty} \frac{1}{x^2+1} dx = \alpha \arctan(x)\big|_1^{+\infty} \\ &= \alpha\big(\arctan(\infty) - \arctan(1)\big) = \alpha\frac{\pi}{4} < \infty.\end{aligned}$$

It is therefore that $\left\{\frac{1}{\sqrt{t}(t+1)}\right\}_{t>0}$ converges and hence

$$\sum_{t=1}^{\infty} \mathbb{E}\big[\delta \mathbb{E}[g_{t+1}(\mathbf{U}_{t+1}) - g_t(\mathbf{U}_t)|\mathcal{F}_t]\big] < \infty. \tag{30}$$

According to quasi-martingale theorem as shown in Proposition 10, we can conclude that $\{g_t(\mathbf{U}_t)\}_{t=1}^{\infty}$ converges almost surely

$$\sum_{t=1}^{\infty} \mathbb{E}[g_{t+1}(\mathbf{U}_{t+1}) - g_t(\mathbf{U}_t)|\mathcal{F}_t] < \infty. \tag{31}$$

We complete the proof.

## IV. Proof of Lemma 4

We investigate the convergence of a surrogate sequence $\left\{\big(g_t(\mathbf{U}_t) - f_t(\mathbf{U}_t)\big)\frac{1}{t+1}\right\}$ as follows

$$\begin{aligned}\frac{g_t(\mathbf{U}_t) - f_t(\mathbf{U}_t)}{t+1} &= u_t - u_{t+1} + \underbrace{g_{t+1}(\mathbf{U}_{t+1}) - g_{t+1}(\mathbf{U}_t)}_{\leq 0} + \underbrace{\frac{t(\lambda-1)}{t+1} g_t(\mathbf{U}_t)}_{\leq 0} + \frac{\ell(\mathbf{U}_t, \mathbf{P}_{t+1}, \mathbf{x}_{t+1}) - f_t(\mathbf{U}_t)}{t+1} \\ &\leq \underbrace{u_t - u_{t+1}}_{\text{(S-1)}} + \underbrace{\frac{\ell(\mathbf{U}_t, \mathbf{P}_{t+1}, \mathbf{x}_{t+1}) - f_t(\mathbf{U}_t)}{t+1}}_{\text{(S-2)}}\end{aligned} \tag{32}$$

because of $u_t = g_t(\mathbf{U}_t)$ and $\lambda \leq 1$. Note that, (S-1) $-$ (S-2) converge almost surely:

- The sequence $\mathbb{E}[u_t - u_{t+1}]$ converges almost surely as proved in Lemma 3.
- The sequence (S-2) also converges, thanks to the fact $\mathbb{E}[\ell(\mathbf{U}_t, \mathbf{P}_{t+1}, \mathbf{x}_{t+1})] = f(\mathbf{U}_t)$ and the convergence of $\frac{\mathbb{E}[f(\mathbf{U}_t) - f_t(\mathbf{U}_t)]}{t+1}$ as mentioned in the appendix III.

It is therefore that the sequence $\left\{\big(g_t(\mathbf{U}_t) - f_t(\mathbf{U}_t)\big)\frac{1}{t+1}\right\}$ converges almost surely, i.e.,

$$\sum_{t=0}^{\infty} \big(g_t(\mathbf{U}_t) - f_t(\mathbf{U}_t)\big)\frac{1}{t+1} < \infty. \tag{33}$$

On the other hand, the real sequence $\left\{\frac{1}{t+1}\right\}_{t\geq 0}$ diverges, $\sum_{t=0}^{\infty} \frac{1}{t+1} = \infty$. It implies that $g_t(\mathbf{U}_t) - f_t(\mathbf{U}_t)$ convergences, thanks to the Proposition 7.

## V. Proof of Corollary 4

Let $\mathbf{U}_t = \underset{\mathbf{U}}{\operatorname{argmin}}\, g_t(\mathbf{U})$ when $t \to \infty$, we have

$$f_t(\mathbf{U}_t) \leq f_t(\mathbf{U}) + \frac{L}{2}\|\mathbf{U} - \mathbf{U}_t\|_F^2, \forall\ \mathbf{U} \in \mathcal{U}, \tag{34}$$

where $L$ is a positive constant. In other words, $\mathbf{U}_t$ is the minimum point of $f(\mathbf{U})$.

*Proof.* Let us denote the error function $e_t(\mathbf{U}) = g_t(\mathbf{U}) - f_t(\mathbf{U})$. Then it is easy to have $\nabla e_t(\mathbf{U}) = \nabla g_t(\mathbf{U}) - \nabla f_t(\mathbf{U})$ because the function $f_t(\mathbf{U})$ and its surrogate $g_t(\mathbf{U})$ are continuous and differentiable. We first have the following facts

$$\begin{aligned}\|\nabla e_t(\mathbf{U}) - \nabla e_t(\mathbf{U}_t)\| &= \big\|\big(\nabla g_t(\mathbf{U}) - \nabla g_t(\mathbf{U}_t)\big) - \big(\nabla f_t(\mathbf{U}) - \nabla f_t(\mathbf{U}_t)\big)\big\| \\ &= \big\|\big(\nabla g_t(\mathbf{U})\big) - \big(\nabla f_t(\mathbf{U}) - \nabla f_t(\mathbf{U}_t)\big)\big\| \\ &\leq \|\nabla g_t(\mathbf{U}) - g_t(\mathbf{U}_t)\| + \|\nabla f_t(\mathbf{U}) - \nabla f_t(\mathbf{U}_t)\|, \end{aligned} \tag{35}$$

thanks to the triangle theorem.

As proved in the Proposition 2, the surrogate function $g_t(\mathbf{U})$ is strongly convex, but also Lipschitz and its second derivative are given by

$$\nabla^2 g_t(\mathbf{U}) = \frac{2}{t}\sum_{i=1}^{t} \lambda_i^{t-i}\mathbf{P}_i\mathbf{w}_i\mathbf{w}_i^\top. \tag{36}$$

Under the given assumption that the subspace coefficient vectors $\{\mathbf{v}_i\}_{i\geq 1}$ are bounded, the $\nabla^2_{\mathbf{U}} g_t(\mathbf{U})$ is then bounded. It is therefore that the first derivative $\nabla g_t(\mathbf{U})$ is also a Lipschitz function, that means,

$$\|\nabla g_t(\mathbf{U}) - \nabla g_t(\mathbf{U}_t)\| \leq L_g\|\mathbf{U} - \mathbf{U}_t\|_F. \tag{37}$$

In parallel, we will show that the first derivative of the cost function $f_t(\mathbf{U})$ is Lipschitz too, as

$$\|\nabla f_t(\mathbf{U}) - \nabla f_t(\mathbf{U}_t)\| \leq L_f\|\mathbf{U} - \mathbf{U}_t\|_F. \tag{38}$$

For any two subspace variables $\mathbf{U}_1, \mathbf{U}_2 \in \mathcal{U}$, we have

$$\|\nabla f_t(\mathbf{U}_1) - \nabla f_t(\mathbf{U}_2)\| \leq \frac{1}{t}\sum_{i=1}^{t}\lambda_i^{t-i}\|\nabla \ell(\mathbf{U}_1, \mathbf{P}_i, \mathbf{x}_i) - \nabla \ell(\mathbf{U}_2, \mathbf{P}_i, \mathbf{x}_i)\|. \tag{39}$$

For any signal $\mathbf{x} \in \mathcal{S}$ at time instant $t$, we also have

$$\begin{aligned}&\|\nabla \ell(\mathbf{U}_1, \mathbf{P}_t, \mathbf{x}) - \nabla \ell(\mathbf{U}_2, \mathbf{P}_t, \mathbf{x})\| \\ &\leq\ \|\mathbf{P}_t\mathbf{U}_1\mathbf{w}^*(\mathbf{U}_1, \mathbf{P}_t, \mathbf{x})\mathbf{w}^*(\mathbf{U}_1, \mathbf{P}_t, \mathbf{x})^\top - \mathbf{P}_t\mathbf{U}_2\mathbf{w}^*(\mathbf{U}_1, \mathbf{P}_t, \mathbf{x})\mathbf{w}^*(\mathbf{U}_1, \mathbf{P}_t, \mathbf{x})^\top\| \\ &+ \|\mathbf{s}^*(\mathbf{U}_1, \mathbf{P}_t, \mathbf{x})\mathbf{w}^*(\mathbf{U}_1, \mathbf{P}_t, \mathbf{x})^\top - \mathbf{s}^*(\mathbf{U}_2, \mathbf{P}_t, \mathbf{x})\mathbf{w}^*(\mathbf{U}_2, \mathbf{P}_t, \mathbf{x})^\top\| + \|\mathbf{x}\mathbf{w}^*(\mathbf{U}_1, \mathbf{P}_t, \mathbf{x})^\top - \mathbf{x}\mathbf{w}^*(\mathbf{U}_2, \mathbf{P}_t, \mathbf{x})^\top\|.\end{aligned}$$

where $(\mathbf{w}^*(\mathbf{U}, \mathbf{P}, \mathbf{x}), \mathbf{s}^*(\mathbf{U}, \mathbf{P}, \mathbf{x})) \triangleq \operatorname{argmin}_{\mathbf{w},\mathbf{s}} \ell(\mathbf{U}, \mathbf{P}, \mathbf{x}, \mathbf{w}, \mathbf{s})$. Note that, $\big(\mathbf{w}^*(\mathbf{U}, \mathbf{P}, \mathbf{x}), \mathbf{s}^*(\mathbf{U}, \mathbf{P}, \mathbf{x})\big)$ can be seen as a continuous function of the two variables. As mentioned in the proof of Lemma 1, the function is not only strongly convex, but also Lipschitz in terms of each variable $\mathbf{s}$ or $\mathbf{w}$. Therefore, we have the following facts:

$$\begin{aligned}\|\mathbf{w}^*(\mathbf{U}_1, \mathbf{P}, \mathbf{x}) - \mathbf{w}^*(\mathbf{U}_2, \mathbf{P}, \mathbf{x})\| &\leq c_1\|\mathbf{P}(\mathbf{U}_1 - \mathbf{U}_2)\|, \\ \|\mathbf{s}^*(\mathbf{U}_1, \mathbf{P}, \mathbf{x}) - \mathbf{s}^*(\mathbf{U}_2, \mathbf{P}, \mathbf{x})\| &\leq c_2\|\mathbf{P}(\mathbf{U}_1 - \mathbf{U}_2)\|,\end{aligned}$$

where $c_1$ and $c_2$ are the Lipschitz number of $\mathbf{w}^*(\mathbf{U}_1, \mathbf{P}, \mathbf{x})$ and $\mathbf{w}^*(\mathbf{U}_1, \mathbf{P}, \mathbf{x})$ respectively.

Denote the upper bound for $\mathbf{x}$, $\mathbf{s}$, $\mathbf{w}$ and $\mathbf{U}$ are $\alpha_1, \alpha_2, \alpha_3$ and $\alpha_4$ respectively. The first part of (E-5) can be bounded as follows:

$$\begin{aligned}
&\|\mathbf{P}_t\mathbf{U}_1\mathbf{w}^*(\mathbf{U}_1,\mathbf{P}_t,\mathbf{x})\mathbf{w}^*(\mathbf{U}_1,\mathbf{P}_t,\mathbf{x})^\top - \mathbf{P}_t\mathbf{U}_2\mathbf{w}^*(\mathbf{U}_1,\mathbf{P}_t,\mathbf{x})\mathbf{w}^*(\mathbf{U}_1,\mathbf{P}_t,\mathbf{x})^\top\| \\
&\le \|\mathbf{P}_t\mathbf{U}_1\|\|\mathbf{w}^*(\mathbf{U}_1,\mathbf{P}_t,\mathbf{x})\|\|\mathbf{w}^*(\mathbf{U}_1,\mathbf{P}_t,\mathbf{x}) - \mathbf{w}^*(\mathbf{U}_2,\mathbf{x})\| \\
&\qquad + \|\mathbf{P}_t\mathbf{U}_1\mathbf{w}^*(\mathbf{U}_1,\mathbf{P}_t,\mathbf{x}) - \mathbf{P}_t\mathbf{U}_2\mathbf{w}^*(\mathbf{U}_1,\mathbf{P}_t,\mathbf{x})\|\|\mathbf{w}^*(\mathbf{U}_1,\mathbf{P}_t,\mathbf{x})\| \\
&\le c_1\alpha_3\alpha_4\|\mathbf{P}_t(\mathbf{U}_1-\mathbf{U}_2)\| + \|\mathbf{w}^*(\mathbf{U}_1,\mathbf{P}_t,\mathbf{x})\|\big(\|\mathbf{P}_t\mathbf{U}_1\|\|\mathbf{w}^*(\mathbf{U}_1,\mathbf{P}_t,\mathbf{x}) - \mathbf{w}^*(\mathbf{U}_2,\mathbf{P}_t,\mathbf{x})\| \\
&\qquad + \|\mathbf{P}_t(\mathbf{U}_1-\mathbf{U}_2)\|\|\mathbf{w}^*(\mathbf{U}_1,\mathbf{P}_t,\mathbf{x})\|\big) \\
&\le \alpha_3\alpha_4\|\mathbf{P}_t(\mathbf{U}_1-\mathbf{U}_2)\| + \alpha_3\big(c_1\alpha_4\|\mathbf{P}_t(\mathbf{U}_1-\mathbf{U}_2)\| + \alpha_3\|\mathbf{P}_t(\mathbf{U}_1-\mathbf{U}_2)\|\big) \\
&= (2c_1\alpha_3\alpha_4 + \alpha_3^2)\|\mathbf{P}_t(\mathbf{U}_1-\mathbf{U}_2)\| \le (2c_1\alpha_3\alpha_4 + \alpha_3^2)\|(\mathbf{U}_1-\mathbf{U}_2)\|, \qquad (40)
\end{aligned}$$

the bounds for the two latter terms are

$$\begin{aligned}
&\|\mathbf{s}^*(\mathbf{U}_1,\mathbf{P}_t,\mathbf{x})\mathbf{w}^*(\mathbf{U}_1,\mathbf{P}_t,\mathbf{x})^\top - \mathbf{s}^*(\mathbf{U}_2,\mathbf{P}_t,\mathbf{x})\mathbf{w}^*(\mathbf{U}_2,\mathbf{P}_t,\mathbf{x})^\top\| \\
&\le \|\mathbf{s}^*(\mathbf{U}_1,\mathbf{P}_t,\mathbf{x})\|\|\mathbf{w}^*(\mathbf{U}_1,\mathbf{P}_t,\mathbf{x})^\top - \mathbf{w}^*(\mathbf{U}_2,\mathbf{P}_t,\mathbf{x})^\top\| + \|\mathbf{s}^*(\mathbf{U}_1,\mathbf{P}_t,\mathbf{x}) - \mathbf{s}^*(\mathbf{U}_2,\mathbf{P}_t,\mathbf{x})\|\|\mathbf{w}^*(\mathbf{U}_2,\mathbf{P}_t,\mathbf{x})\| \\
&\le c_1\alpha_2\|\mathbf{P}_t(\mathbf{U}_1-\mathbf{U}_2)\| + c_2\alpha_3\|\mathbf{P}_t(\mathbf{U}_1-\mathbf{U}_2)\| \\
&\le (c_1\alpha_2 + c_2\alpha_3)\|\mathbf{P}_t(\mathbf{U}_1-\mathbf{U}_2)\| + \alpha_3\|(\mathbf{U}_1-\mathbf{U}_2)\|, \qquad (41)
\end{aligned}$$

and

$$\|\mathbf{x}\mathbf{w}^*(\mathbf{U}_1,\mathbf{P}_t,\mathbf{x})^\top - \mathbf{x}\mathbf{w}^*(\mathbf{U}_2,\mathbf{P}_t,\mathbf{x})^\top\| \le c_1\alpha_1\|(\mathbf{U}_1-\mathbf{U}_2)\|. \qquad (42)$$

From (40), (41) and (42), we can conclude the inequality (38).

From the three facts above above and $g_t(\mathbf{U}_t) \overset{a.s.}{\to} f_t(\mathbf{U}_t)$ when $t \to \infty$, we have $\nabla e_t(\mathbf{U}_t) = \mathbf{0}$ and hence the following inequality

$$|\nabla e_t(\mathbf{U})| \le \frac{L}{2}\|\mathbf{U}-\mathbf{U}_t\|_F.$$

It is therefore that

$$\frac{|e_t(\mathbf{U}) - e_t(\mathbf{U}_t)|}{\|\mathbf{U}-\mathbf{U}_t\|_F} \le \frac{L}{2}\|\mathbf{U}-\mathbf{U}_t\|_F, \qquad (43)$$

thanks to the mean value theorem. In other word, we have $|e_t(\mathbf{U})| \le \frac{L}{2}\|\mathbf{U}-\mathbf{U}_t\|_F^2$ because of $e_t(\mathbf{U}_t) \overset{a.s.}{\to} 0$. In addition, for all $\mathbf{U} \in \mathbf{R}^{n\times r}$, we always have $f_t(\mathbf{U}_t) \le g_t(\mathbf{U})$. Therefore, we can conclude the corollary as follows

$$f_t(\mathbf{U}_t) \le g_t(\mathbf{U}_t) = f_t(\mathbf{U}) + e_t(\mathbf{U}) \le f_t(\mathbf{U}) + \frac{L}{2}\|\mathbf{U}-\mathbf{U}_t\|_F^2. \qquad (44)$$

It ends the proof. □

## VI. Technical Propositions

In this section, we would provide the following propositions which help us to derive several important results in the proofs. Their details are provided in well-known materials. [3], [6]–[10].

**Proposition 1.** *(Strongly Convex): The function $f$ is strongly convex if and only if for all $\mathbf{u}, \mathbf{v} \in \boldsymbol{dom}(f)$ we always have*

$$f(\mathbf{v}) - f(\mathbf{u}) - \frac{1}{2}\|\mathbf{v}-\mathbf{u}\|_2^2 \ge \langle \mathbf{v}-\mathbf{u}, \boldsymbol{\theta}\rangle, \quad \forall \boldsymbol{\theta} \in \partial f(\mathbf{u}).$$

**Proposition 2.** *The function $f$ is $m$-strongly convex, with a constant $m$ if and only if for all $\mathbf{u}, \mathbf{v} \in \textbf{\textit{dom}}(f)$, we always have*

$$|f(\mathbf{v}) - f(\mathbf{u})| \geq \frac{m}{2} \|\mathbf{v} - \mathbf{u}\|_2^2 .$$

**Proposition 3.** *Every norm on $\mathbb{R}^n$ is convex and the sum of convex functions is convex.*

**Proposition 4.** *(Lipschitz Function) A function $f : \mathcal{V} \to \mathbf{R}$ is called Lipschitz function if there exist a a positive number $L > 0$ such that for all $\mathbf{A}, \mathbf{B} \in \mathcal{V}$, we always have*

$$|f(\mathbf{A}) - f(\mathbf{B})| \leq L\|\mathbf{A} - \mathbf{B}\|.$$

**Proposition 5.** *(Huber Function): The Huber penalty function replaces the $\ell_1$-norm $\|\mathbf{x}\|_1, \mathbf{x} \in \mathbb{R}^n$ is given by the sum $\sum_{i=1}^n f_\mu^{Hub}(x(i))$, where*

$$f_\mu^{Hub}(x(i)) = \begin{cases} \frac{x(i)^2}{2\mu}, & |x(i)| \leq \mu, \\ |x(i)| - \mu/2, & |x| > \mu. \end{cases}$$

*There exists a smooth version of the Huber function $f_\mu^{Hub}$, which has derivatives of all degrees, i.e.,*

$$\psi_\mu(\mathbf{x}) = \sum_{i=1}^{n} \big((x(i)^2 + \mu^2)^{1/2} - \mu\big).$$

*and the first derivative of the pseudo-Huber function $\psi_\mu$ is defined by*

$$\nabla\psi_\mu(\mathbf{x}) = \big[x(1)(x(1)^2 + \mu^2)^{-1/2}, \ldots, x(n)(x(n)^2 + \mu^2)^{-1/2}\big]^\top.$$

**Proposition 6.** *Let $\mathcal{V}$ and $\mathcal{W}$ are two vector spaces, and $\mathcal{U} \subset \mathcal{V}$. A function $f : \mathcal{U} \to \mathcal{W}$ is called (Frechet) differentiable at $\mathbf{x} \in \mathcal{U}$ if there exists a bounded linear map $\mathbf{A} : \mathcal{V} \to \mathcal{W}$ such that*

$$\lim_{\|\mathbf{h}\| \to 0} \frac{\|f(\mathbf{x} + \mathbf{h}) - f(\mathbf{x}) - \mathbf{A}\mathbf{x}\|_{\mathcal{W}}}{\|\mathbf{h}\|_{\mathcal{V}}} = 0.$$

**Proposition 7.** *(Convergence): Let $\{a_t\}_{t=1}^\infty$ and $\{b_t\}_{t=1}^\infty$ be two nonnegative sequences such that $\sum_{i=1}^\infty a_i = \infty$ and $\sum_{i=1}^\infty a_i b_i < \infty$, $|b_{t+1} - b_t| < K a_t$ with some constant $K$, then $\lim_{t\to\infty} b_t = 0$ or $\sum_{i=1}^\infty b_i < \infty$.*

**Proposition 8.** *(Convergence): If $\{f_t\}_{t\geq 1}$ and $\{g_t\}_{t\geq 1}$ are sequences of bounded functions which converge uniformly on a set $\mathcal{E}$, then $\{f_t + g_t\}_{t\geq 1}$ and $\{f_t g_t\}_{t\geq 1}$ converge uniformly on $\mathcal{E}$.*

**Proposition 9.** *($\mathbb{P}$-Donsker classes, Donsker theorem [6, Section 19.2]): Let $F = \{\ell_\theta : \mathcal{X} \to \mathbb{R}\}$ be a set of measurable functions defined on a bounded subset of $\mathbb{R}^n$. For every $\theta_1, \theta_2$ and $x$, if there exists a constant $c$ such that*

$$|\ell_{\theta_1}(x) - \ell_{\theta_2}(x)| < c \|\theta_1 - \theta_2\|_2 ,$$

*then $F$ is $\mathbb{P}$-Donsker. For any function $\ell$ in $F$, let us define the following functions*

$$f_t = \frac{1}{t}\sum_{i=1}^{t} \ell(\mathbf{U}_i), \quad \textit{and} \quad f = \mathbb{E}[f_t(\mathbf{U})].$$

*Assume that for all $\ell$, $\|\ell\|_\infty < M$ and random variables $\{\mathbf{U}_i\}_{i\geq 1}$ are Borel-measurable, we then have*

$$\mathbb{E}[\sqrt{t}\|f_t - f\|_\infty] = \mathcal{O}(1),$$

*where $\|\ell\|_\infty \triangleq \inf\{C \geq 0, |f(x)| < C \ \forall\ x\}$.*

**Proposition 10.** *(Quasi Martingales [11, Section 4.4]): Let $(\Omega, \mathcal{F}, \mathbb{P})$ be a probability space, $\{u_t\}_{t>0}$ be a stochastic process on the probability space and $\{\mathcal{F}_t\}_{t>0}$ be a filtration by the past information at time instant $t$. Let us define the indicator function $\delta_t$ as follows*

$$\delta_t \triangleq \begin{cases} 1 & \text{if} \quad \mathbb{E}[u_{t+1} - u_t | \mathcal{F}_t] > 0, \\ 0 & \text{otherwise.} \end{cases}$$

*For all $t$, if $u_t \geq 0$ and $\sum_{i=1}^{\infty} \mathbb{E}[\delta_i (u_{i+1} - u_i) | \mathcal{F}_i] < \infty$, then $u_t$ is a quasi-martingale and converges almost surely, i.e.,*

$$\sum_{t=1}^{\infty} \mathbb{E}[u_{t+1} - u_t | \mathcal{F}_t] < \infty.$$

## VII. Additional Experimental Results

### A. Convergence of PETRELS-ADMM

Fig. 1 shows the typical convergence behavior of PETRELS-ADMM at three noise levels (i.e. $\mathrm{SNR} = \{0, 10, 20\}$ dB) w.r.t the two variables: $\mathrm{fac\text{-}outlier}$ and the weight $\rho$. The experimental results are practical evidences of Lemma 1 in the main manuscript. Particularly, the variation of $\{\mathbf{s}^k\}_{k\geq 1}$ always converges in all testing cases (i.e., approximate $10^{-14}$ on average). When the regularization weight $\rho \geq 0.5$, the convergence rate is fast which the variation $\left\|\mathbf{s}^{k+1} - \mathbf{s}^k\right\|_2$ can converge in 50 iterations in both low- and high-noise cases. Similarly, the variations of the sequence $\{\mathbf{U}_t\}_{t\geq 0}$ generated by PETRELS-ADMM also have asymptotic converged behavior as shown in Fig. 2.

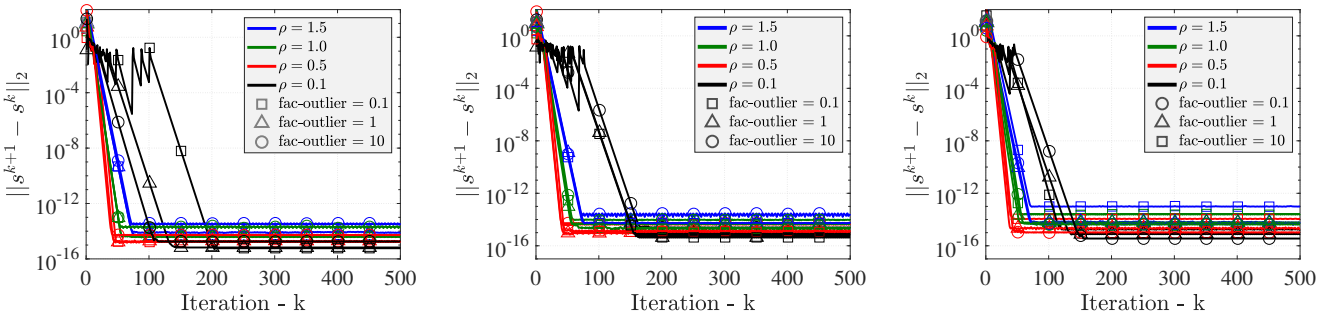


(a) SNR = 0 dB (b) SNR = 10 dB (c) SNR = 20 dB

Fig. 1: Convergence of PETRELS-ADMM in terms of the variation $\left\|\mathbf{s}^{k+1} - \mathbf{s}^k\right\|_2$: $n = 50, r = 2$, $90\%$ entries observed and outlier density of $5\%$.

### B. Outlier Detection

To demonstrate the effectiveness of PETRELS-ADMM, we assess the outlier detection performance of the proposed method in comparison with the well-known GRASTA algorithm [12]. We use a synthetic data whose number of row $n = 50$, rank $r = 2$ and $5000$ observations. Outlier density and intensity are varied in the range $[5\% - 40\%]$ and $[0.1, 1, 10]$ respectively, while the value of $\mathrm{SNR}$ is set at high (20 dB), moderate (10 dB) and low (5 dB) level.

The results are shown as in Fig. 3-6. Particularly, at low outlier density (e.g. $20\%$) and high $\mathrm{SNR}$ (20 dB), both algorithms can detect outliers effectively. Their detection performance may be degraded when

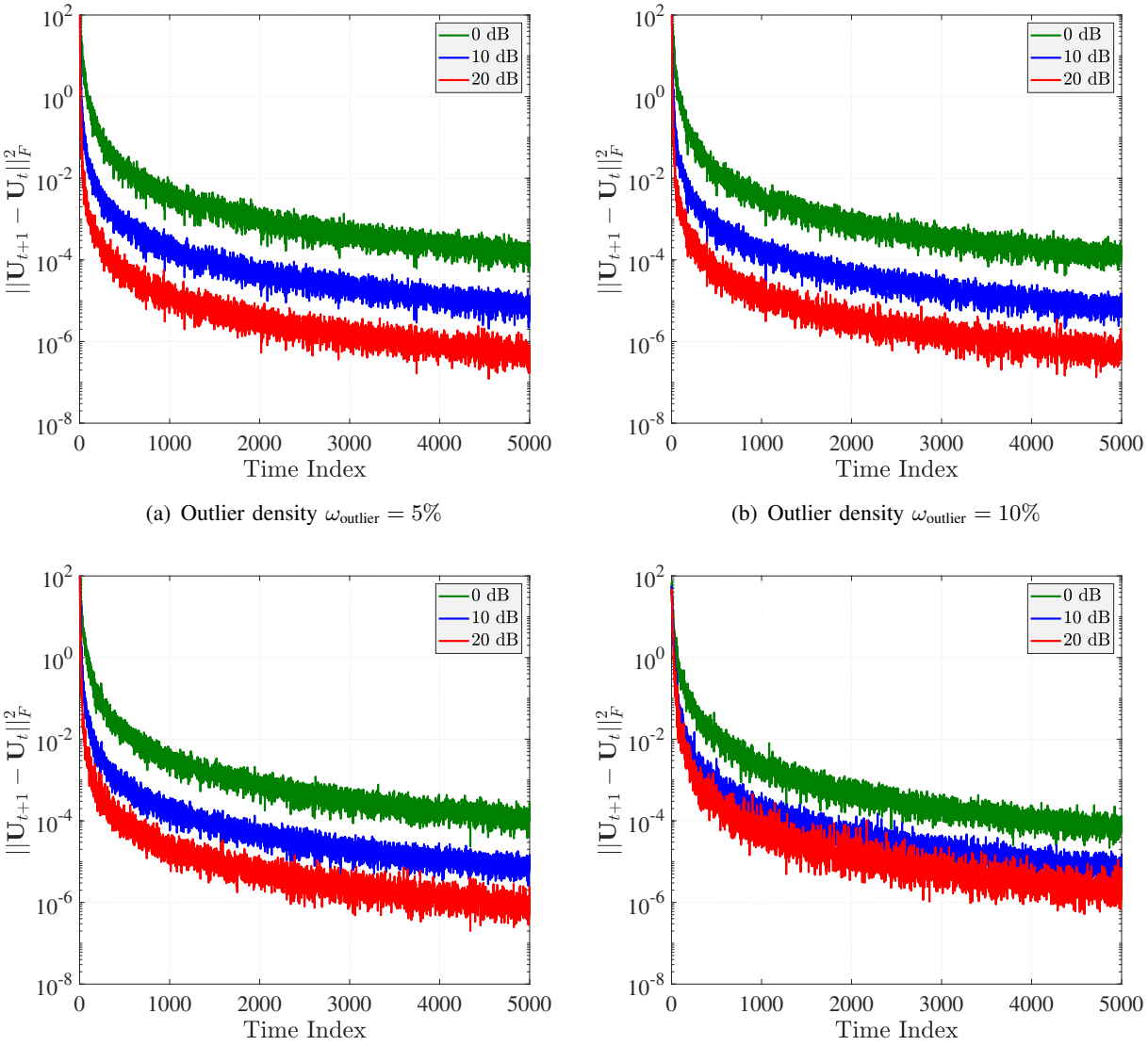


(a) Outlier density $\omega_{\text{outlier}} = 5\%$

(b) Outlier density $\omega_{\text{outlier}} = 10\%$

(c) Outlier density $\omega_{\text{outlier}} = 20\%$

(d) Outlier density $\omega_{\text{outlier}} = 40\%$

Fig. 2: Convergence of PETRELS-ADMM in terms of the variation $\|\mathbf{U}_{t+1} - \mathbf{U}_t\|_F$: $n = 50, r = 2$, $90\%$ entries observed and outlier intensity $\text{fac-outlier} = 10$.

the effect of the noise is increased (i.e. low $\text{SNR}$). Although the location of outliers can be identified correctly, PERTRELS-ADMM provides better results than GRASTA in terms of sparsity, see Fig. 3(b)-(c). The effect of outlier intensity and density on their outlier detection performance are illustrated in Fig. 4 and Fig. 5 respectively. Our method outperforms GRASTA again. We can see that, when the data is corrupted by "strong" outliers, both methods are able to detect them efficiently. At low $\text{SNR}$, outliers are effectively localized by PETRELS-ADMM even in the presence of high corruptions, while GRASTA labels many locations as outliers, see Fig. 4(a) and Fig. 5(b) for examples. Besides, GRASTA fails to detect outliers in cases of low outlier intensity (e.g. $\text{fac-outlier} = 0.1$), as shown in Fig. 4(a). The overall detection performance of PETRELS-ADMM and GRASTA is reported in Fig. 6.

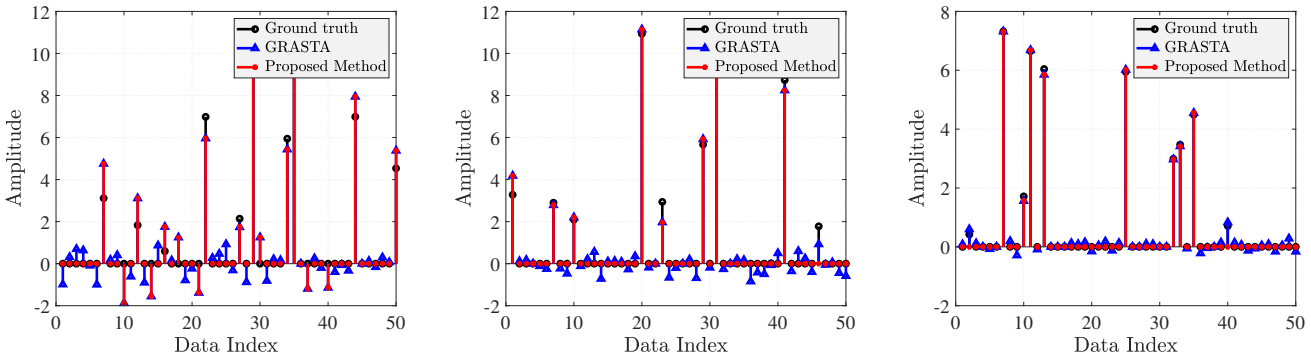


(a) SNR = 5dB (b) SNR = 10dB (c) SNR = 20dB

Fig. 3: Effect of the noise on the outlier detection performance: $n = 50, r = 2$, outlier density of $20\%$ and outlier intensity $\text{fac-outlier} = 1$.

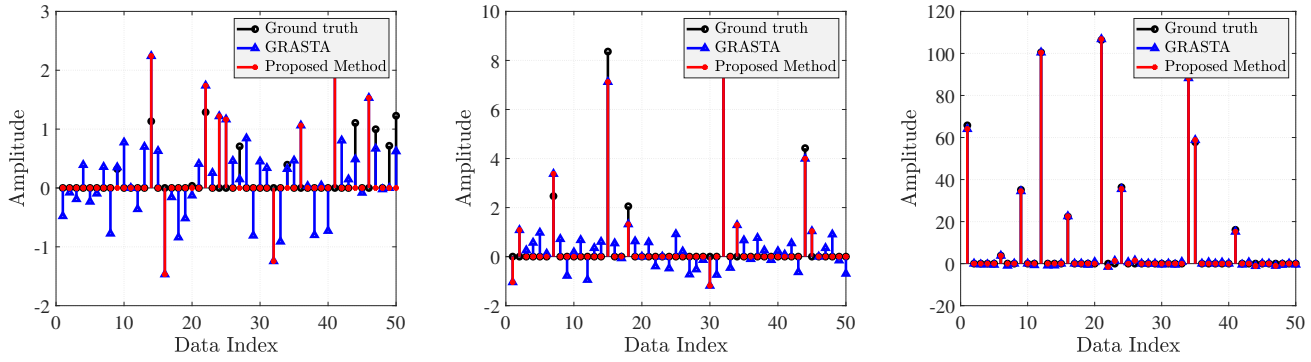


(a) Outlier intensity, fac-outlier = 0.1 (b) Outlier intensity, fac-outlier = 1 (c) Outlier intensity, fac-outlier = 10

Fig. 4: Effect of outlier intensity on the outlier detection performance: $n = 50, r = 2, \text{SNR} = 5$ dB and outlier density of $20\%$.

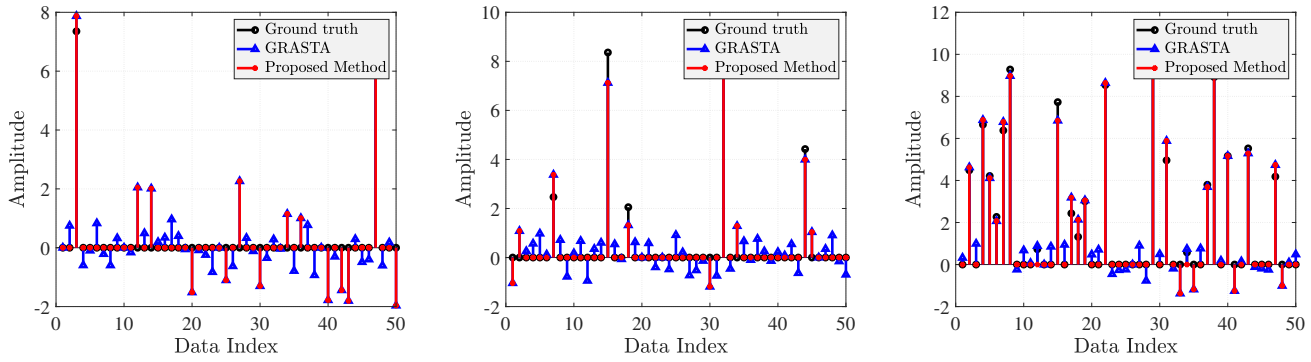


(a) Outlier density = 5% (b) Outlier density = 10% (c) Outlier density = 40%

Fig. 5: Effect of outlier density on the outlier detection performance: $n = 50, r = 2, \text{SNR} = 5$ dB and $\text{fac-outlier} = 1$.

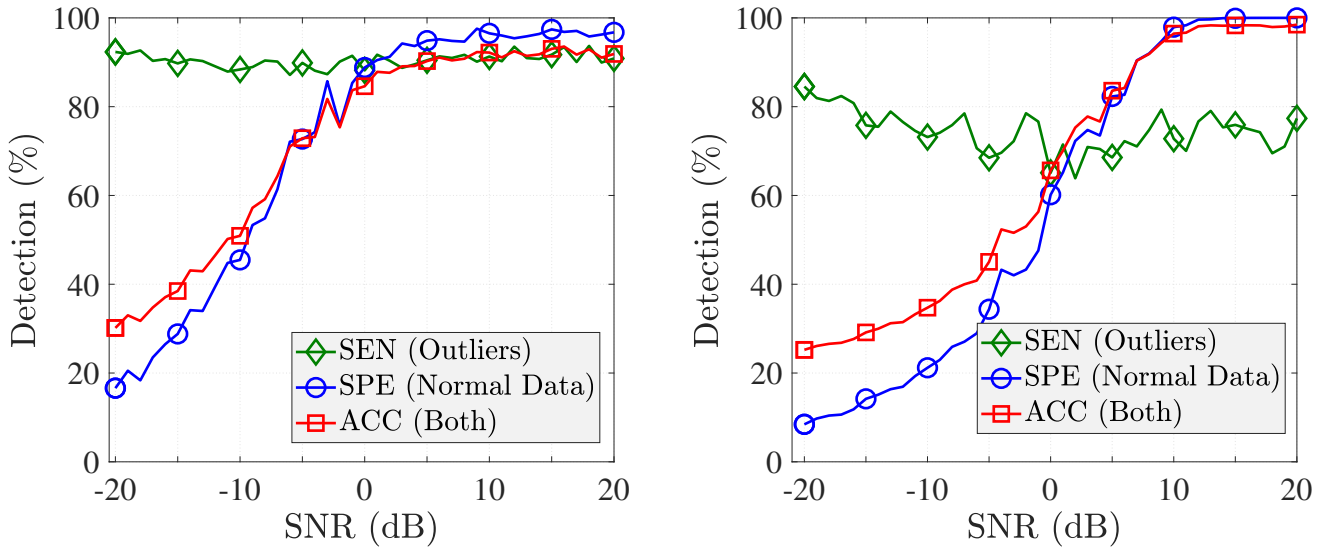


(a) PETRELS-ADMM. (b) GRASTA.

Fig. 6: Outlier detection accuracy versus the noise level: $n = 50$, $r = 2$, $80\%$ entries observed and $20\%$ outliers, $\text{fac-outlier} = 1$.

### *C. Highly Incomplete Observations*

In order to illustrate the efficiency and effectiveness of the proposed algorithm for subspace tracking from (very) highly incomplete observations, a performance comparison of PETRELS-ADMM against the original PETRELS [13] and a well-known GROUSE algorithm [14] is conducted. For a fair comparison, effect of outliers is ignored in this task. Following the above experiments, we consider the same data model of $n = 500$, rank $r = 10$ and $5000$ observations. The underlying subspace is corrupted abruptly at the time index $3000$. The noise level $\text{SNR}$ is set at $10$ dB and $20$ dB.

The results are shown as in Fig. 7. All three algorithms can successfully track the underlying subspace, but PETRELS-ADMM provides better subspace estimation performance than the original PETRELS and GROUSE. Particularly, PETRELS-based algorithms converge faster than GROUSE even with a small number of entries observed at each time. PETRELS-ADMM yields a much better subspace estimation accuracy than the original PETRELS in terms of $\text{SEP}$ metric, see Fig. 7.

### *D. Robustness of PETRELS-ADMM at low Signal-to-Noise Ratio (*$\text{SNR}$*)*

Following the same experiment setup in the main manuscript, we demonstrate the effectiveness of PETRELS-ADMM against the-state-of-the-art algorithms at low $\text{SNR}$ levels (e.g. $\text{SNR} \in \{0, 5, 10\}$ dB). In particular, the performance of PETRELS-ADMM is investigated with respect to three main aspects: (i) impact of outlier intensity, (ii) impact of outlier density, and (iii) impact of missing density on the subspace estimation accuracy. The results are illustrated in Fig. 8, 9, and 10. In the same manner as in cases of high $\text{SNR}$ ($20$ dB), PETRELS-ADMM outperforms the state-of-the-art subspace tracking algorithms again.

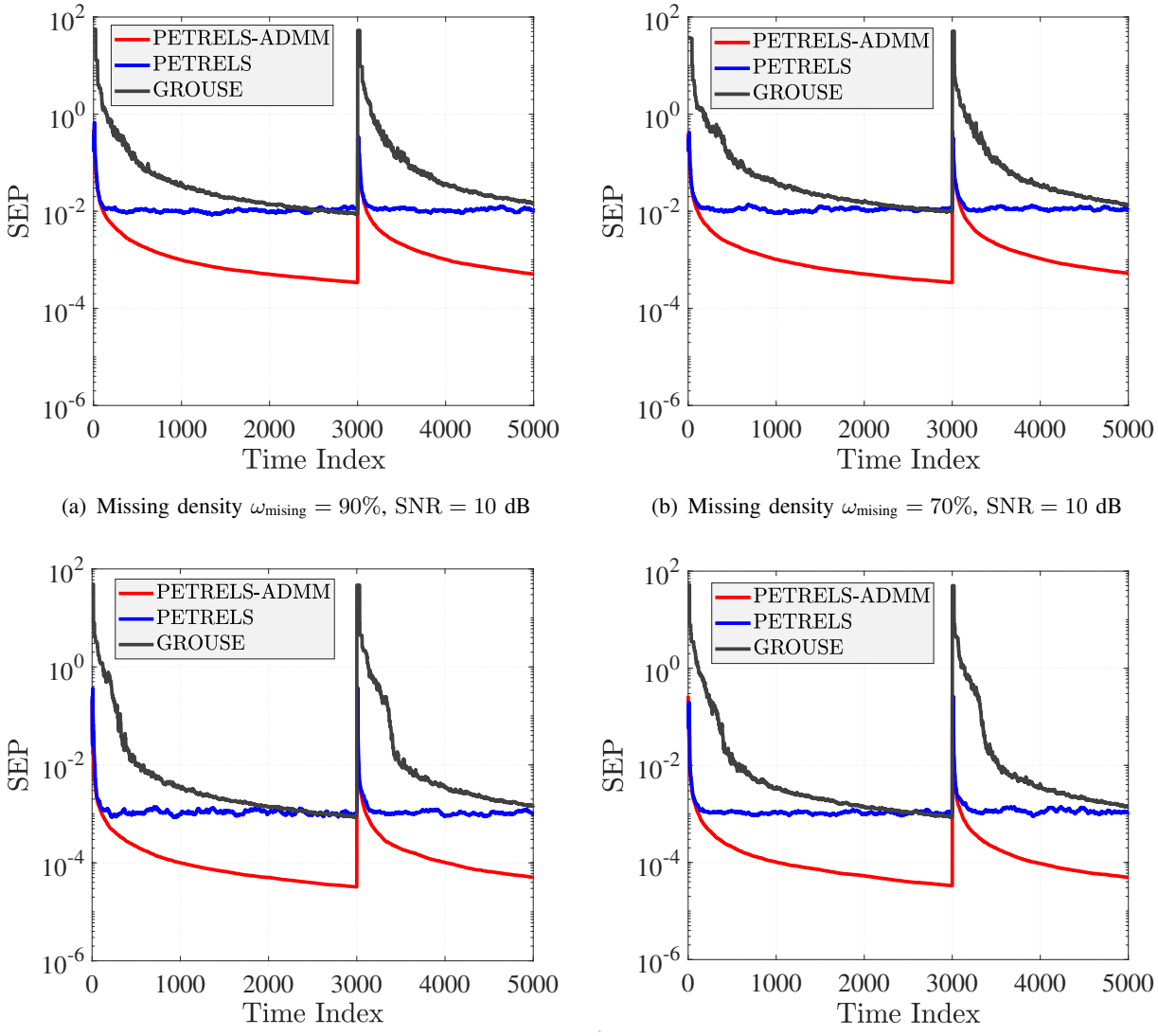


(a) Missing density $\omega_{\text{mising}} = 90\%$, SNR $= 10$ dB

(b) Missing density $\omega_{\text{mising}} = 70\%$, SNR $= 10$ dB

(c) Missing density $\omega_{\text{mising}} = 90\%$, SNR $= 20$ dB

(d) Missing density $\omega_{\text{mising}} = 70\%$, SNR $= 20$ dB

Fig. 7: Performance comparison between the subspace tracking algorithms from highly incomplete observation: $n = 500$, $r = 10$.

## REFERENCES


[1] G. Li and T. K. Pong, "Global convergence of splitting methods for nonconvex composite optimization," *SIAM J. Optim.*, vol. 25, no. 4, pp. 2434–2460, 2015.

[2] Y. Wang, W. Yin, and J. Zeng, "Global convergence of ADMM in nonconvex nonsmooth optimization," *J. Sci. Comput.*, vol. 78, no. 1, pp. 29–63, 2019.

[3] S. Boyd and L. Vandenberghe, *Convex optimization*. Cambridge University Press, 2004.

[4] J. Mairal, F. Bach, J. Ponce, and G. Sapiro, "Online learning for matrix factorization and sparse coding," *J. Mach. Learn. Res.*, vol. 11, no. Jan, pp. 19–60, 2010.

[5] K. Knopp, *Theory and application of infinite series*. Courier Corporation, 2013.

[6] A. W. Van der Vaart, *Asymptotic statistics*. Cambridge University Press, 2000.

[7] S. Shalev-Shwartz and Y. Singer, "Online learning: Theory, algorithms, and applications," 2007.

[8] K. Fountoulakis and J. Gondzio, "A second-order method for strongly convex $\ell_1$-regularization problems," *Math. Program.*, vol. 156, no. 1-2, pp. 189–219, 2016.

[9] D. P. Bertsekas, "Nonlinear programming," *J Oper. Res. Soc.*, vol. 48, no. 3, pp. 334–334, 1997.

[10] R. Coleman, *Calculus on normed vector spaces*. Springer Science & Business Media, 2012.

[11] L. Bottou, *On-Line Learning and Stochastic Approximations*. USA: Cambridge University Press, 1999, p. 9–42.

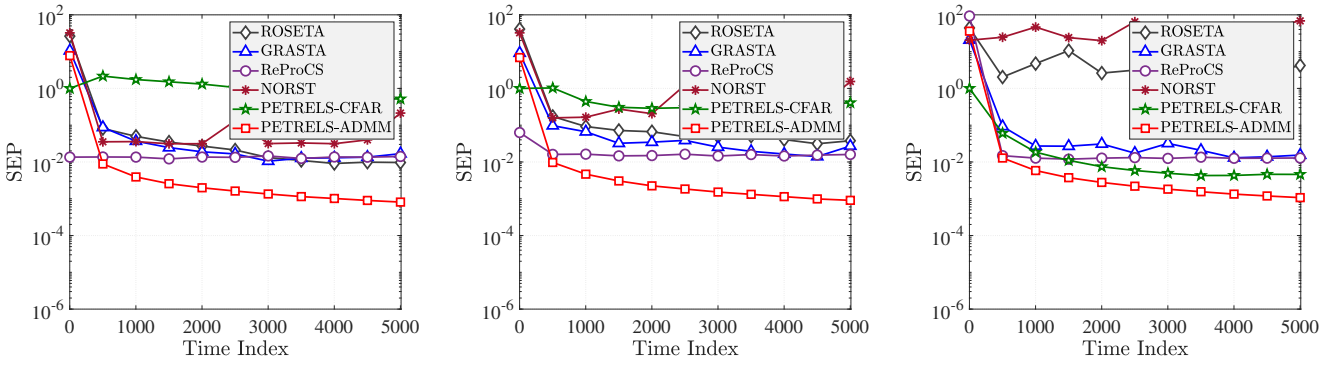


(a) SNR $= 0$ dB and fac-outlier $= 0.1$. (b) SNR $= 0$ dB and fac-outlier $= 1$. (c) SNR $= 0$ dB and fac-outlier $= 10$.

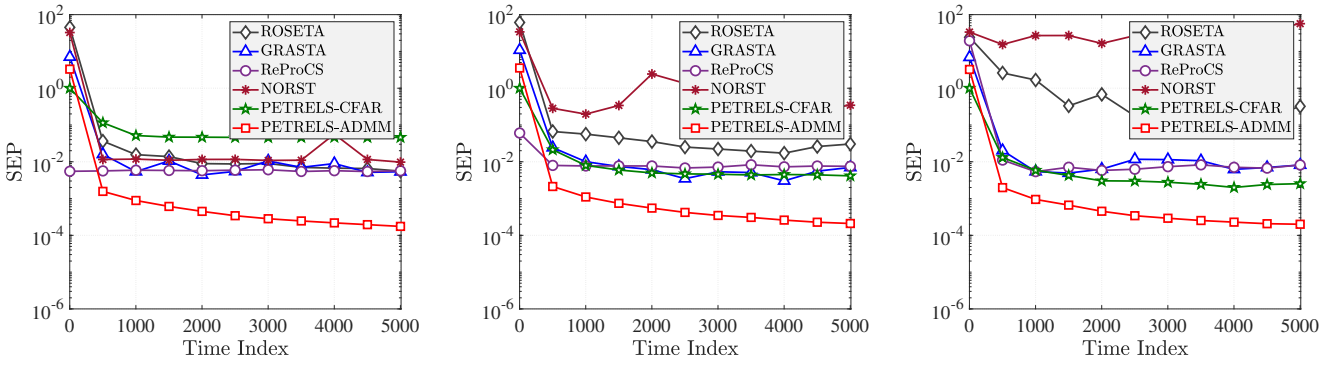


(d) SNR $= 5$ dB and fac-outlier $= 0.1$. (e) SNR $= 5$ dB and fac-outlier $= 1$. (f) SNR $= 5$ dB and fac-outlier $= 10$.

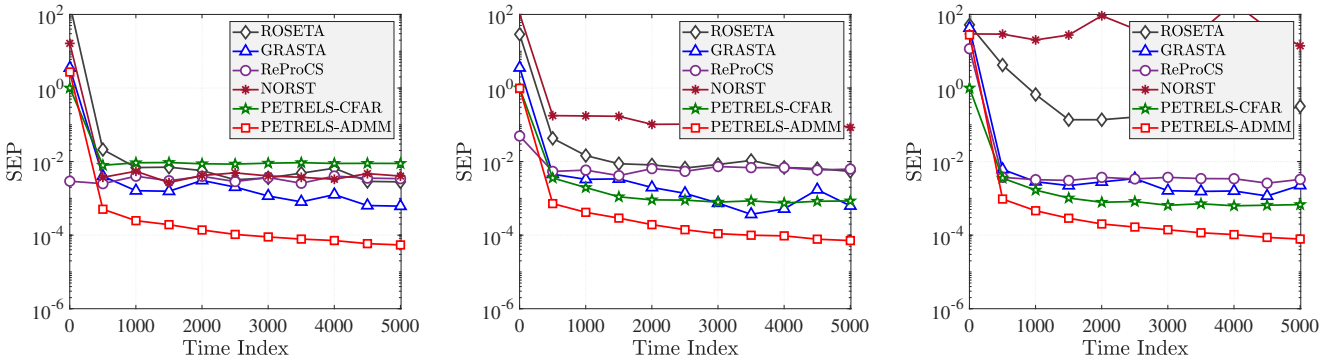


(g) SNR $= 10$ dB and fac-outlier $= 0.1$. (h) SNR $= 10$ dB and fac-outlier $= 1$. (i) SNR $= 10$ dB and fac-outlier $= 10$.

Fig. 8: Impact of outlier intensity on algorithm performance at different (low) noise levels (SNR is chosen among $\{0, 5, 10\}$ dB): $n = 50$, $r = 2$, $90\%$ entries observed, outlier density $\omega_{\text{outlier}} = 0.1$.

[12] J. He, L. Balzano, and A. Szlam, "Incremental gradient on the Grassmannian for online foreground and background separation in subsampled video," in *IEEE Comput. Soc. Conf. Comput. Vis. Pattern Recognit.* IEEE, 2012, pp. 1568–1575.

[13] Y. Chi, Y. C. Eldar, and R. Calderbank, "PETRELS: Parallel subspace estimation and tracking by recursive least squares from partial observations," *IEEE Trans. Signal Process.*, vol. 61, no. 23, pp. 5947–5959, 2013.

[14] L. Balzano, R. Nowak, and B. Recht, "Online identification and tracking of subspaces from highly incomplete information," in *Ann. Allerton Conf. Commun., Cont. Comput.* IEEE, 2010, pp. 704–711.

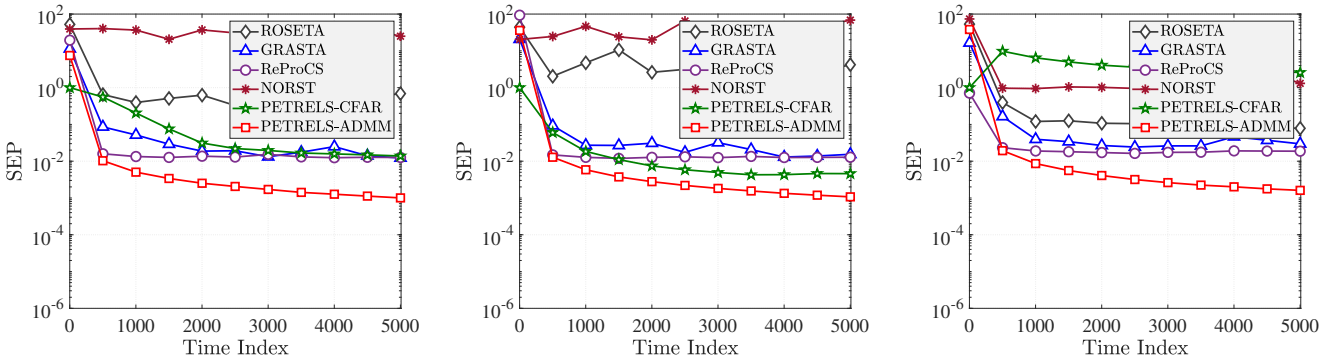


(a) SNR $= 0$ dB and $\omega_{\text{outlier}} = 0.05$ (b) SNR $= 0$ dB and $\omega_{\text{outlier}} = 0.1$ (c) SNR $= 0$ dB and $\omega_{\text{outlier}} = 0.2$

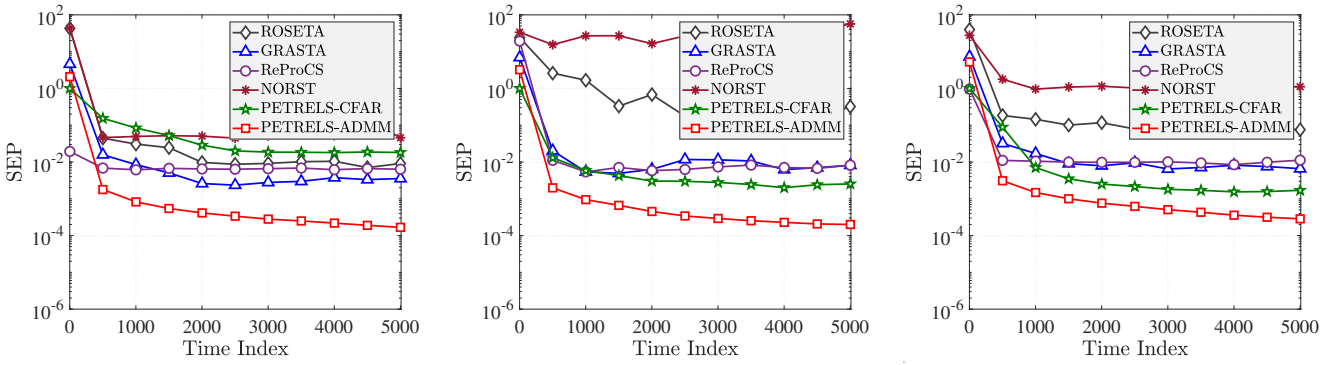


(d) SNR $= 5$ dB and $\omega_{\text{outlier}} = 0.05$ (e) SNR $= 5$ dB and $\omega_{\text{outlier}} = 0.1$ (f) SNR $= 5$ dB and $\omega_{\text{outlier}} = 0.2$

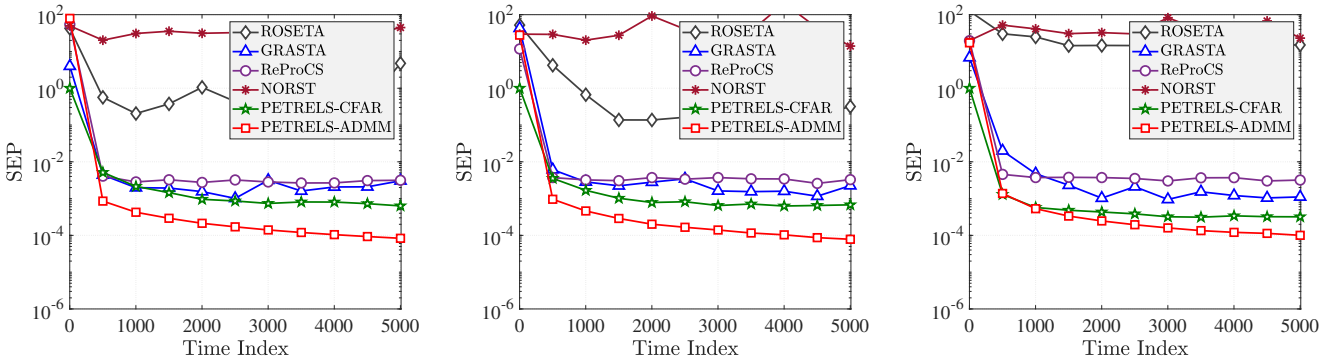


(g) SNR $= 10$ dB and $\omega_{\text{outlier}} = 0.05$ (h) SNR $= 10$ dB and $\omega_{\text{outlier}} = 0.1$ (i) SNR $= 10$ dB and $\omega_{\text{outlier}} = 0.2$

Fig. 9: Impact of outlier density on algorithm performance at different (low) noise levels (SNR is chosen among $\{0, 5, 10\}$ dB): $n = 50$, $r = 2$, $90\%$ entries observed, outlier intensity fac-outlier $= 10$.

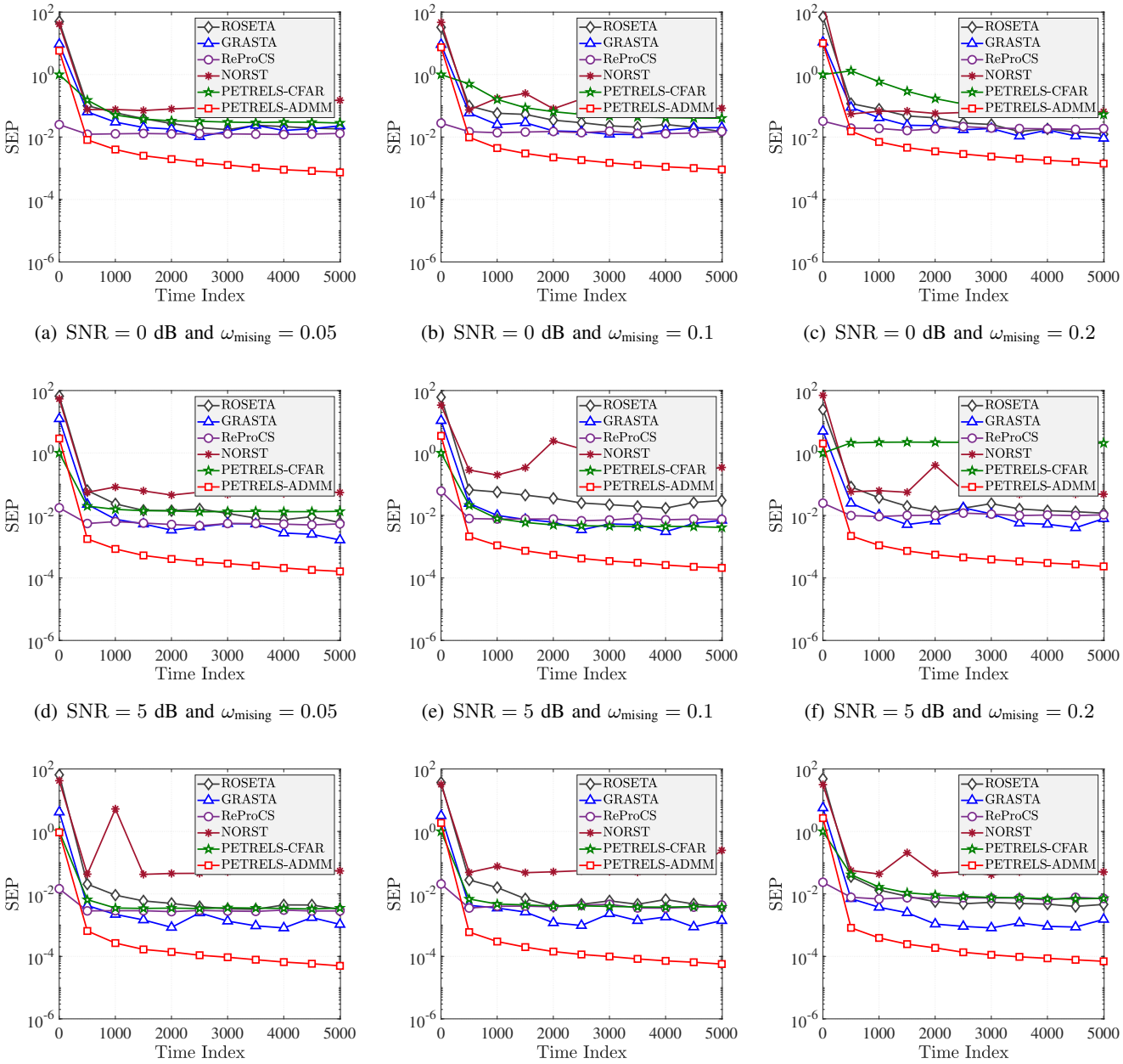


(a) SNR $= 0$ dB and $\omega_{\text{mising}} = 0.05$ (b) SNR $= 0$ dB and $\omega_{\text{mising}} = 0.1$ (c) SNR $= 0$ dB and $\omega_{\text{mising}} = 0.2$

(d) SNR $= 5$ dB and $\omega_{\text{mising}} = 0.05$ (e) SNR $= 5$ dB and $\omega_{\text{mising}} = 0.1$ (f) SNR $= 5$ dB and $\omega_{\text{mising}} = 0.2$

(g) SNR $= 10$ dB and $\omega_{\text{mising}} = 0.05$ (h) SNR $= 10$ dB and $\omega_{\text{mising}} = 0.1$ (i) SNR $= 10$ dB and $\omega_{\text{mising}} = 0.2$

Fig. 10: Impact of the density of missing entries on algorithm performance at different (low) noise levels (SNR is chosen among $\{0, 5, 10\}$ dB): $n = 50, r = 2$, outlier density $\omega_{\text{outlier}} = 0.05$, outlier intensity fac-outlier $= 1$.